INFORMATION TO USERS

This manuscript has been reproduced from the microfilm master. UMI films the text directly from the original or copy submitted. Thus, some thesis and dissertation copies are in typewriter face, while others may be from any type of computer printer.

The quality of this reproduction is dependent upon the quality of the copy submitted. Broken or indistinct print, colored or poor quality illustrations and photographs, print bleedthrough, substandard margins, and improper alignment can adversely affect reproduction.

In the unlikely event that the author did not send UMI a complete manuscript and there are missing pages, these will be noted. Also, if unauthorized copyright material had to be removed, a note will indicate the deletion.

Oversize materials (e.g., maps, drawings, charts) are reproduced by sectioning the original, beginning at the upper left-hand corner and continuing from left to right in equal sections with small overlaps. Each original is also photographed in one exposure and is included in reduced form at the back of the book.

Photographs included in the original manuscript have been reproduced xerographically in this copy. Higher quality 6" x 9" black and white photographic prints are available for any photographs or illustrations appearing in this copy for an additional charge. Contact UMI directly to order.

UMI

A Bell & Howell Information Company
300 North Zeeb Road, Ann Arbor MI 48106-1346 USA
313/761-4700 800/521-0600

Université d'Ottawa · University of Ottawa

العِلْم

ما من شك على الإطلاق في أن للعلم إجمالاً . وللحديث منه بنوع أخص . فضلاً لا يُقدر على المدنيّة التي نقدرها فوق ما تستحق . فالعلم قد ذلل عقبات كثيرة كانت تعترض سبيل الإنسان في دنياه . ولكنه ما ذلل عقبة حتى خلق عقبات . والناس ، مع ذلك ، يؤمنون به إيماناً أعمى ويعبدونه عبادة لا تفتر . فكل ما يقرّه العلم حقيقة في نظرهم لا تُدحض . وكل ما ينفيه وهمٌ وخرافة . وأما القضايا التي ما تزال تحت البحث فقضايا معلّقة بين الشك واليقين . وليس لنا أن نقبلها أو أن نرذلها ريثما يبدي العلم حكمه النهائي فيها .

ميخائيل نعيمة

ABSTRACT

{[(TMS)NCH$_2$CH$_2$]$_2$N(TMS)}$_2$V$_2$(μ-Cl)$_2$ was prepared by reaction of VCl$_3$(THF)$_3$ with the corresponding amide, and then reacted with sulfur to yield what it is thought to be {[(TMS)NCH$_2$CH$_2$]$_2$N(TMS)}$_2$V$_2$(μ-S)$_2$. X-ray crystallographic analysis was not possible due to the poor quality of the crystals. However reaction of [(Me$_3$Si)$_2$N]$_2$VCI(THF) with S$_8$ yielded crystals of {[(Me$_3$Si$_2$N]$_2$V}$_2$(μ-S)$_2$}. On the other hand reaction of VCl$_2$(TMEDA)$_2$ with S$_8$ led to the formation of VCl$_3$(TMEDA)(THF) and V$_3$S$_7$Cl(TMEDA)$_3$ which precipitated as a black powder. Reaction of V$_3$S$_7$Cl(TMEDA)$_3$ with mercaptopyridine led to the formation of [V$_3$(μ_3-Cl)-(μ-S$_2$)$_3$](PyS)$_3$Li(THF)$_4$ meanwhile the reaction of Me$_3$Si$_2$NLi yielded a high valent tetrameric structure {[(TMS)$_2$N]VS$_3$Li(THF)$_2$Li}$_4$ complex.

Alternative sources of sulfur atoms such as diphenyl disulfide was also used. In that particular case the reaction yielded a dimer which the X-ray structure confirmed as (TMEDA)$_2$V$_2$Cl$_2$(μ-SPh)$_2$(μ-Cl).

Ab initio and extended Huckel calculations were carried out on several clusters in order to understand the electronic structures of the complexes and the interactions between the metal centers. Calculations on a vanadium-sulfur cubane cluster revealed the

presence of an intricate "web" of molecular orbitals showing electronic communication between all four metallic centers.

PUBLICATIONS

Preparation and Characterization of a Diamagnetic Sulfido-Bridged Divanadium Amide Complex.

Moore M. Feghali K. Gambarotta S.
Inorganic Chemistry 1997, 36, 2191 - 2194

Preparation and Characterization of a Diamagnetic and Dinuclear Titanium (III) Formamidinate Complex. Evidence for the Existence of a Ti-Ti Bond.

Hao S. Feghali K. Gambarotta S.
Inorganic Chemistry 1997, 36, 1745 - 1748

Reactivity of Coordinatively Unsaturated Trivalent Chromium Complexes with Sulfur: Preparation of Novel Sulfide-Bridged Dinuclear Cr^{IV} Derivatives.

Reardon D. Kovacs I. Ruppa K. B. P. Feghali K.Gambarotta S. Petersen J.
Chemistry, A European Journal 1997, 3, No.9, 1481 - 1488

Amide C-N Bond Cleavage And Formation of Nitride Promoted by A Niobium(II) Cluster.

Tayebani M. Feghali K. Gambarotta S. Bensimon C.
Organometallics. 1997, 16, No.23, 5084-5088

The Reduction of Nb2Cl6(TMEDA)(2) by R2NLi - Formation of a Diamagnetic Niobium(II) Cluster With Short Nb-Nb Triple Bond And Amide C-N Bond Cleavage.

Tayebani M. Kasani A. Feghali K. Gambarotta S. Bensimon C.
Chemical Communications. (20):2001-2002, 1997 Oct 21.

ACKNOWLEDGEMENTS

I would like to thank my supervisor Dr. Sandro Gambarotta for his support and guidance through this work and my labmates, Dr. M. Moore, Dr. K. B. Ruppa, Dr. A. Kasani, Dr. F. Conan, D. Reardon, M. Tayebani, T. Dube, and Y. Ma for all the help and skilled guidance throughout this work.

I would like to take this opportunity to thank Dr. Alain St-Amant for his guidance through the theoretical part of this work, as well as Dr. Darrin Richeson for many fruitful discussions.

I would also like to thank my parents and my brother who gave me support and encouragement troughout my life.

TABLE OF CONTENT

CHAPTER I

Introduction

The high stability of dinitrogen is very well known and reflected in its physical-chemical characteristics. The presence of a N-N triple bond is responsible for a very high bond dissociation energy (225 kcal/mol), high ionization potential (15.058 eV) and negative value of electron affinity (-1.8 eV). The proton affinity, though positive (5.12 eV), is smaller than, for example, methane (5.3 eV). Therefore, dinitrogen acts as a very weak base and does not interact even with the strongest acids. The strength of the triple bond does not by itself explain the inertness of dinitrogen. The triple bond dissociation energy in acetylene (230 kcal/mol) is approximately the same as that for dinitrogen, while in carbon monoxide the bond energy is even higher (256 kcal/mol). In contrast to N_2 however, CO and acetylene display a wide spectrum of reactivity unknown for dinitrogen.

Important conclusions about the reasons for dinitrogen's inertness, as well as clues to overcoming it, may be drawn by considering the energies required for consecutive cleavage of the three bonds in the molecule. Dissociation of the first of the three bonds (requiring more than 100 kcal/mol) corresponds to about half of the total triple bond energy. This distinguishes this molecule from others with multiple bonds [e.g. acetylene whose first splitting bond energy is the weakest (53

kcal/mol)]. This is a peculiar characteristic of N_2 and is not affected by the nature of the species reacting with it. The strength of the first of the three N-N bonds has a correspondence in the values of redox potentials E_o [1].

In the first step of reduction, diazene is formed via transfer of one and two electrons with simultaneous addition of protons. This process requires strongly negative values of E_o (-3.2 V) thus requiring the use of a reducing agent stronger than dihydrogen. In aprotic media, strong reductants such as metallic lithium are capable of reacting with dinitrogen to form nitrides. These reactions are very unlikely to occur in protic media since the conditions favour dihydrogen formation :

$$2H^+ + 2e^- \rightleftharpoons H_2$$

Dinitrogen reduction in aprotic media

- Stoichiometric systems:

In 1965, the discovery by Allen and Senoff [2] of the first dinitrogen complex $[Ru(NH_3)_5(N_2)]^{2+}$ marked a milestone in the chemistry of dinitrogen fixation. This result prompted further the research into this field and synthesis and reactivity of dinitrogen complexes of various transition metals were actively pursued by several groups around the world.

In the early experiments transition metal chlorides ($CrCl_3$, $MoCl_5$, WCl_6, $FeCl_3$, $TiCl_4$) were reduced with strong reducing agents, such as $LiAlH_4$, EtMgBr or i-Bu_3Al. Ammonia was detected in variable amounts in the hydrolysis of the

reaction products. Appreciable yields of the reaction product (up to 25% of ammonia relative to the amount of transition metal employed) were observed at comparatively high dinitrogen pressure (100-150 atm.). Later, Vol'pin and his co-workers succeeded in obtaining more active systems. Thus, in the reaction of N_2 with the products of the reaction of Cp_2TiCl_2 with EtMgBr in ether, the yield of ammonia (after hydrolysis) was 67% per mol of titanium compound employed, even at atmospheric pressure [3,4]. On increasing the pressure, the yield of ammonia became nearly quantitative.

The activity of the systems towards dinitrogen varies widely, depending on the nature of the transition metal and reaction conditions. However, some generalizations can be made. Firstly, the number of transition metal compounds capable of taking part in the nitrogen-fixing systems is very large. The strongest N_2 reducing capacity is displayed by transition metals of Groups 4, 5 and 6 of the periodic table, e.g, Ti, V, Cr, Mo and W. Particularly active are titanium and zirconium compounds. With first row transition metals, the yields of ammonia generally decrease while moving in the periodic table from left to right as a possible result of a decreased stability of nitrides. However, it must be observed that iron compounds are in general, more efficient than manganese compounds. Cobalt and nickel derivatives usually possess low or no activity. Palladium, copper and platinum complexes apparently demonstrate no activity in any of the tested systems.

Yields of ammonia strongly depend on the reducing agent. The reductants include organometallic compounds (RMgX, RLi, R_3Al), metal hydrides ($LiAlH_4$, LiH), free metals (alkali, alkaline earth, rare earth), aromatic radical anions and dianions and dihydrogen (in combination with other reductants). The role of the reducing agent is to produce a low-valent transition metal complex activating dinitrogen.

- Catalytic systems:

Attempts have been made to design systems for the catalytic hydrogenation of N_2. However, excess dihydrogen usually inhibits the reaction, thus decreasing the yield of NH_3 even in systems that normally catalyze hydrogenation of unsaturated compounds. In some cases however, the concentration of H_2 does not affect the yield of NH_3, and in a few cases, for example $Ti(OEt)_4$ +$(i\text{-}Bu)_3Al$ + N_2, an appreciable increase in the yield of ammonia (after hydrolysis) was observed following the introduction of H_2. However, with increase of dihydrogen pressure, the yield of ammonia passes through a maximum, which is still less than 100%, before decreasing. Nevertheless, these systems demonstrate the possibility of the participation of dihydrogen in the N_2 reduction process (perhaps forming hydrides and subsequently some NH containing compounds in the process of reduction).

Vol'pin and co-workers achieved the catalytic reduction of dinitrogen by

using a potent reducing agent. For example, aluminum metal reduces dinitrogen at 130 °C and a pressure of 100 atm in the presence of titanium tetrachloride and aluminum bromide. Lithium aluminum hydride can be used as a reducing agent instead of aluminum in catalytic systems. In the case of the catalytic system $TiCl_4$ + $LiAlH_4$ + $AlBr_3$, more than 100 mol of ammonia (after hydrolysis) per mole of initial titanium tetrachloride were obtained at relatively low temperatures (60-70 °C) when the reaction was performed in a molten mixture of aluminum chloride and bromide. When the ternary mixture $AlBr_3$-$AlCl_3$-C_6H_6 was used as a solvent, some catalytic reduction to ammonia was observed [NH_3:Ti is approx. 5] even at 30 °C.

Although catalytic hydrogenation of dinitrogen has not been observed in aprotic solutions, Japanese workers have shown that the introduction of alkali metal strongly activates the heterogeneous catalyst employed for the large scale synthesis of ammonia from dinitrogen and dihydrogen [5]. Thus, Tamaru et al. observed that the reaction of iron, cobalt, titanium and molybdenum phthalocyanine complexes with metallic sodium resulted in the formation of a donor acceptor complex which can catalyze the synthesis of ammonia from dinitrogen and dihydrogen starting from temperatures as low as 110 °C. Ozaki, Aika and Hori showed that alkali metals sharply increase the catalytic activity of ruthenium, osmium, iron, molybdenum and other metals in the synthesis of ammonia. Ruthenium activated by potassium is capable of catalyzing the reaction

at 146 °C and atmospheric pressure [5].

Dinitrogen reduction in protic media

- Stoichiometric systems:

In protic media, V(II) hydroxide turned out to be most active, and remains one of the simplest, dinitrogen reducing systems. The reduction of N_2 occurs in aqueous or alcohol suspensions of freshly prepared hydroxide formed by adding excess alkali to a solution of a mixture of VCl_2 and $MgCl_2$. Apparently, V(II) (d^3) in the mixed hydroxide combines the ability to both activate and reduce dinitrogen. The reaction produces hydrazine and ammonia at high rates at ambient conditions. Dinitrogen fixation takes place even from air, as dioxygen diminishes the yield only to a minor extant [6].

At high concentrations of alkali and high dinitrogen pressures the reaction forms hydrazine according to the stoichiometry

$$4V(OH)_2 + N_2 + 4H_2O \xrightarrow{Mg(OH)_2} 4V(OH)_3 + N_2H_4$$

The hydrazine formed in this process competes for electrons of V(II), with dinitrogen, particularly at low N_2 pressures, and ammonia can be the final product. The highest yields of hydrazine and ammonia reach approximately 65% .

As already mentioned, at low alkali concentrations (pH 8~ 12), ammonia

is directly produced from dinitrogen without intermediate formation of free hydrazine. The overall reaction is the following:

$$6V(OH)_2 + N_2 + 6H_2O \xrightarrow{Mg(OH)_2} 6V(OH)_3 + 2\,NH_3$$

The role of excess $Mg(OH)_2$ was never completely elucidated. However, there is a general agreement that $Mg(OH)_2$ prevents the formation of a rigid cluster structure of $V(OH)_2$ which is inactive towards N_2. In the absence of $Mg(OH)_2$, vanadium(II) hydroxide is active only in the first few seconds after its formation and quickly loses its activity.

- Catalytic systems:

A catalytic system for dinitrogen reduction requires the presence of a sufficiently strong reducing agent that would reduce dinitrogen coordinated on the catalyst. The catalyst may participate in the reduction, by increasing its oxidation state. The role of the reductant is to restore the initial state of the catalyst. To perform successive catalytic cycles, the catalyst with coordinated N_2 should react with new molecules of the reducing agent. Another possibility is to construct a system able to transfer both electrons and protons to the coordinated N_2 from the reductant. Thus, the catalyst must posses electroconductivity to ensure the electron flow. Another alternative would be a catalyst adsorbed at a cathode of an electrochemical cell.

Mo (III) activates dinitrogen in a bi- or polynuclear complex, forming an intermediate e.g. of the type (Mo=N=N=Mo) which is unable to produce hydrazine or ammonia at the expense of Mo oxidation. In no instance does reduction take place with Mo (III) complexes alone in protic media. The reaction may become thermodynamically favorable if a stronger reducing agent, situated nearby, can simultaneously reduce Mo to its initial trivalent state.

The first catalytic system for dinitrogen reduction in protic media was realized with Mo (III) as a catalyst and titanium(III) hydroxide as a reductant. With pure $Ti(OH)_3$, the yield of the products of N_2 reduction, in the presence of Mo (III) formed in the process of coprecipitation of both metal hydroxides by addition of alkali, only reaches, at best, equimolar amounts with respect to Mo, even at elevated temperatures and pressures of dinitrogen. In the presence of salts of some other metals in solution before the addition of alkali, e.g. Mg^{2+}, Ca^{2+} or Sr^{2+}, the yields increase and the system becomes catalytic. The effect of magnesium salts turned out to be particularly pronounced. The yields of hydrazine and ammonia greatly increase and, at high temperatures and at pressures can reach several hundred turnovers per Mo present. The highest yields are obtained when the ratio of Mg^{2+}: Ti^{3+} is 1:2. At this ratio, a compound of formula $MgTi_2O_2$ is produced that forms fine crystals. The catalytic effect of Mo (III) is observed when the complex is adsorbed at the surface of $MgTi_2O_2$.

Experimental results show that the mechanism of catalytic action involves

a cooperative reductive action of the titanium ions surrounding the Mo catalyst and oxidation of these ions to titanium (IV). During this process, coordinated dinitrogen is reduced to hydrazine. Subsequent electron transfer from the remote titanium ions to the catalytic center, cleave the N-N bond forming possibly an amide and ammonia. The magnesium titanium compound, $MgTi_2O_2$, possesses semiconducting properties, and evidently the Mo-dinitrogen complex on its surface forms an electron trap. Accordingly dihydrogen is evolved in a fast reaction in the absence of dinitrogen, particularly at high temperatures. The introduction of the Mo catalyst, even in a very small amount compared with titanium, strongly inhibits H_2 evolution in the presence of dinitrogen. This may be explained by a mechanism in which the Mo complexes are adsorbed at the active sites of $MgTi_2O_2$; dinitrogen forms intermediate complexes with Mo (III), preventing the electron flow to the hydrogen evolution centers. Coordinated dinitrogen can then be reduced to hydrazine or to ammonia with the participation of the solvent protons.

The mechanism proposed for the catalytic N_2 reduction by an electroconductive reductant has prompted the use of amalgams, particularly sodium amalgam, as reducing agents. Sodium amalgam is a strong reductant (redox potential for $Na/Hg \Rightarrow Na^+/Hg^+ + e$ is -1.84 V). However in contact with alcohol it is reasonably stable. Further, the amalgam can be prepared electrochemically using a mercury cathode and passing electric current through a

solution containing sodium ions. Therefore, it can be conveniently used in the electrochemical reduction of dinitrogen.

Introduction of the sodium amalgam in the catalytic system based on Mo (III) and $MgTi_2O_2$ described above, increased the yield of hydrazine and ammonia. Apparently, amalgam transfers its electrons through the magnesium-titanium mixed oxide to the Mo catalytic center. Obviously the electron-transferring material is unnecessary, and the amalgam can serve, in principle, as the only reducing agent. Accordingly, if one shakes the Mo (V) compound formed by dissolving $MoCl_5$ in methanol (without titanium-magnesium reductant), under 100 atm N_2 with sodium amalgam, formation of hydrazine can be observed in solution. However, the yields are extremely small and poorly reproducible. Nevertheless, the system was subsequently developed and transformed into the most active among the known non-biological catalytic systems for the reduction of dinitrogen at ambient temperature and pressure.

The first improvement of the system was achieved when the magnesium salt was added to the solution of $MoCl_5$ in methanol before reducing the latter by sodium amalgam [7,8]. The yields, albeit still low, became reproducible and the reaction kinetics could be measured to draw conclusions about the nature of the rate determining step. Apparently, magnesium ions which are involved in the formation of polynuclear structures (vide infra) stabilize the complexes and may make them more suitable for the activation of dinitrogen. The system's low

activity was most probably due to insufficient contact of the complexes with the surface of the amalgam. Therefore, it was necessary to find a means to bind the complex to the amalgam to improve the electron transfer from the reductant to the catalytic complex. After a long search, and following the example of living nature, a phospholipid (phosphatidylcholine) was proven to strongly increase the reaction rate and the product yield. It became possible to study the reaction at atmospheric pressure and room temperature. This further facilitated the search for system improvement.

Hydrazine and ammonia are produced in parallel reactions. Their ratio depends mainly on the nature of the catalytic complex and also on the length of phosphatidylcholine aliphatic chains. In the case of a specially prepared polynuclear Mo complex (vide infra), hydrazine is the main product and the yield of ammonia amounts to only approximately 10% of total dinitrogen reduction.

After all the improvements, the specific activity of the catalytic system in dinitrogen reduction (per catalytic complex) reached or exceeded that of nitrogenase. Up to 1000 turnovers can be observed with respect to Mo catalytic complex at atmospheric pressure, and more than 10000 turnovers at elevated pressure. It is believed that the role of the phospholipid is to form a thin film on the surface of the amalgam with the catalyst incorporated and thus bound to the electron donor (Figure 1). The film is kept at the surface, presumably because of the attachment of the phosphatidylcholine positive heads to the negatively

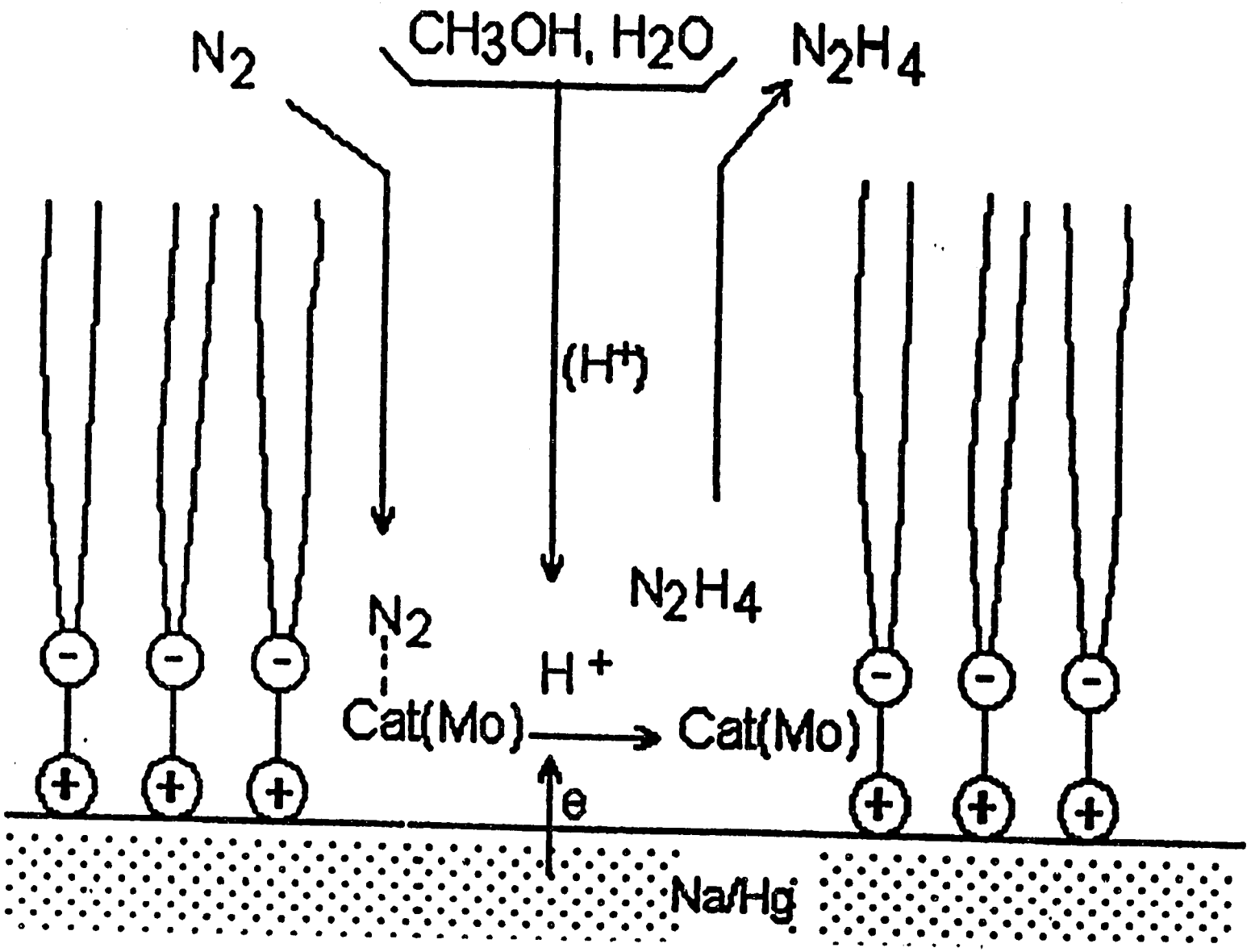

Figure 1

charged surface. Electrons move from the amalgam to the complex to perform the reduction. Proton containing molecules (water and alcohol) diffuse through the hydrophobic part of the film to protonate the activated dinitrogen and to form the final products. The hydrophobic film helps to keep the amalgam droplets separated and prevents their fast agglutination. This leads to an increase in the surface to volume ratio, and thus to an increase in catalytic activity. Presumably, the hydrophobic film also helps to control the proton flow to the catalyst from the solution. Indeed, the dihydrogen evolution is also catalyzed by the Mo complexes and facilitated by the presence of the phospholipid, but its rate increase is much less pronounced than that of dinitrogen reduction.

Apparently, the chemical nature of the polar heads of the phospholipid is important for the incorporation of the catalyst, since many other surface-active materials, including other phospholipids, proved to be inactive; e.g. tetraalkylammonium salts with long aliphatic chains. Although they form a film on the surface of the amalgam, they failed to make a catalytic system with the Mo complexes.

- Biological dinitrogen fixation:

In striking contrast to the synthetic systems, biological N2-fixing systems can reduce N_2 gas into NH_3 under very mild conditions (1 atm, aqueous medium, pH ~ neutral, RT). The ability of some bacteria to efficiently perform nitrogen fixation, established in the last century, has served as a continuous source of

inspiration to search for synthetic chemical systems capable of catalytically fixing dinitrogen under mild conditions. Until the 1960's, all efforts to react dinitrogen reactions at low temperature and pressures were unsuccessful and the reaction with lithium to form nitrides remained the only example. Also attempts to isolate enzymes able to interact with N_2 and to observe an in vitro reaction with N_2 failed.

In 1960, reduction of dinitrogen was observed in supernatant solution produced from cells in the presence of an ATP generating system. This work marked a milestone in the field and stimulated investigations on nitrogenase chemistry. The nitrogen fixing enzyme consists of two proteins, an Fe-protein and an MoFe-protein. While in combination, these two proteins perform dinitrogen reduction to ammonia under ambient conditions.

Fe-proteins from nitrogenase of different microorganisms, as well as from Mo-containing and alternative nitrogenases, have been isolated, purified and thoroughly studied. Fe-proteins have much in common in terms of size, structure and properties. The proteins are dimers of identical subunits with the total molecular mass about 60 kDa. They contain one [4Fe-4S]-cluster that, as shown by recent X- ray structural analysis [9] of single crystals of Fe-protein, binds its subunits using sulfur atoms of cysteines from both subunits as ligands. The cluster is located virtually on the surface of the protein globules and is easily accessible to solvent. This is likely to be the reason for the strong sensitivity of protein to oxidation, and seems to be necessary for its catalytic activity.

The large protein components of nitrogenase have a molecular mass of about 220 kDa. The MoFe-protein is a tetramer of two types of subunits $\alpha_2\beta_2$. Each protein molecule contains two Mo atoms, 32 Fe atoms, and 32 S atoms in the form of inorganic sulfides. All the transition metal atoms in MoFe-proteins are organized into two types of redox centers. About half of the Fe is in the composition of four [Fe_4S_4]-clusters, named P-clusters, and the rest, together with Mo (or V), is in M-centers, also named FeMo-cofactors. The FeMo-cofactor consists of two cubane fragments [Fe_4S_3] and [Fe_3MoS_3] bound by three bridging ligands which are most likely all S (S^{2-}), although one of them was originally considered as a different ligand and was designated as Y atom[10] (Figure 2).

Conditions for the performance of the nitrogenase reaction cycle include the presence of MoFe-protein, Fe-protein, MgATP, and the absence of air or oxygen. Under these conditions dihydrogen evolution occurs with simultaneous hydrolysis of ATP to ADP and phosphate. The introduction of dinitrogen causes a decrease in the amount of dihydrogen produced and formation of ammonia, whereas the rates of the ATP hydrolysis and the reductant oxidation do not change. Under optimum conditions the main nitrogenase reaction can be presented by the equation:

$$N_2 + 8H^+ + 8e^- + 16MgATP \longrightarrow 2NH_3 + H_2 + 16MgADP + 16PO_4^{2-}$$

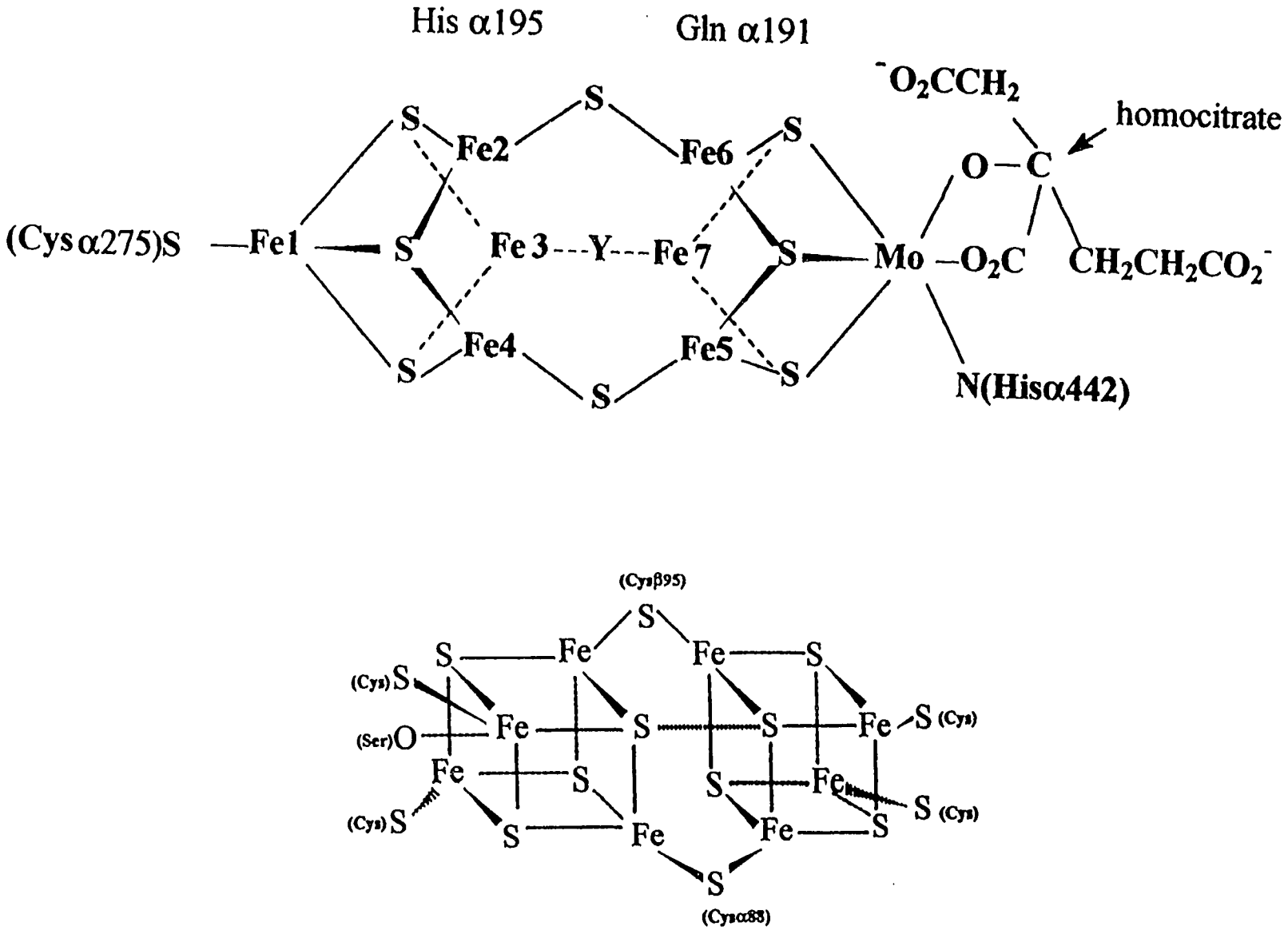
His α195
Gln α191
$^{-}O_2CCH_2$
homocitrate
(Cys α275)S
Fe1
Fe2
Fe3
Y
Fe4
Fe5
Fe6
Fe7
Mo
O_2C
$CH_2CH_2CO_2^-$
N(His α442)
(Cys β95)
(Cys)S
(Ser)O
(Cys α88)

Figure 2

In addition to dinitrogen reduction, nitrogenase catalyzes the reduction of many other substrates of small size, mostly triple bonds [11].

During the catalytic cycle of dinitrogen reduction performed by nitrogenase, several reactions proceed consecutively and/or in parallel: formation of the MgATP complex with Fe-protein, reduction of MoFe-protein by this complex, ATP hydrolysis releasing ADP and phosphate, coordination and reduction of a substrate, reduction of Fe-protein, and release of product molecules. The dinitrogen transformation to ammonia is the result of a series of electron and proton transfers. The agents responsible for the sequence of electron transfer are well established: an external reducing agent, flavodoxine or ferredoxine in vivo, or dithionite in vitro, transfers electrons to the Fe-protein, then, one by one, from the latter to the MoFe-protein where N_2, is reduced to NH_3. Presumably, electrons go to the P-cluster in the first stage , then to FeMoco and finally to the substrate. The detailed mechanism of the electron transfer and coupled ATP hydrolysis process remains unclear: such problems as the interaction of the proteins, the electron and protons paths through the proteins, the exact nature of intermediates. etc., remain unknown.

A full schematic description of the reactions in the nitrogenase cycle, based on the experimental kinetic results, was proposed by Thorneley and Lowe. The mechanism involves two reaction cycles, shown in Figures 3 and 4 [12]. Figure 3 describes the Fe-protein redox cycle of nitrogenase and shows the reactions

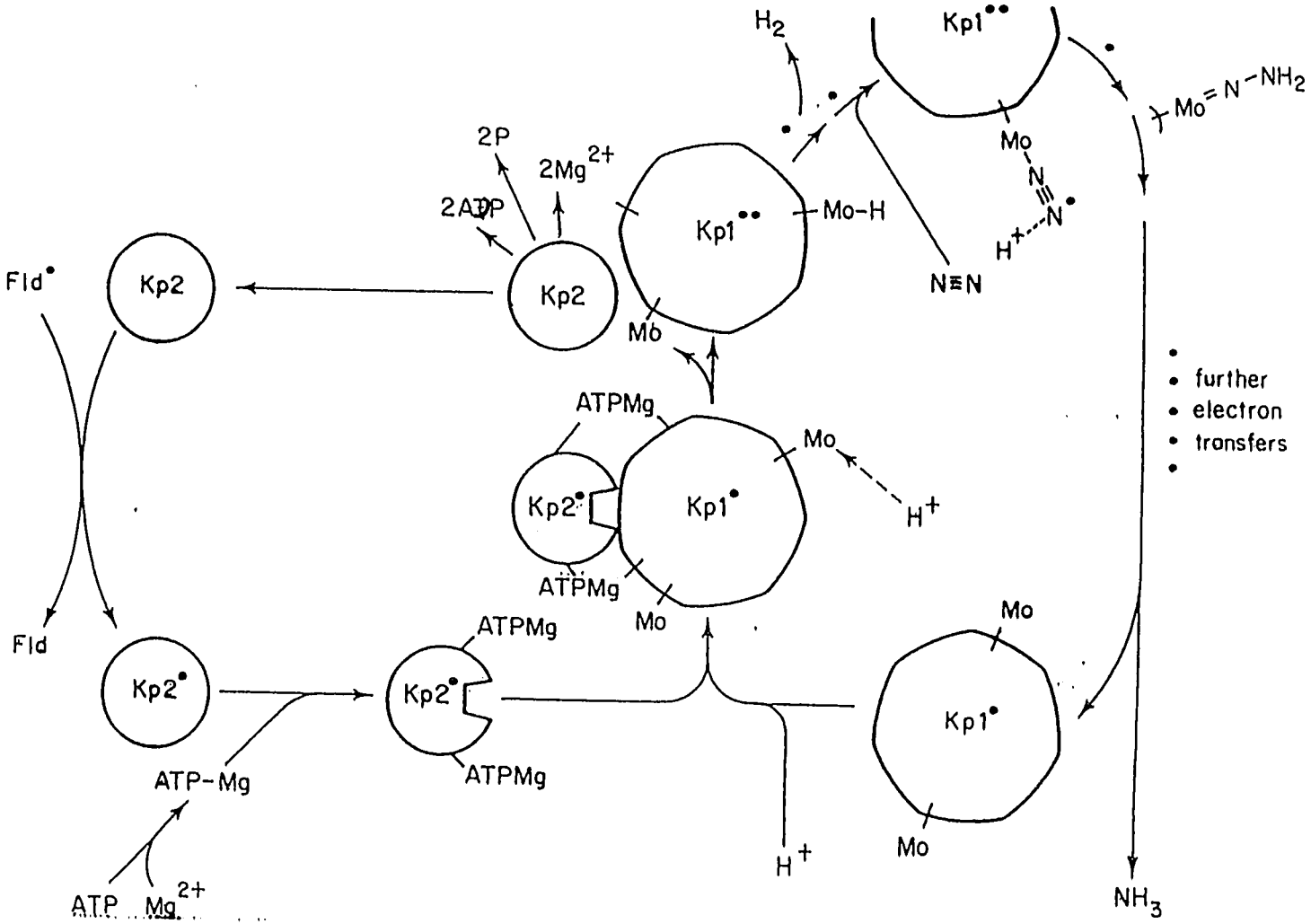
H2
Kp1••
Mo=N-NH2
2P
2Mg2+
2ATP
Kp1••
Mo-H
Mo
N
N
H+
N≡N
Fld•
Kp2
Kp2
Mo
• further
• electron
• transfers
ATPMg
Mo
Kp2•
Kp1•
H+
ATPMg
Mo
Fld
Kp2•
ATPMg
Kp2•
Kp1•
Mo
ATP-Mg
ATPMg
H+
Mo
ATP
Mg2+
NH3

Figure 3

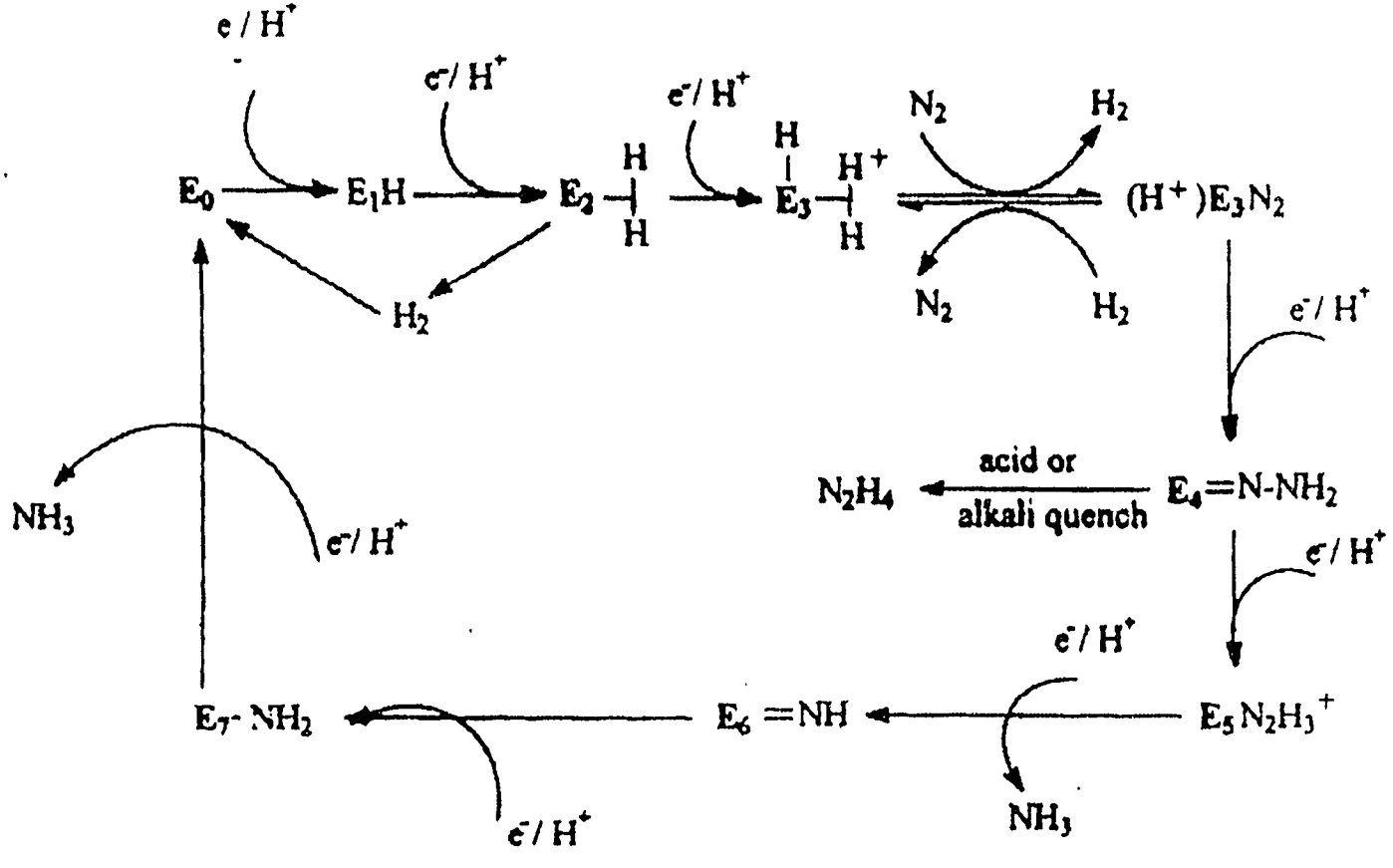
e / H+
e-/ H+
e-/ H+
N2
H2
E0
E1H
E2
E3
(H+)E3N2
H2
N2
H2
e-/ H+
NH3
e-/ H+
N2H4
acid or
alkali quench
E4=N-NH2
e-/ H+
e-/ H+
E7- NH2
E6 =NH
E5 N2H3+
e-/ H+
NH3

Figure 4

which proceed on transfer of electrons from the reduced Fe-protein to the MoFe-protein.

The rate determining step is proposed to be dissociation of the complex of the oxidized Fe-protein and the reduced MoFe-protein.

Figure 4 presents the changes in the MoFe-protein in the process of electron accumulation in its active center. Here E is MoFe-protein, and the associated subscript corresponds to the number of electrons transferred to it; each step of Figure 4 is the result of the total cycle of Figure 3.

To be able to coordinate and activate dinitrogen, the FeMo-cofactor of the MoFe-protein must be sufficiently reduced: according to Figure 4 this corresponds to the transfer of three electrons to the MoFe-protein from the Fe-protein. At step E_3, FeMoco can already reversibly coordinate N_2. Recently, it was experimentally confirmed [13] that the transition from the E_3 state (the reversible binding of N_2) to the E_4 state is connected with the oxidation of the P-centers. This is a critical point of the catalytic cycle of the MoFe-protein: dinitrogen becomes irreversibly reduced to the intermediate state, and corresponds to the hydrazine derivative producing hydrazine when decomposed by acid or alkali. Consecutive addition of two more electrons and two protons leads to the liberation of two molecules of ammonia.

A valid chemical mechanism for the interaction of dinitrogen with FeMoco is central to understanding the catalytic action of nitrogenase. Before the

molecular model of the M-centers was reported, almost all the mechanistic hypothesis of N_2 substrate reduction was based on the participation of the Mo atom: the differences in opinion concerning the mechanism were usually dealing with the number of Mo atoms (one or two), and with the possible participation of Fe in the intermediate complex with dinitrogen formed in the process of the reduction (a binuclear MoFe-complex was often proposed).

The discovery of alternative Mo-independent nitrogenases has already questioned the participation of Mo as an essential prerequisite. The catalytic properties and physical characteristics of the M-centers in the nitrogenases are very similar to each other and to the Mo-containing nitrogenase. Therefore, if dinitrogen can be reduced on the Fe center of the FeFe-cofactor, why should the Fe center not function in Mo- and V-nitrogenases?

On the basis of the current knowledge, an answer cannot be provided to this question since the problem of the detailed mechanism and the site of dinitrogen activation and reduction has not been conclusively resolved. However, there is a general agreement that the molecular structure of the cofactor is more suitable for the dinitrogen coordination on the central coordinatively unsaturated Fe atoms than on the coordinately saturated Mo, rather than forming a mononuclear complex with Mo or a binuclear complex involving both Mo and Fe. The role of Mo (or of V in the corresponding V-nitrogenase) might be that of stabilizing the cluster, as is suggested by the shortening of the Fe- Fe distance at

the side close to Mo. The atom of Mo in the tetravalent state (d^2), decreases the number of electrons in the cluster without causing a serious change of its reducing ability. One might suggest that in an Fe-only containing cluster the larger number of electrons (if all the Fe atoms are in the +2 oxidation state there are four electrons more) is a destabilizing factor, perhaps via population of antibonding molecular orbitals. Therefore, there seem to be more similarities between Mo- and V-nitrogenases (presumably V is in the V(III) state with the same number of electrons) than between these nitrogenases and the Fe-only nitrogenase. The difference between Mo- and V-nitrogenases is due to somewhat different reducing properties: the reduced VFe-cofactor is probably a reductant stronger than its Mo analog, and, therefore, a small amount of hydrazine is formed in parallel with ammonia in the case of V-nitrogenase; in the case of Mo-containing enzyme, hydrazine is observed only upon the addition of acid or alkali [14], when there is proton or OH coaction. The final product is ammonia only at neutral pH.

If dinitrogen activation does occur at the central Fe atoms then the intermediate complex might involve four Fe atoms, and a diagonal arrangement of dinitrogen may be suggested: it will be then coordinated side-on to two Fe atoms and end-on to the other two (Figure 5). Other possibilities for dinitrogen coordinating to the cofactor have been proposed from X-ray structural data [15,16], including N_2 coordination with one and two Fe atoms. They are not necessarily alternatives for a single step of dinitrogen activation on the cofactor, since the

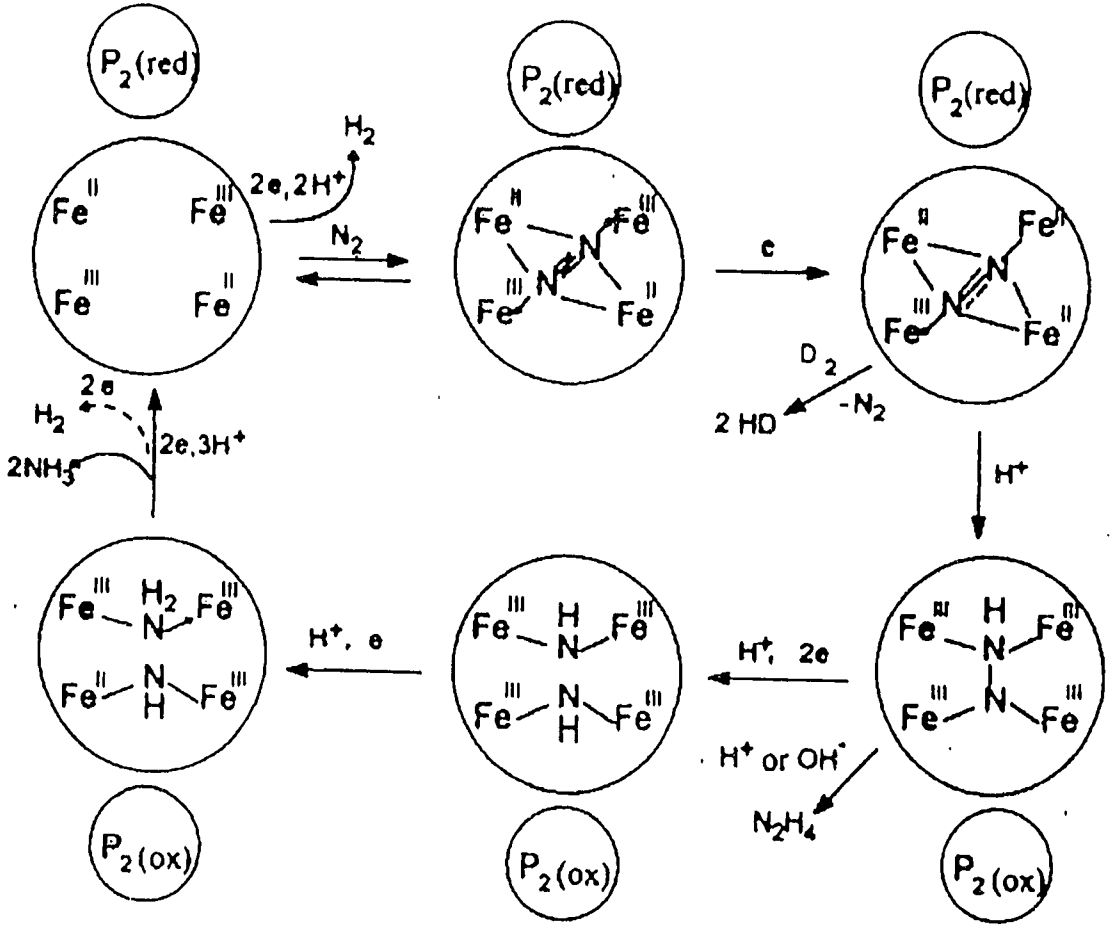
P2(red)
P2(red)
P2(red)
H2
2e,2H+
N2
e
D2
2 HD
-N2
H+
2e
H2
2e,3H+
2NH3
H+, e
H+, 2e
H+ or OH-
N2H4
P2(ox)
P2(ox)
P2(ox)

Figure 5

number of contacts may increase with time if the coordination is actually a multistep process, e.g. N_2 might start to coordinate first to one Fe atom and then include other atoms of the reaction center. The diagonal four coordinated N_2 for activation is preferred because both end-on and side-on binuclear dinitrogen complexes are known. There are few examples of trinuclear complexes, and some indirect evidence indicates the existence of tetranuclear ones (vide infra). Four contacts will strongly activate dinitrogen and facilitate the subsequent formation of a hydrazine derivative. At the same time, the involvement of all six central Fe atoms of the cofactor in the activation suggested by Kim and Rees [10] seem less probable: firstly, the Fe-N distances inside the Fe_6 trigonal prism are too short [16]; secondly there are some evidence that a hydrazine derivative is formed as an intermediate in enzymatic N_2 reduction, and even some free N_2H_2 is produced in parallel with NH_3 on V-nitrogenase. The involvement of six atoms would probably have produced only ammonia. However the remaining two Fe atoms may take part in the process in the later stages e.g. in cleavage of the N-N bond.

Since the X-ray structure of nitrogenase gives very strong support to the hypothesis that the mechanism of dinitrogen activation on the enzyme involves Fe atoms of the FeMo-cofactor, more attention was paid to Fe complexes coordinating and reducing dinitrogen. An Fe catalyst for the conventional ammonia synthesis from dinitrogen involves a polynuclear Fe cluster. Although the catalytic cycle requires high temperature, dihydrogen can be used as a

reducing agent in spite of being the weakest reducing agents among those reacting with dinitrogen. There is no doubt that dinitrogen is activated in a side-on fashion and the structure of a surface dinitrogen complex forming a bridge between two Fe atoms has been proposed [17]. From what is known about nitrogen fixing systems, the conventional catalyst for ammonia synthesis still seems to be the closest analog of the nitrogenase active center, at least as far as the nature of metal atoms involved in dinitrogen activation and reduction is concerned.

Fe complexes are known to reduce dinitrogen in aprotic media. They reduce dinitrogen to nitrides with moderate yields in the presence of reducing agents such as RMgX and with almost 100% yield with lithium naphthalene. Fe(0), formed in the LiAr reduction of $FeCl_3$, activates dinitrogen and reduces it upon protonation. The structures of Fe complexes active towards N_2 were elucidated [18]. Dinitrogen Fe complexes have been known for many years since Sacco and Aresta published their paper [19] on mononuclear dinitrogen iron(II) hydride phosphine complexes. These and many similar complexes were found to be inactive in N_2 protonation and reduction, but later conditions were found to protonate a dinitrogen Fe(0) phosphine complex with at least partial reduction to ammonia [20]. The tetraphenyliron complex $[FePh_4][Li(OEt_2)]_4$ is also active towards N_2 producing a complex which yields N_2H_4, NH_3 and N_2 upon protonation [21]. Another Fe complex that may be considered analogous with the FeMo-cofactor of nitrogenase is formed in the reaction of tetraphenyliron(II) dihydride in

tetrahydrofuran [22] . A binuclear Fe(II) complex is formed which includes three μ_2-H and three μ_2-Li bridges; the Fe-Fe distance in the complex (2.4 Å) is very close to that in Fe metal and in the Fe Mo-cofactor.

Dinitrogen is coordinated by the complex ($\nu(N_2)$ = 1660 cm^{-1}) and is weakly bound. Spontaneous release of N_2 is observed during the crystallization process. At the same time, dinitrogen can be reduced and upon protonation, produces hydrazine. It is interesting to observe that the electrons to produce N_2H_4 are taken from Fe (and not from LiPh ligand as in the case of a similar nickel complex) since the amount of hydrazine formed corresponds to the Fe(II), Fe(III) transformation.

Since it became known that FeS clusters are involved in nitrogenase, many Fe-S complexes have been synthesized in attempts to prepare models for the active center of the enzyme. Entry to the field of synthetic analogs of Fe-S protein sites was afforded by the discovery in 1972 that the reaction system $FeCl_3$/NaHS/3$NaSCH_2Ph$ in methanol yielded the cluster $[Fe_4S_4(SCH2Ph)_4]^{2-}$, which was readily isolated and purified as its Et_4N^+ salt. Very soon thereafter the procedure was shown to be general for a variety of thiolate salts NaSR [23], producing many of the existing $[Fe_4S_4(SR)_4]^{2-}$ clusters. The proposed reaction scheme consisted of the formation of a polymeric Fe(III) thiolate in the reaction:

$$4FeCl_3 + 12RS^- \longrightarrow 4Fe(SR)_3 + 12Cl^-$$

followed by cluster formation:

$$4Fe(SR)_3 + 4HS^- + 4MeO^- \longrightarrow [Fe_4S_4(SR)_4]^{2-} + RSSR + 6RS^- + 4MeOH$$

The overall process has the limiting stoichiometry of the following reaction:

$$4FeCl_3 + 4HS^- + 6RS^- + 4MeO^- \longrightarrow [Fe_4S_4(SR)_4]^{2-} + RSSR + 12Cl^- + 4MeOH$$

The method remained unchanged until it was shown in 1979 [24] that elemental sulfur in the presence of sufficient amount of thiolate reductant could be substituted for sulfide, as shown in these reactions:

$$4FeCl_3 + 14RS^- + 4S \longrightarrow [Fe_4S_4(SR)_4]^{2-} + 5RSSR + 12Cl^-$$

$$4FeCl_2 + 10RS^- + 4S \longrightarrow [Fe_4S_4(SR)_4]^{2-} + 3RSSR + 8Cl^-$$

Both preparative methods were extended to $[Fe_4S_4(SR)_4]^{2-}$ clusters [25]. While it has been clear for some time that cluster formation is thermodynamically controlled, the nature of the thermodynamic product could not have been uniquely predicted. This situation is indigenous to most initial cluster syntheses and, in the present case, the term "spontaneous self-assembly" has been applied as a reminder of the thermodynamic origin of cluster formation. The presence of trinuclear cluster,

whose cuboidal structure has been widely verified by protein crystallography [26-28], had not yet yielded to synthesis in stable isolable form [29]. The finding that unfolding of inactive oxidised aconitase causes isomerization of the $[Fe_3S_4]^+$cluster core to linear $[Fe_3(\mu_2\text{-}S_4)]^+$ [30], which has otherwise been isolated in the form of the stable clusters $[Fe_3S_4(SR)_4]^{3-}$ [31], implies that the cuboidal geometry is probably sustained by protein structure. However, Fe_3S_4 has been obtained as a constituent of many heterometal MFe_3S_4 cubane type cores [32]. However the activity of the tetranuclear and trinuclear cubane clusters towards dinitrogen remains unknown. In an recent attempt to mimic the M cluster of nitrogenase, Coucouvanis [33] studied the reaction of $(Et_4N)_2[(Cl_4\text{-cat})(CH_3NH_2)\ MoFe_3S_4Cl_3]$ with cis-1,2-dimethyldiazene in acetonitrile. The reduction products were expected to be ammonia and methane but once the experiments were carried out methylamine was found to be the major product. Other data indicated that the substrate was exclusively activated and reduced by the $[MoFe_3S_4]^{3+}$ core, while methylamine was obtained only from reduction of cis-1,2-dimethyldiazene and that the Mo atom is the active site the substrate reduction.

The fact that ammonia was not produced in this type of system is not a surprise, mainly because the substructure of catalyst used, is different from the nitrogenase M cluster, where dinitrogen fixation takes place in the iron cage and not on the Mo centre. Even though ammonia was a major product in this reaction, this is still

far from achieving the ultimate goal, (catalytic dinitrogen fixation) since the substract was methyldiazene, and not N_2.

Nevertheless this experiment shows that at least the cubane cluster possesses a catalytic activity towards N=N system which is a first step in the long quest for dinitrogen fixation by cubane clusters under mild conditions.

References:

1. A. E. Shilov F.Hardey Bottomley and R. C. Burns, *A Treatise on Dinitrogen Fixation,* Wiley, New York, **1979**, p.31.
2. A. D. Allen and C. V. Senoff, *J. Chem. Soc., Chem. Commun.*, **1965,** 621.
3. M. E. Vol'pin and V. B. Shur, New Trends in the Chemistry of Nitrogen Fixation, Academic Press, London, **1980**, p.67.
4. M. E. Vol'pin and V. B. Shur, *J. Organomet. Chem.*, **1980**, 200, 319.
5. A. Ozaki and K. Aika, in R.W.F. Hardy, F. Bottomley and R.C. Burns (eds.), *A Treatise on Dinitrogen Fixation*, Wiley, New York, **1979** p. 169.
6. A. E. Shilov, *New Trends in the Chemistry of Nitrogen Fixation*, Academic Press, London, **1980**, p.130.
7. A. E. Shilov, *J. Molec. Catal.*, **1987,** 41, 221.
8. A. E. Shilov, Perspectives in Catalysis, Blackwell, Boston, **1992**, p.169.
9. M. M. Georgiadis, H. Komiya, P.Chakrabarti, D. Woo, J. J. Kornuc and D. C. Rees, *Science*, **1992,** 257, 1653.
10. M. K. Chann, J. Kim and D. C. Rees, *Science*, **1993,** 260, 792.
11. I. Bertiny, S. Lippard and J. Valentine, *Bioinorganic Chemistry*, Mill Valley, Calif. : University Science Books, **1994.**
12. B. E. Smith and R. R. Eady, *Eur. J. Biochem.*, **1992,** 205, 1.

13. B. E. Smith, P. E. Bishop, P. J. Bottomley and W.E. Newton, *Nitrogen Fixation Research Progress*, **1985,** p.597.

14. R. C. Burns and R. W. F. Hardy, *Methods in Enzymol. B*, **1972,** 24, 480.

15. W. H. Orme-Johnson, *Science*, **1992,** 257, 1639.

16. H. Deng and R. Hoffmann, *Angew. Chem., Int. Ed. Engl.*, **1993,** 1062.

17. C. W. Bauschlicher, G. M. Petterson and P. E. M. Siegbahn, *J. Chem. Phys.* **1987,** 87, 2129.

18. R. A. Forder and K. Prout, *Acta Crystallogr. Sect. B,* **1974,** 30, 3778.

19. M. Aresta, P. Giannocaro, M.Rossi and A. Sacco, *Inorg. Chim. Acta,* **1971,** 5, 115.

20. G. J. Leigh and Jimenez-Tenorio, *J. Am. Chem. Soc.,* **1991,** 113, 5862.

21. T. A. Bazhenova, R. M. Lobkovskaya, A. E. Shilov, A. K. Shilova, M. Gruselle, G. LeNy and B. Tchoubar, *J. Organomet. Chem.,* **1983,** 244, 265.

22. T. A. Bazhenova, L. M. Kachapina, A. E. Shilov, *J. Organomet. Chem.,* **1992,** 428, 107.

23. B. A. Averill, T. Herskovitz, R. H. Holm, J. A. Ibers, *J. Am. Chem. Soc.*, **1973,** 95, 3523.

24. G. Christou, C. D. Garner, *J. Chem. Soc. Dalton Trans.*, **1979,** 1093.

25. G. Christou, B. Ridge, H. N. Rydon, *J. Chem. Soc. Dalton Trans.*, **1978,** 1423.

26. A. H. Robbins, C. D. Stout, *Proteins*, **1989,** 5, 289.

27. C. R. Kissinger, E. T. Adman L. C. Sieker and L. H. Jensen, *J. Am. Chem. Soc.*, **1988,** 110, 8721.

28. C. D. Stout, *J. Mol. Biol.* **1989,** 205, 545.

29. J. P. Weterings, T. A.Kent, R. Prins, *Inorg. Chem.* **1987,** 26, 324.

30. M. C. Kennedy, T. A. Kent, M. Emptage, H. Merkle, H. Beinert, E. Münck, *J. Biol. Chem.* **1984,** 259, 14463.

31. K. S. Hagen, A. D. Watson, R. H. Holm, *J. Am. Chem. Soc.* **1983,** 105, 3905.

32. R. H. Holm, S. Ciurli, *Inorg. Chem.* **1986,** 30, 743.

33. S. M. Malinak, A. M. Simeonov, P. E. Mosier, C.E. Mckenna, D. Coucouvanis *J. Am. Chem. Soc.* **1997**, 119, 1662.

CHAPTER II

The high reactivity of low-valent early transition metals and their strong reducing power is the key to the ability of these species to react with exceptionally stable molecules, such as dinitrogen. Recently, there has been a considerable growth of interest for the synthesis of V(II) complexes to explore its chemistry and in particular the reactivity with N_2. The d^3 electronic configuration of V(II) was regarded as particularly promising since a dinuclear V(II) system potentially has the ability to transfer the 6 electrons necessary for the cleavage of the N-N triple bond. Conversely, the d^2 or d^1 electronic configuration of V(III) and V(IV) respectively may be regarded as promising for the reduction of N_2 and formation of reactive intermediates (nitride, hydrazido, etc...)

The first example of fixation of dinitrogen on vanadium center was observed when $VCl_2(TMEDA)_2$ [1] was reacted with two equivalents of [o-$C_6H_4CH_2N(CH_3)_2$]Li followed by addition of one equivalent of pyridine to give (μ-N_2){[(o-$C_6H_4CH_2N(CH_3)_2$]$_2$V(py)}$(THF)_2$ as product (Figure 1). The reaction initially formed an unidentified intermediate, which upon treatment with pyridine reacted with dinitrogen to form the final complex. The magnetic moment (μ_{eff}= 3.47μ_B) is slightly lower than expected for a d^3 electronic configuration, thus indicating that only a minimal reduction of dinitrogen occurred. Nevertheless, the

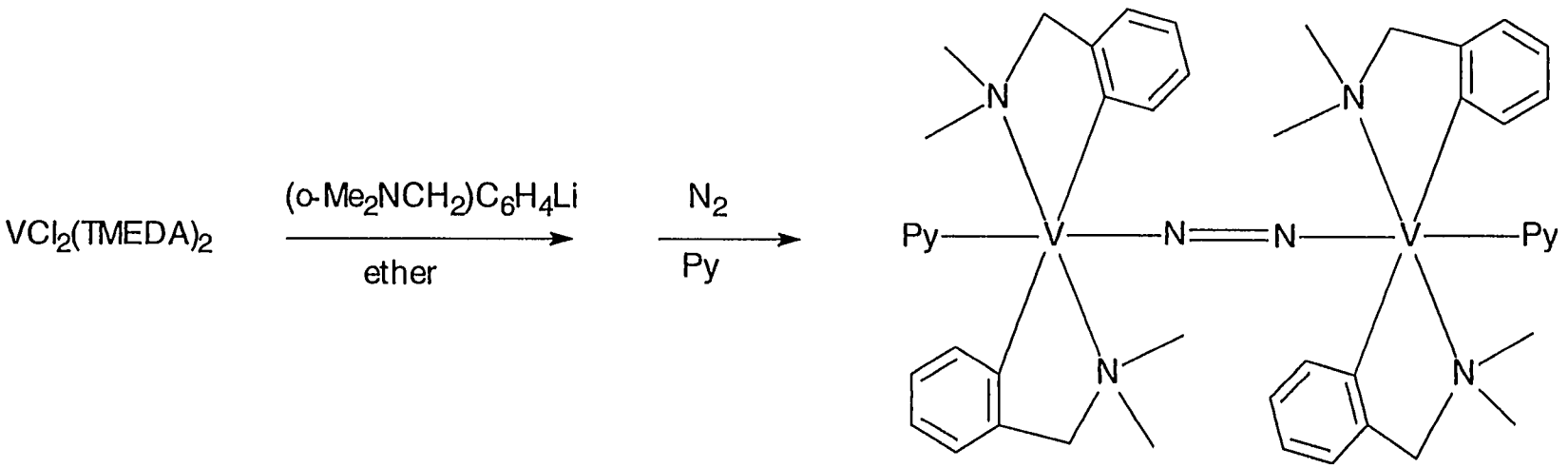

Figure 1

coordination of dinitrogen appears to be rather robust, since exposure to vacuum did not remove nitrogen. However, simple treatment with Lewis bases such as CO, alkynes or pyridine, released N_2 to form a monomeric vanadium(II) complexes. In the case of pyridine the mononuclear $[o\text{-}C_6H_4CH_2N(CH_3)_2]_2V(py)_2$ was isolated and fully characterized.

It is well known that the formation and the structures of dinitrogen complexes are very sensitive to the nature of the ligands. Among the ligands successfully used for the stabilization of dinitrogen complexes with other metals were organophosphines [2], alkyls/aryls and cyclopentadienyl groups. In contrast to the catalytic transformation of N_2 promoted by in situ generated V(II) hydroxide, there is no report of dinitrogen complex of V(II) or V(III) using Cp or Cp* as the supporting ligand. Even in the case of titanium, another versatile substrate for dinitrogen activation, most of the complexes were characterized on the basis of microanalytical data. Since the isolation of the first dinitrogen complex on titanium, a few dinitrogen complexes having titanium in different oxidation states with different bonding modes (Figure 2) of dinitrogen have been isolated and reported.

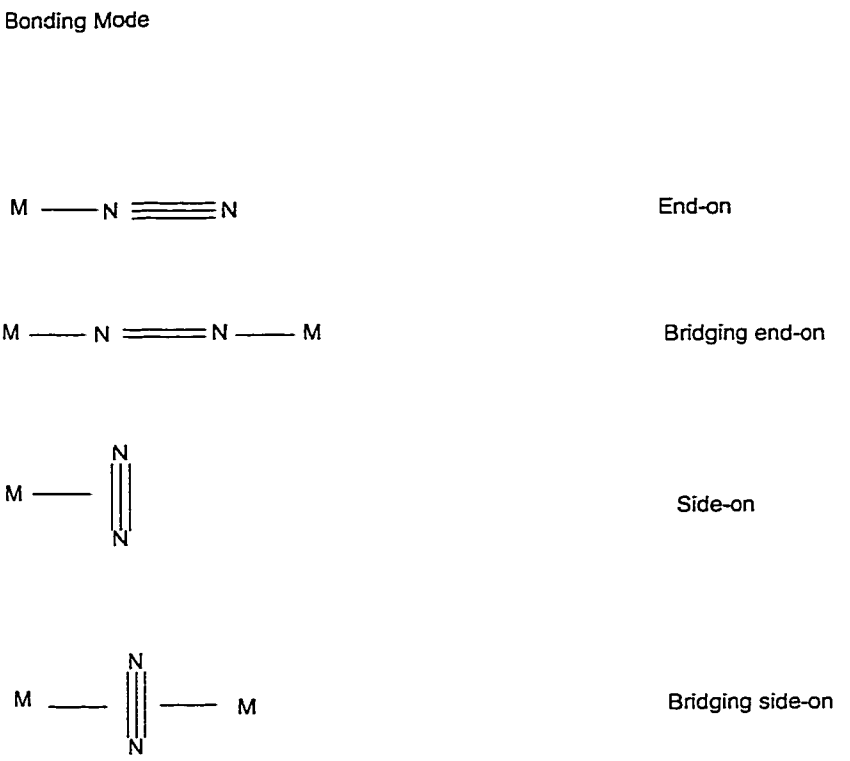

Figure 2

Transition metal alkyl/aryl complexes constitute a very important class of compounds because of the pivotal role played by these species in both synthesis and catalysis [3]. In the case of vanadium in +2 and +3 oxidation states, the carbon - donor based ligands have promoted the coordination of dinitrogen. The very first vanadium dinitrogen complex [4] was isolated and characterized only in 1989 (Figure1) as mentioned above. The formation of this complex proved the high reactivity of divalent vanadium towards dinitrogen. Following this, two organometallic dinitrogen complexes of V(II) [4] and V(III) [5] were obtained (Figure 3). The reduction of $V(mes)_3(THF)$ [mes = 2,4,6-$Me_3C_6H_2$] by sodium metal in the presence of nitrogen in diglyme, produces the dinuclear complex (μ-

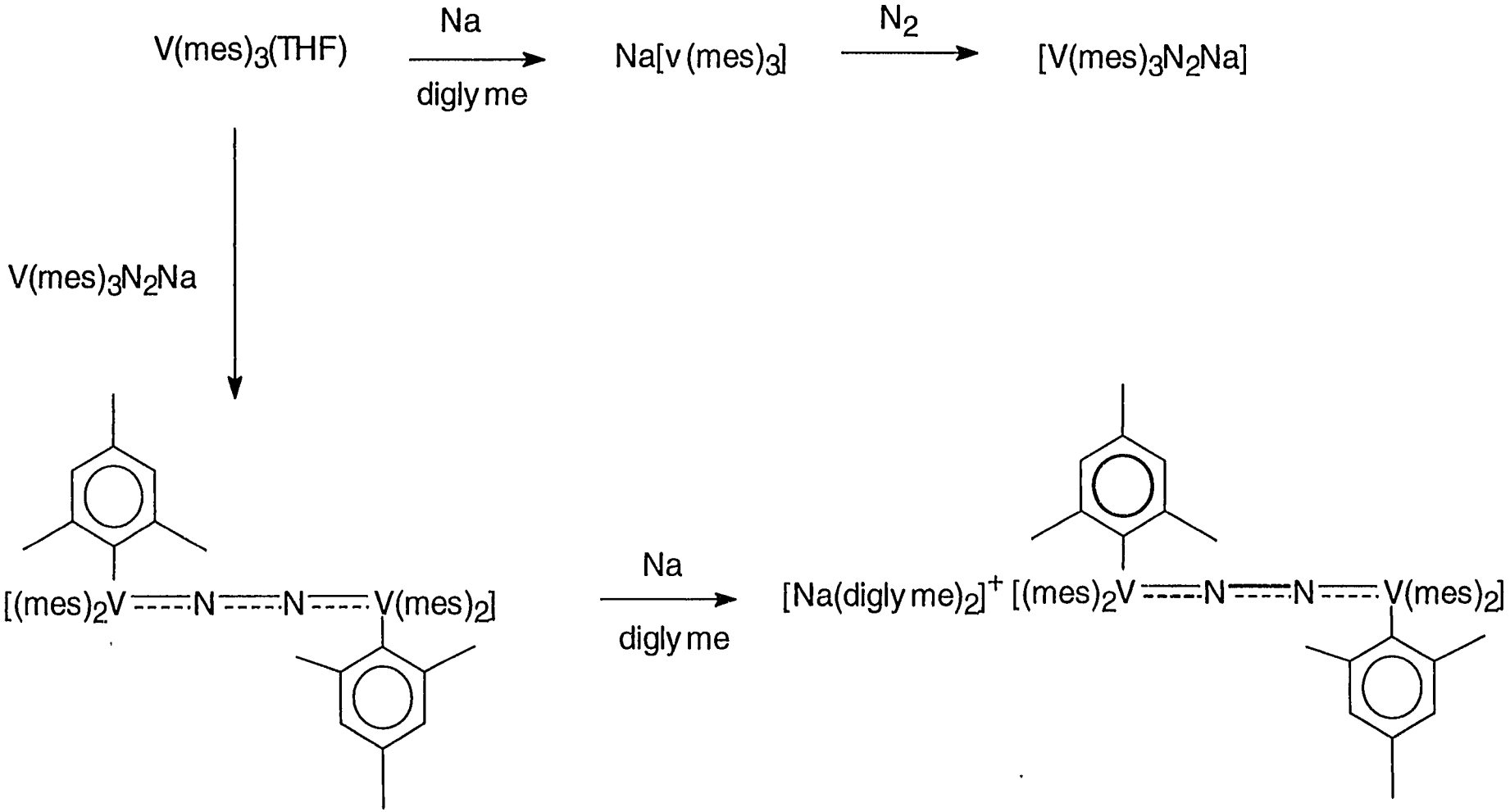
V(mes)3(THF)
Na
diglyme
Na[v(mes)3]
N2
[V(mes)3N2Na]
V(mes)3N2Na
[(mes)2V N N V(mes)2]
Na
diglyme
[Na(diglyme)2]+ [(mes)2V N N V(mes)2]

Figure 4

$N_2)N[(mes)_2Me_3C_6H_2]^-[Na(diglyme)_2]^+$ (Figure 4) [6]

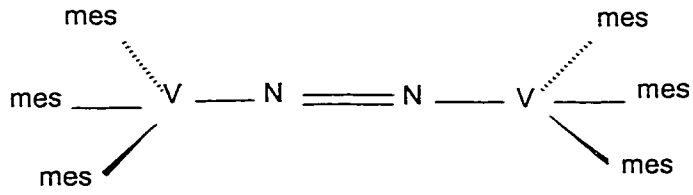

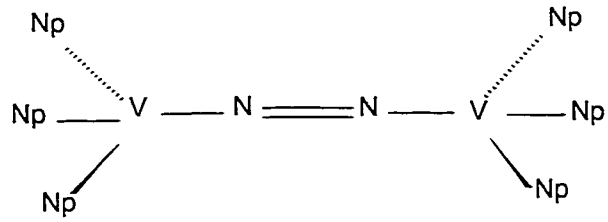

Figure 3

The V-N distance of 1.763(15) Å is very short and suggests multiple bond character, while the N-N bond length of 1.280(21) Å is longer than the bond distance in the free dinitrogen molecule (1.098 Å). These two bond distances suggest that dinitrogen was reduced to some extent in this species. The magnetic moment of 1.69 μ_B per metal center is significantly lower than expected for a d^3-d^3 system. The lowering of the magnetic moment can either be a consequence of a strong electronic coupling of the two vanadium atoms through the dinitrogen bridge, or may reflect a change in the oxidation state of the metal atom. The coordination of dinitrogen to V(III) is quite interesting due to the occurrence of

this oxidation state in some metalloenzymes. In addition, the studies on V-nitrogenases predict the involvement of medium-valent vanadium as the active species responsible for the activation of dinitrogen in biological systems. Although di- and tri-valent vanadium organometallic complexes have been proved to be able to interact with dinitrogen, yet the reversibility of dinitrogen coordination, the high reactivity and thermal unstability render these complexes unsuitable for further activation studies.

Alkoxides / Aryloxides:

Interest in the chemistry of low- and medium-valent transition metal alkoxides has been steadily increasing in recent years [7]. Ligands with oxygen based donors atom seem to be the most promising for the vanadium and titanium promoted activation of dinitrogen. Other interesting characteristics of these ligands are: (i) the electronic configuration of the oxygen donor atom which allows different molecular complexity by adopting different bonding modes, (ii) the unlimited choice of organic substituents which allows to adjust the steric hindrance, (iii) the possibility of introducing optical activity by using optically active alkoxides / aryloxides. The interest in V(III) aryloxides was mainly stimulated due to the similarity with the $V(OH)_2$ system which is able to perform catalytic reduction of N_2. However the only two anionic V(II) aryloxides [8]

reported in the literature, were found to be unreactive with N_2. Even ligand replacement on preformed N_2 complexes by alkoxide systematically released N_2 thus indicating a scarce ability of this particular ligand system to support this type of reactivity.

Macrocyclic Ligands:

The employment of a macrocyclic ligand and nitrogen-donor based ligands enhanced the ability of vanadium to interact with dinitrogen. The reaction of $VCl_2(TMEDA)_2$ with the tetralithium salt of octaethylporphyrinogen (OEPG) under nitrogen, yielded the paramagnetic (μ_{eff}=2.85μ_B per dimer) nitrido-bridged dinuclear complex [{(OEPG)V}2(μ-N)(μ-Li)$_4$][Li(TMEDA)$_2$] (Figure 5) [9]. The structure is formed by two parallel planar V(OEPG) units linked by a nitride function. The magnetic moment lower than expected for a d^2 electronic configuration, can be explained by the presence of a magnetic coupling between the two vanadium centers. The formation of the nitrido-bridged complex arises from a complicated series of reactions. The first complex formed from the reaction between $(OEPG)Li_4$ and $VCl_2(TMEDA)_2$ is the divalent vanadium species $[(OEPG)VLi_4Cl_2(THF)_4]$. In an attempt to remove LiCl the complex was treated with excess of TMEDA. The reaction gave $[(OEPG)V(THF)_4][Li(TMEDA)_2]$ which was isolated and characterized. The formation of this species was

accompanied by formation of a nitrido-bridged complex. This species probably arises from the cleavage of dinitrogen by the low-valent OEPG-vanadium complex [(OEPG)$Vli_4Cl_2(THF)_4$].

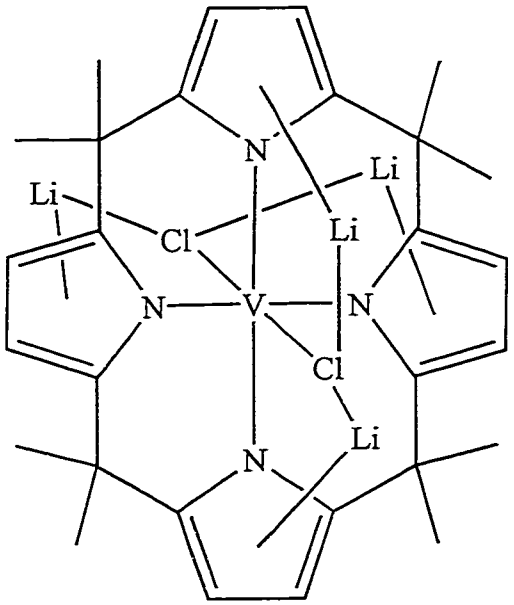

Figure 5

Amides:

The employment of ligands with nitrogen based donor atoms for the preparation of low- and medium- valent titanium and vanadium complexes was advised by some unique characteristics of these ligands. (i) The overlap of nitrogen lone pair with an appropriate empty *d* orbital of the metal atom, may give partial π-bond character to the M-N bond [10] and introduce some electronic flexibility. (ii) The ability to act as a bridging ligand between two or more metal

centers may promote formation of polynuclear species. The electron deficiency of the early transition metal atoms and the consequent tendency to achieve a partial saturation (Figure 6) by sharing the amido ligands may be regarded as the driving force behind this behavior. (iii) The steric bulk may be considerably varied by selecting the appropriate organic substituents on the nitrogen atom. (iv) The strong reducing power stabilizes a wide range of oxidation states.

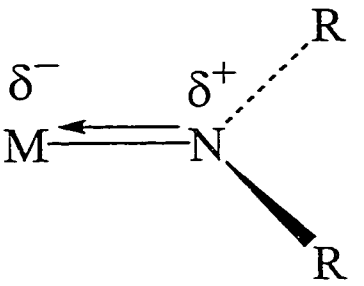

Figure 6

The chemistry of amido vanadium complexes is poorly developed. Early studies [11] mainly focused on the synthesis of amido vanadium(IV) complexes. In 1957 the synthesis of what was formulated as $VCl_2N(Me_2)_2$ was achieved [12] from VCl_4 and gaseous $HNMe_2$. Even though the nature of the final product was never conclusively demonstrated, this methodology can be extended to other primary amines [13]. Substitution of more than two chlorides is commonly achieved by using the amide lithium salt [14]. The majority of vanadium amide derivatives characterized so far was prepared by using the salt method [15], or by reduction of amido vanadium(IV) compounds [16].

As discussed earlier, the reduction of N_2 to form two nitride moieties requires six electrons. Therefore, the dinitrogen complex of a dinuclear d^3 V(II) moiety should be the ideal system, since each of the two d^3 V(II) atoms can easily undergo a 3 electron reduction to d^0 V(V) centers. This was recently observed in the case of a d^3 Mo(III) complex, which upon reaction with N_2 gave preliminary formation of an end-on dinitrogen complex which further evolved into a terminal Mo-N species [17]. The formation of a dinuclear end-on dinitrogen complex by reaction of $Mo(NRAr)_3$ complex with N_2 was followed by N-N cleavage and subsequent formation of a nitrido complex $NMO(NRAr)_3$ [R = $C(CD_3)_2CH_3$, Ar = 3,5-$C_6H_3Me_2$] (Figure 7).

This observation encouraged further attempts to synthesize low- or medium valent amides of vanadium, which, however, displayed a remarkably different behavior. For example, the reaction of trans-$VCl_2(TMEDA)_2$ with Cy_2NLi, prepared *in situ* from Cy_2NH and n-BuLi in THF, formed an unprecedented complex $[(Cy_2N)_2V]_2Li(\mu_3\text{-}O)(\mu_2,\eta_1\text{:}\ \eta_1\text{-}CMe)$ (Figure 8). The μ_3-O and $\mu_2,\eta_1\text{:}\ \eta_1$-CMe moieties are probably obtained *via* fragmentation of the THF solvent. Treatment of $VCl_2(TMEDA)_2$ with Ph_2NNa in THF gave the olive green ionic complex $[V_3C1_5(TMEDA)_3][V(NPh_2)_4]$. The cationic unit is composed by a triangular cluster of trivanadium with three bridging chlorine coplanar with theV_3 unit and the other two symmetrically placed above and below the molecular plane. The mononuclear anionic unit features a vanadium atom

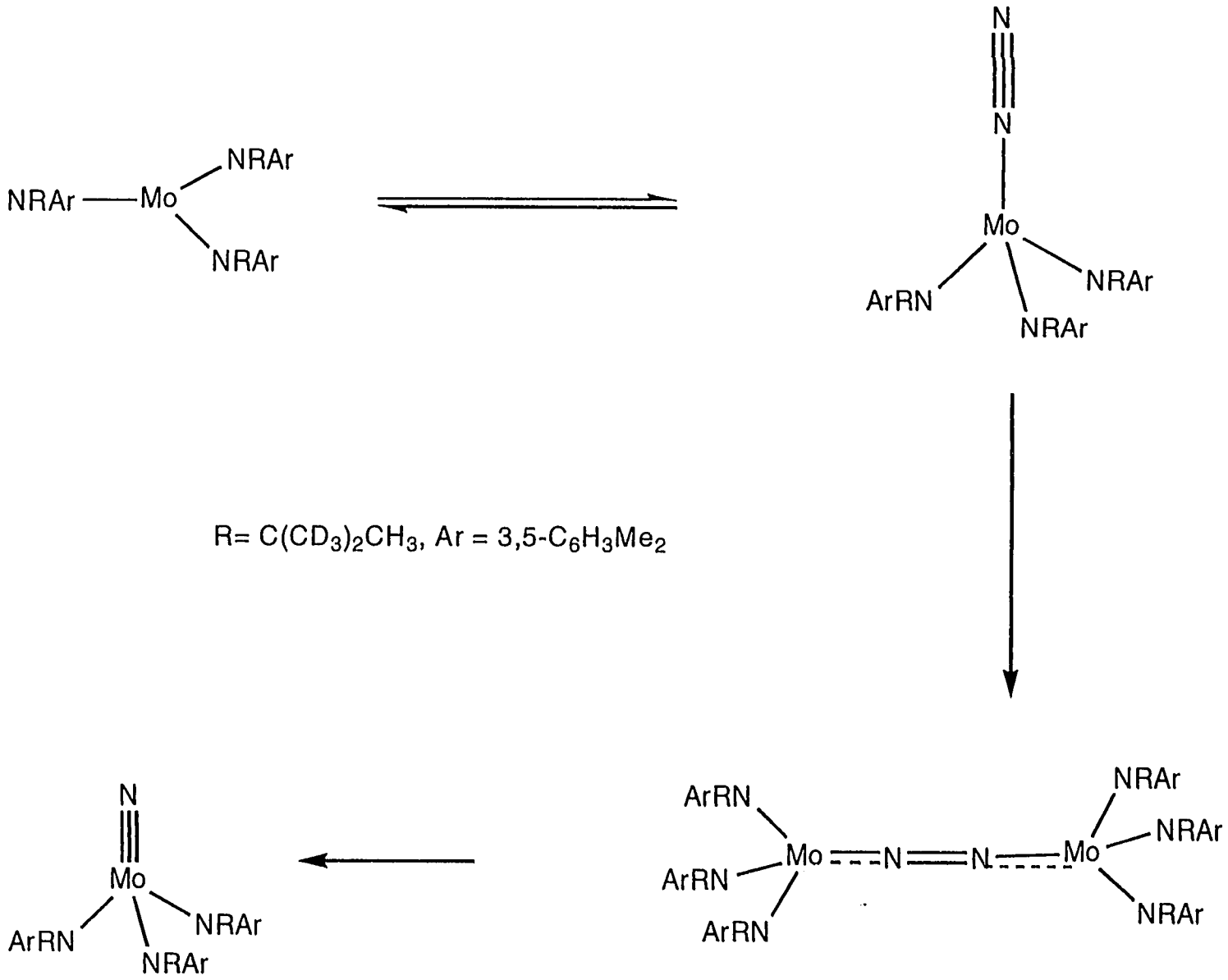
NRAr
NRAr
Mo
NRAr
N
N
Mo
ArRN
NRAr
NRAr
R= C(CD3)2CH3, Ar = 3,5-C6H3Me2
ArRN
ArRN
ArRN
Mo
N
N
Mo
NRAr
NRAr
NRAr
N
Mo
ArRN
NRAr
NRAr

Figure 7

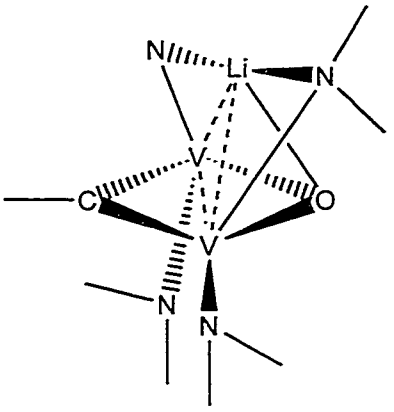

Figure 8

placed in the center of a tetrahedron bound by four nitrogen atoms of four amido ligands. Attempts to form amidinate V(II) derivatives yielded either multiple V-V bonded complexes or extremely labile N_2 end-on complex depending on the nature of the amidinate substituents.

Rather unexpected results were obtained from the reaction of V(III) dinitrogen complexes with amides as supporting ligands. Similar to the case of closely related d^2 titanium systems it was possible to isolate very robust dinitrogen complexes. Reaction of $VCl_3(THF)_3$ with $(i\text{-}Pr)_2NLi$ provided end-on bonded dinitrogen complex $([(i\text{-}Pr)_2N]_3V\}_2(N_2)$ [18] whose cyclic voltammograms did not show reduction or oxidation in a wide range of potentials (Figure 9). In addition these complexes were unreactive towards several reagents (PR_3, py, C), RNC, RCN, azide, diazo). This observation contrasts with the nature of the dinitrogen organometallic complexes of vanadium in the +2 and +3 oxidation states where dinitrogen is always liberated upon treatment with Lewis base. This result

suggests that the d^2 electronic configuration, in combination with N-donor based ligands, can provide exceptionally stable dinitrogen complexes.

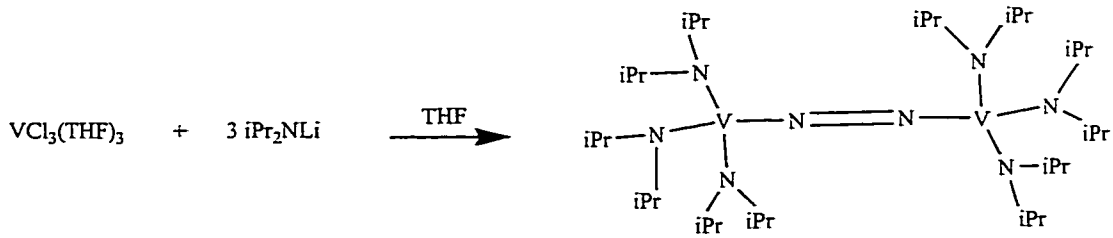

Figure 9

The reaction of $VCl_3(THF)_3$ with LDA gave a surprisingly different result when 1:6 molar ratio was used, thus giving some insight into possible reaction pathways alternative to N_2 activation process. Rather than giving the dinitrogen complex, a dimeric $\{[(i\text{-}Pr)_2N_2V[\mu\text{ - }CH_2C(=CH_2)N(i\text{-}Pr)]Li\}_2$ [19] was formed. The metallacycle was originated by one amido group which chelates the vanadium atom by using both the nitrogen and one deprotonated methyl group, thus forming a four-membered vanadacyclobutane ring (Figure 10). The second carbon atom and the methylene carbon of same isopropyl group engaged in the formation of metallacycle have also been dehydrogenated to form an exocyclic $C=CH_2$ double bond.

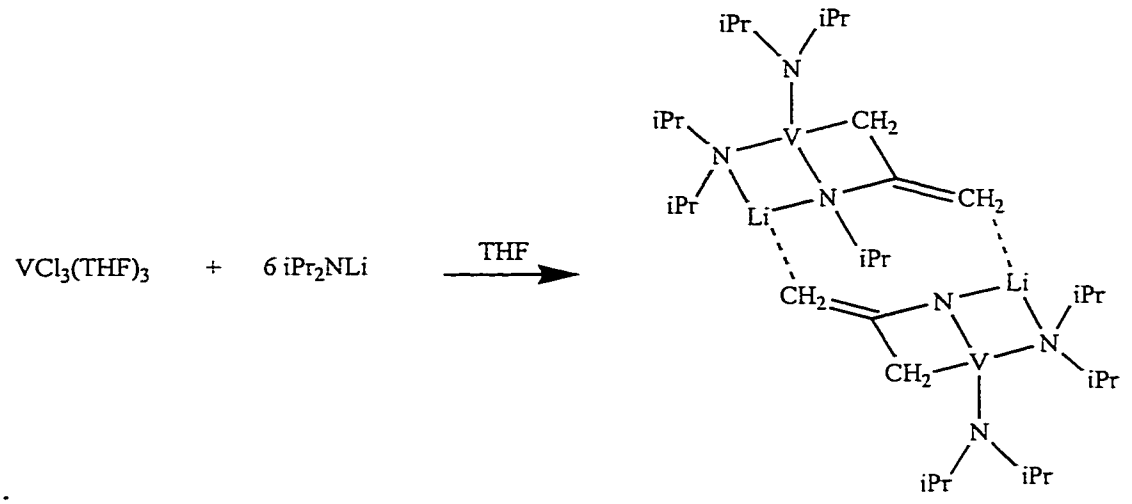

Figure 10

These observations showed that organic amides are able to transfer H_2 from the alkylamide to a substrate and to form in the process metallacyclobutane rings and olefinic functions. Even though the fate of the hydrogen atoms was not elucidated in this case, the possibility that H_2 might be transferred directly from the ligand side chain to several substrates opens interesting perspectives in terms of dinitrogen reduction. Formation of metallocycle occurred also in the reaction of $VCl_3(THF)_3$ with 2 equivalents of $LiN(SiMe_3)_2$ in THF which gave the monomeric $[(SiMe_3)_2N]_2VCl(THF)$. Instead of forming the corresponding homoleptic derivative, addition of a third equivalent of $LiN(SiMe_3)_2$ formed the dimeric $\{[(MeSi)_2N]V[\mu\text{-}CH_2SiMe_2N(SiMe_3)]\}_2$ (Figure 11) via C-H bond metathesis of one methyl group [19]. This dimer can be cleaved by Py or PMe_3 forming very reactive $\{[(MeSi)_2N]V[CH_2SiMe_2N(SiMe_3)]L$ [20] (L = Py or PMe_3) where the vanadaazacyclobutane ring was preserved.

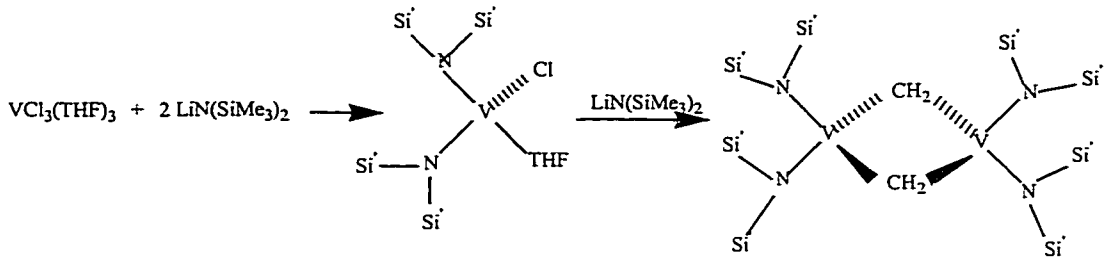

Figure 11

In the case of the phosphine derivative, the V-C bond can be hydrolyzed under pressure and at room temperature forming an unusual mixed valence ionic complex [21] $\{[(PMe)_3V]_2\ (\mu\text{-}H)_3)^+/\{([(Me_3Si)_2N]_2V)_2(\mu\text{-}N_2)\}^-$. The presence of hydrides was supported by the formation of three equivalents of H_2 during a degradation experiment with seven equivalents of HCl. The two nitrides were identified by the formation of NH_3 during hydrolysis.

On the basis of this literature survey it seems rather legitimate to conclude that anionic organic amides are the most promising ligand system of the vanadium-promoted activation of N_2

Scope of the thesis

The scope of this thesis was to study the synthesis, characterization and reactivity of novel low- and medium valent vanadium complexes. The long term goal of this research was to find a new and easier synthetic route for the vanadium-sulfur cubane clusters, to verify their reactivity towards N_2 and to understand the steps through which dinitrogen is reduced to ammonia or hydrazine. The aim was to carry out a preliminary exploratory work to test a few synthetic strategies. For this purpose sulfur and nitrogen donor–based compounds were used as ligand systems.

We also carried out molecular orbital calculation on the compounds obtained during this work, and on other related systems. Several levels of theory were used in order to evaluate the magnetic and chemical properties of the newly prepared compounds and correlate these results with the V-S cubane clusters.

Results and discussion

As mentioned above, dinitrogen reduction in synthetic systems requires strong reducing agents such as RLi in aprotic media and OH or Na/Hg in protic media. By contrast, biological dinitrogen fixation does not require such harsh reducing agents, but uses ferrodoxin as an electron source, since FeMo-cofactor is a very well organised molecular system. Therefore in order to find milder

conditions for reduction, more sophisticated fixing agents must be developed. The system should possess the following characteristics:

1- a structure as similar as possible to the M cluster of nitrogenase,

2- the metal used should be an element belonging to the first row transition series i.e. vanadium, iron, ..., in medium oxidation state

3- oxidation-reduction voltage barrier must be small,

4- resistance to water or other protic solvents.

Since the cuboid Fe_4S_4 clusters available in literature do not react with dinitrogen, it will be tempting to try to synthesize cubane clusters with other metallic elements such as vanadium in the +3 oxidation state which, conversely, have been proven versatile for this purpose. As a matter of fact several V_4S_4 cluster were built but the synthesis involved several steps, unusual starting material and suffered from relatively low yield. In 1982 T.B. Rauchfuss [22] prepared $[CpV]_2(\mu_3\text{-}S)\ \eta^2\text{:}\mu S_2^{2-}$ using $CpV(CO)_4$ [23] as a starting material. The final cuboid structure was obtained by abstracting a sulfur atom by tributylphospine to yield $[CpV]_2(\mu_2\text{-}S)\ \eta^2\text{:}\mu S_2^{2-}$ [24] . Subsequent addition of two more equivalents of PBu_3 yielded the vanadium cubane sulfur cluster [25]. Unfortunately this complex proved to be generally stable and unreactive towards N_2.

Our ultimate target was to build alternate and more reactive V_4S_4 cuboid structures supported by anionic organic amides which may act as a reduction catalyst for dinitrogen activation. As a possible synthetic strategy towards the preparation of cuboidal cluster, we decided to preliminarily test the reactivity of low valent vanadium complexes with S_8. In this chapter we describe the results of our attempts to prepare a (amide)V=S compound, possibly tetrameric with a cuboid V_4S_4 core.

The ligands used in the experiments were selected in the view of the special requirement of dinitrogen fixation. Alkoxides and aryloxides were dismissed, since these ligands lead to the formation of complexes incapable of fixing free dinitrogen [9]. Conversely, nitrogen donor based ligands have shown a marked tendency to stabilize dinitrogen complexes. The denticity may be another important factor. One might think that choosing monodentate amides might provide the simplest solution to start with. However, monodentate amides are very dynamic. They may be occasionally unstable and sometimes lead to complicated reactions which might include disproportionation pathways. At the opposite extreme, tridentate ligands are stable and occupy three coordination sites, not to mention the steric hindrance factor which prevent ligand scrambling. Given this rationale, tridentate ligands complexes were chosen as models at this preliminary stage of research to explore the chemistry of vanadium with elemental sulfur.

As summarized in Figure 12, reaction of $VCl_3(THF)_3$ with one equivalent of $[(TMS)NLiCH_2CH_2]_2NTMS$, led to the formation of the corresponding $\{[(TMS)NCH_2CH_2]_2N(TMS)\}_2V_2(\mu\text{-}Cl)_2$ **(4)** which was isolated in good yield as a crystalline complex. The magnetic moment of **4** was determined with a Gouy balance at room temperature, which indicated a value in agreement with the d^2 electronic configuration expected for V(III). The molecular structure was elucidated by an X-ray diffraction analysis (Figure 12-a). The dimer consists of a distorted trigonal bipyramidal vanadium atom [N2-V1-N3=82.73°, N1-V1-N2=83.98°, N3-V1-Cl1=98.37°, N1-V1-N3=117.44°, N1-V1-Cl1a=114.80°, N3-V1-Cl1a=126.52°] surrounded by a tridentate ligand. The V-N distances are rather short [V1-N1=1.910(6) Å, V1-N3=1.909(6) Å] and suggest the presence of a significant extent of π-donation. The value of the magnetic moment as well as the V-V distance [V-V=3.631(5) Å] indicate the absence of significant metal-metal interaction. Unlike vanadium complexes of monodentate silazanates, which decompose spontaneously upon heating to yield a $[N(TMS)SiCH_2]V$ metalocycle, complex **4** was found to be thermally stable in coordinating and non-coordinating solvents.

Reaction of **4** with sulfur under nitrogen atmosphere gave a brown amorphous powder **(6)** and all attempts to isolate crystalline solid failed. Nevertheless the complex is diamagnetic and the ^1H NMR spectrum clearly shows the silazanate ligand peak as a singlet at 0.51 (s 3H TMS). Elemental analysis data

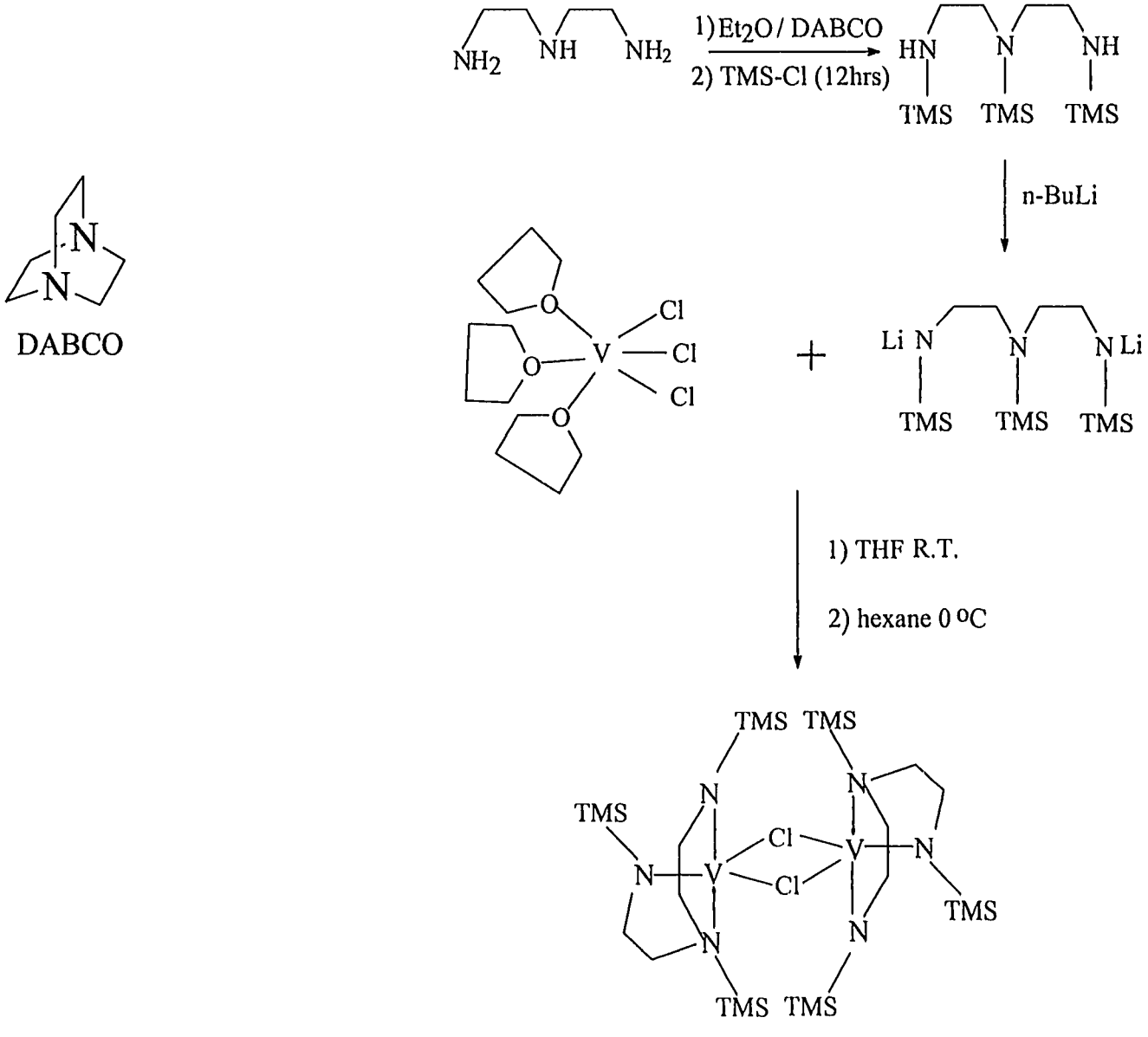
DABCO
1) Et2O / DABCO
2) TMS-Cl (12hrs)
n-BuLi
1) THF R.T.
2) hexane 0 °C
TMS
Cl
V
N
O

Figure 12

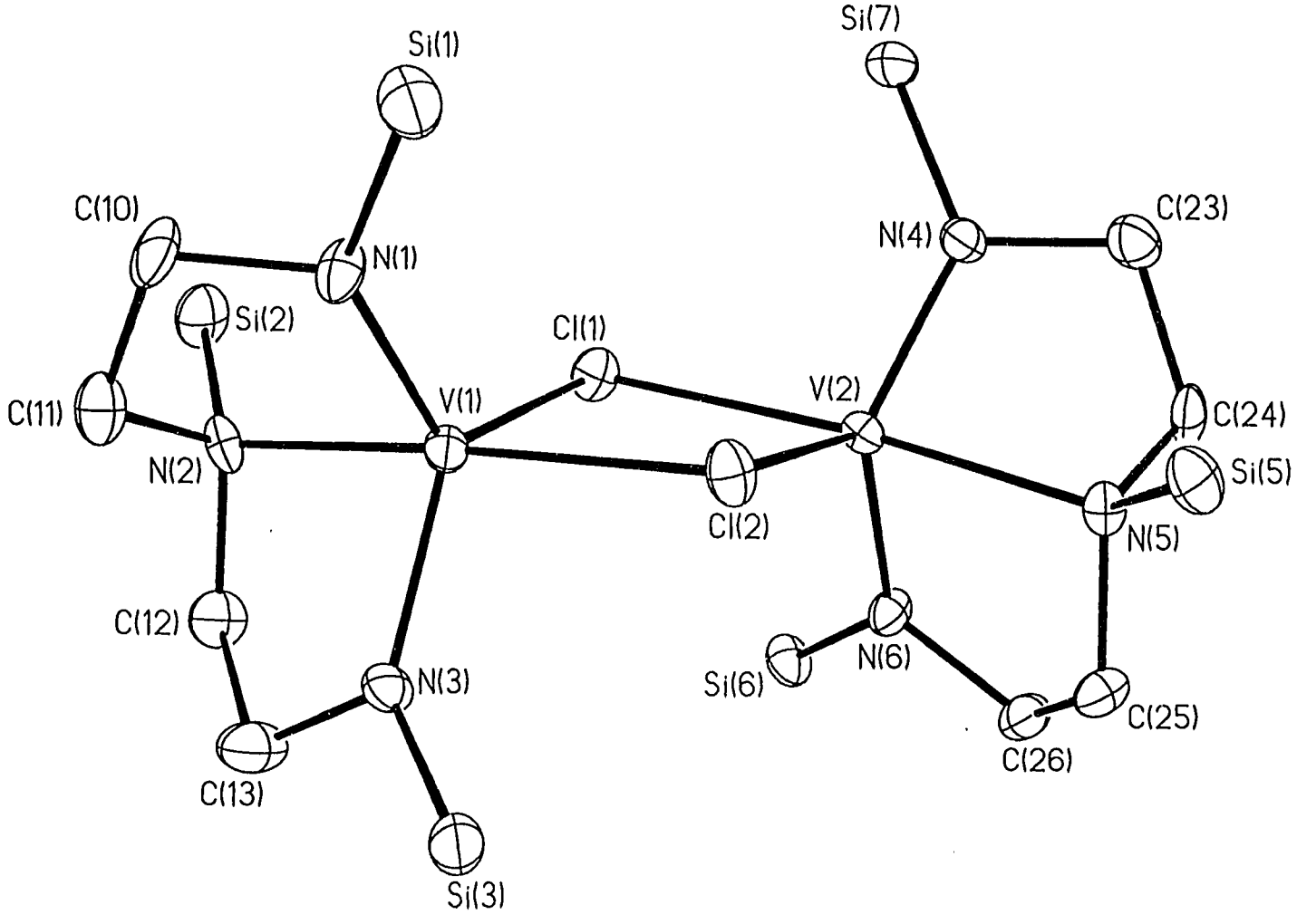

Figure 12-a: ORTEP plot of **4** : N2-V1-N3=82.73°, N1-V1-N2=83.98°, N3-V1-Cl1=98.37°, N1-V1-N3=117.44°, N1-V1-Cl1a=114.80°, N3-V1-Cl1a=126.52°, V1-N1=1.910(6) Å, V1-N3=1.909(6) Å, V-V=3.631(5) Å.

were consistent with the formulation $\{[(TMS)NCH_2CH_2]_2N(TMS)\}_2V\}S$ probably dimeric. The absence of chlorine was indicated by both qualitative tests and XRF data. Unfortunately, poor crystal quality prevented structural crystallographic investigations. Thus in order to gain insight, reaction was carried out by reacting $[(Me_3Si)_2N]_2VCI(THF)$ with sulfur yielding the diamagnetic $\{[(Me_3Si_2N]_2V\}_2(\mu\text{-}S)_2$ **(7)** complex which was isolated from ether in a crystalline form. The NMR spectra showed the characteristic absorptions of the ligand. Combustion analysis data consistent with the proposed formulation were obtained (Figure 13).

The molecular connectivity were elucidated by single- crystal X-ray analysis. The structure is formed by two almost identical $\{(Me_3Si)_2N]_2V$ units, bridged by two sulfur atoms. The coordination geometry around each vanadium atom is distorted tetrahedral [N1-V1-S1 = 108.8(1)°. N1-V1 -S2 = 111.7(1)°. N1-V1-N2 = 114.8(2)°. N2-V1-Si = 111.2(1)°, N2-V1-S2 = 108.0(1)°] and is defined by two nitrogens [V1–N1 = 1.878(4) Å, V1-N2 = 1.874(4) Å] of the two amide groups and the two bridging sulfur atoms. The distortion around vanadium is probably caused by the steric bulk of the two large trimethylsilyl groups [N1-V1-N2 = 114.8(1)°, N3-V2-N4 = 115.3(2)°]. The coordination geometry around each nitrogen atom is trigonal planar [V1-N1-Sil = 130.4(2)°, VI-NI-Si2 = 113.8(2)°, S1-N1-Si2 = 115.7(2)°] with rather short V-N distances. The V_2S_2 core is nearly planar [SI-VI-S2-V2 = 3.4(1)° torsion angle] with rather short V-S distances [V1-S1 =2.211(1) Å, V1-S2 = 2.206(l) Å,V2-Sl =2.216(1) Å, V2-S2 = 2.206(2) Å]

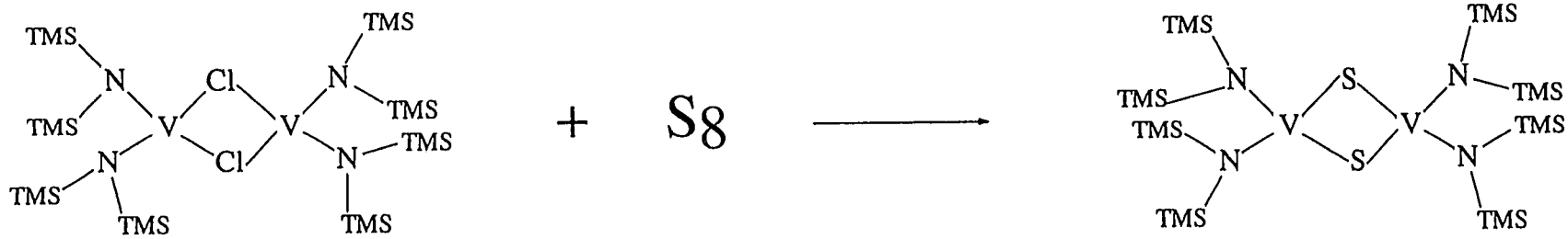

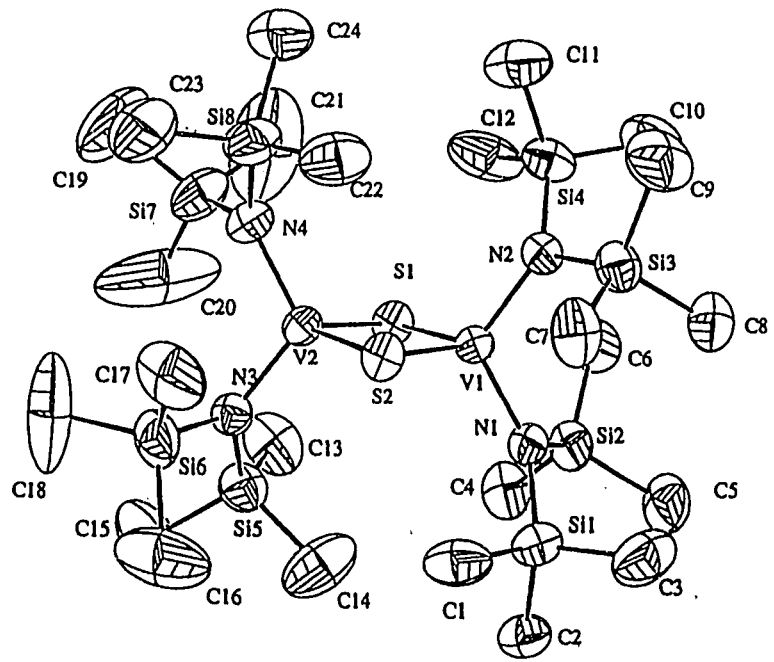

Figure 13: ORTEP plot of **7** : N1-V1-S1 = 108.8(1)°. N1-V1 -S2 = 111.7(1)°. N1-V1-N2 = 114.8(2)°. N2-V1-Si = 111.2-(1)°, N2-V1-S2 = 108.0(1)° , V1 –N1 = 1.878(4) Å, V1 -N2 = 1.874(4) Å , N1-V1-N2 = 114.8(1)°, N3-V2-N4 = 115.3(2)° , V1-N1-Sil = 130.4(2)°, VI-NI-Si2 = 113.8(2)°, S1-N1-Si2 = 115.7(2)° , SI-VI-S2-V2 = 3.4(1)° , V1-S1 =2.211(1) Å, V1-S2 = 2.206(l) Å,V2-Sl =2.216(1) Å, V2-S2 = 2.206(2) Å ,V1-S1-V2 = 81.70(5)°, V1-S2-V2 = 82.04(5)°.

possibly indicative of some V-S multiple bond character. This new compound, *in spite of having a longer intermetallic distance, is diamagnetic* compared to the isostructural oxo compound synthesized by Verkade et al [26]. The long V-V distance [V1-V2 = 2.857(1) Å] compared to the shorter [V1-V2 = 2.612(3) Å] in the oxo compound, and the diamagnetism of the complex raises questions about the nature of the intermetallic interaction and the possible mechanism for the magnetic coupling between the two d^1 metal centers. A database search on dinuclear tetravalent vanadium complexes yielded 31 crystal structures [26]. In all of these d^1 species the M_2X_2 cores featured intermetallic separations ranging from 2.459 to 3.033 Å depending on the nature of the bridging ligands. In the case of complex **7**, the longer intermetallic distance with respect to $\{[(Me_3Si)_2N]_2V\}_2(\mu\text{-}O)_2$ (0.25 Å) is not surprising given the larger atomic dimensions of the bridging atom (S versus O) and the consequent longer V-S distances with respect to V-O. However, the fact that in the identical ligand system the elongation of the intermetallic distance led to a more efficient coupling of the d^1 electrons seems to indicate that a significant V-V bond is unlikely to exist in the sulfido complex. The nature of these interactions will be discussed in further details in chapter III. The angles subtended at the bridging sulfur atoms, significantly narrower than 90°, are possibly the result of the tetrahedral coordination geometry of vanadium which dictates relatively large S-V-S angles. In addition, angles as narrow as 71° are rather common among sulfide and persulfide-bridged divanadium complexes,

which are almost invariably diamagnetic regardless of the size of intermetallic separation (typically in the range 2.5-2.87 Å) [27,28]. The angles subtended at the bridging sulfur atoms in complex **7** are rather small [V1-S1-V2 = 81.70(5)°, V1-S2-V2 = 82.04(5)°] but compare well with others of similar M_2S_2 frameworks[29].

Complex **4** was then reacted with methyllithium. In order to enhance crystallinity, one equivalent of pyridine was added. This reaction led to the formation of $\{[(TMS)NCH_2CH_2]_2N(TMS)\}VCH_3Py$ (**5**) which was isolated in crystalline form from hexane as intensely purple paramagnetic crystals (Figure 14). Due to the extremely high air-sensitivity of this species, single crystal X-ray analysis was the only possibility to elucidate the structure. The molecule features a trigonal bipyramidal vanadium atom connected to a methyl group and to a molecule of pyridine while the other three coordination sites are occupied by the ligand N atoms [C19-V-N1 = 116.65(6)°, C19-V-N3 = 113.85(7)°, C19-V-N4 = 92.62(5)°, C19-V-N2 = 100.94(5)°] (Figure 14-a). The coordination geometry around the terminal nitrogens is trigonal planar, suggesting a considerable extent of V-N π-donation. In agreement, the V-N distances are noticeably short [V-N1 = 1.972(1) Å, V-N3 = 1.925(2) Å] in spite of the considerable steric bulk.

Treatment of **5** with elemental sulfur in a THF solution gave an immediate color change to dark brown. Unfortunately attempts to isolate crystalline products suitable for X-ray analysis failed.

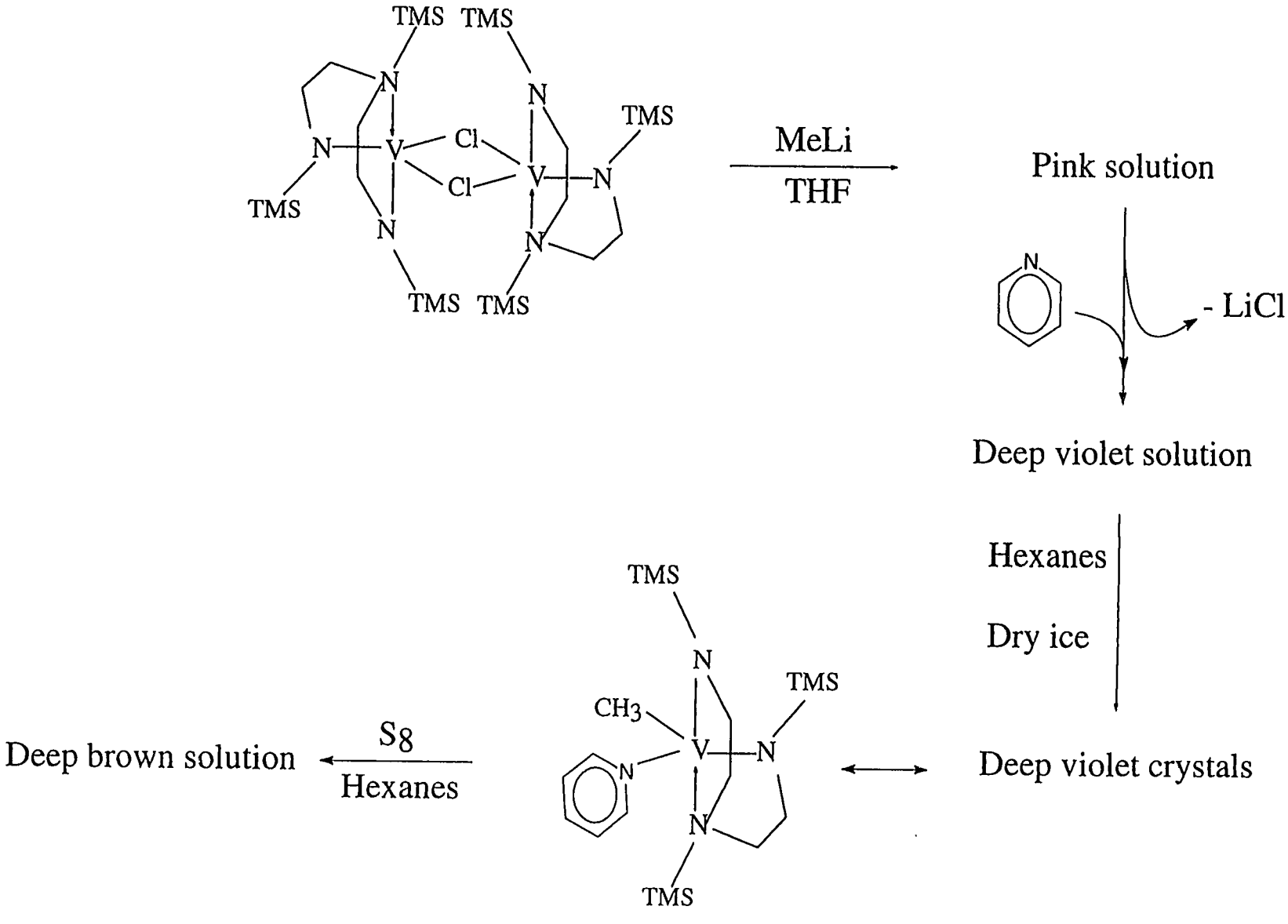
TMS TMS
N
N
TMS
N
V
Cl
V
N
Cl
TMS
N
N
TMS TMS
MeLi
THF
Pink solution
N
- LiCl
Deep violet solution
Hexanes
Dry ice
TMS
N
TMS
CH3
V
N
N
N
TMS
Deep violet crystals
S8
Hexanes
Deep brown solution

Figure 14

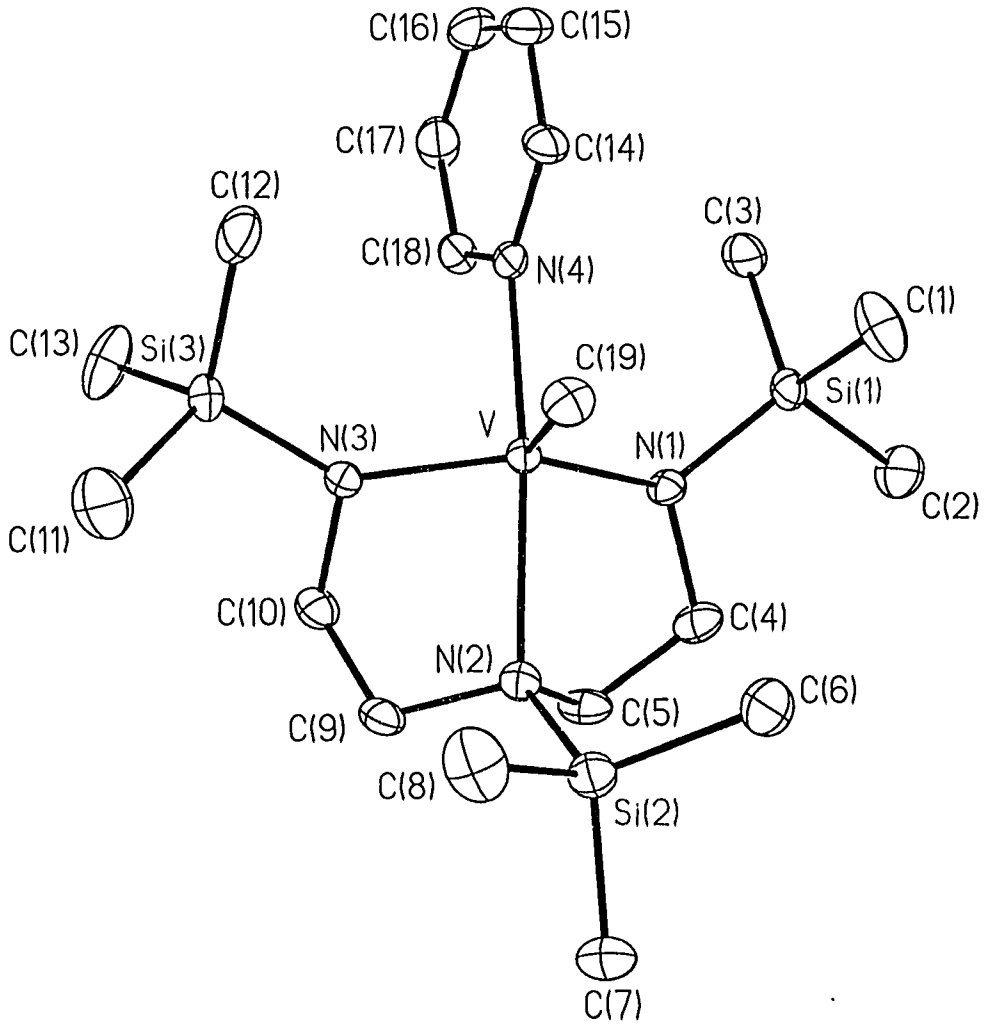

Figure 14-a: ORTEP plot of **5** : C19-V-N1 = 116.65(6)°, C19-V-N3 = 113.85(7)°, C19-V-N4 = 92.62(5)°, C19-V-N2 = 100.94(5)°.

Given that the reaction of vanadium (III) with sulfur resulted in the formation of stable vanadium (IV) dimers, our efforts were focused on reactions of vanadium (II) with sulfur or with sulfur providing molecules. This was advised by several reasons : Firstly, the reactivity of divalent vanadium with sulfur is not well developed, secondly $VCl_2(TMEDA)_2$ (TMEDA = N,N,N',N'-tetramethylethylenediamine) used in these reactions is closer from an oxidation point of view to the starting material used in literature to synthesize the vanadium-sulfur cubane cluster. Thirdly, by reacting V(II) with S_8 it was hoped that V(III) will be the final product, thus sparing a subsequent reduction step.

For this purpose $VCl_2(TMEDA)_2$ was reacted with a few sulfurizing agents. Elemental sulfur S_8 was used in the first instance. As summarized in Figure 15, the reaction led to the formation of a mixture of two compounds. The first was identified as $VCl_3(TMEDA)(THF)$ by IR and X-ray analysis. The second compound was a black precipitate, and unfortunately all attempts to crystallize this black compound failed due to its low solubility in the most common solvents. Reaction with nitric acid produced elemental sulfur thus suggesting possible presence of persulfido S_2^{2-} units. Elemental analysis on all elements and XRF tests were carried out. The results of these tests were consistent and indicated the formula $V_3S_7Cl(TMEDA)_3$ **(7c)**. The presence of chloride was confirmed by the precipitation of silver chloride after the addition of silver nitrate to an acidic solution of the black powder.

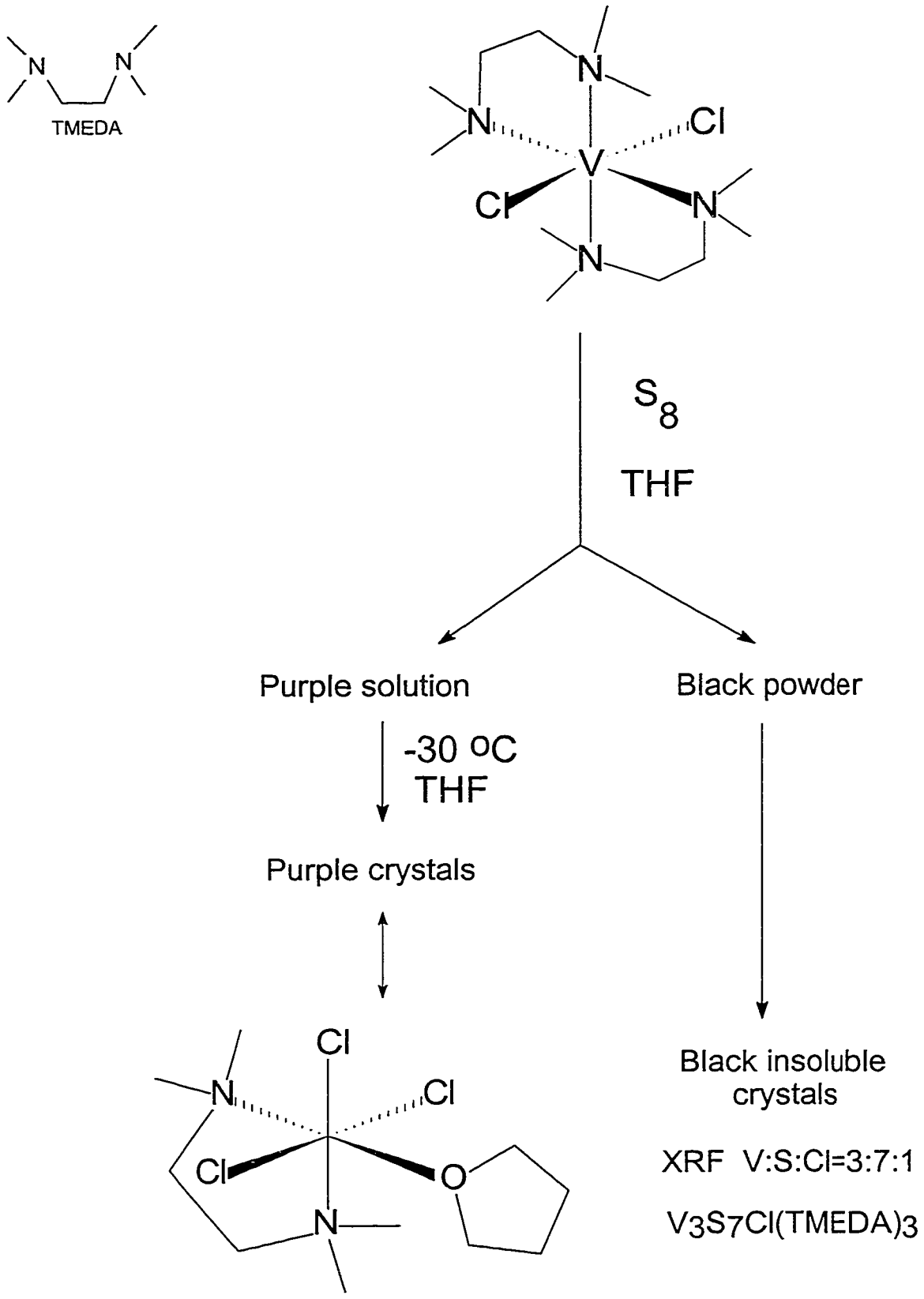
TMEDA
N
N
Cl
V
Cl
N
N
S_8
THF
Purple solution
Black powder
-30 °C
THF
Purple crystals
Cl
N
Cl
Cl
O
N
Black insoluble
crystals
XRF V:S:Cl=3:7:1
$V_3S_7Cl(TMEDA)_3$

Figure 15

In order to shed some light on the molecular structure attempts were made to grow better quality crystals. One of these methods consists of layering a THF solution of sulfur over a THF solution of $VCl_2(TMEDA)_2$. After standing for a few days, black needle shaped crystals separated. Unfortunately the quality was unsuitable for X-ray analysis. Repeated attempts by changing concentrations also failed in producing sufficient quality crystals. Since growing crystals of **7c** seems to be an extremely difficult task, a series of experiments were performed, to derivatize **7c** with ligands which will hopefully produce better quality crystals allowing us to elucidate the structure via X-ray analysis and, indirectly that of **7c**. For this purpose compound **7c** was reacted with a variety of ligands, such as alkoxides, amides, and hydrogen. This compound proved to be unreactive towards alkoxides. Reaction of **7c** with phenyl, substituted phenoxide and silanates were unsuccessful, and unreacted starting material was always recovered after several days of reflux (Figure 16). Reactions with amides and sulfides were more promising. Among the several attempts which were conducted (Figure 17), reaction of **7c** with $(C_5H_5N)SLi$ yielded crystalline material. The formulation $[V_3(\mu_3\text{-}Cl)\text{-}(\mu\text{-}S_2)_3](PyS)_3Li(THF)_4$ **(9)** yielded by combustion analysis data and were in agreement with XRF and single crystal X-ray data. The structure of **9** consists of a triangulo-$[V_3(\mu_3\text{-}Cl)]$ unit with three edge-bridging $\eta^2{:}\eta^2{:}\mu S_2^{2-}$ groups. One pyridinemercaptate ligand is attached to each V of the complex structure. The bridging S_2^{2-} units are slightly asymmetric having one shorter [V1-

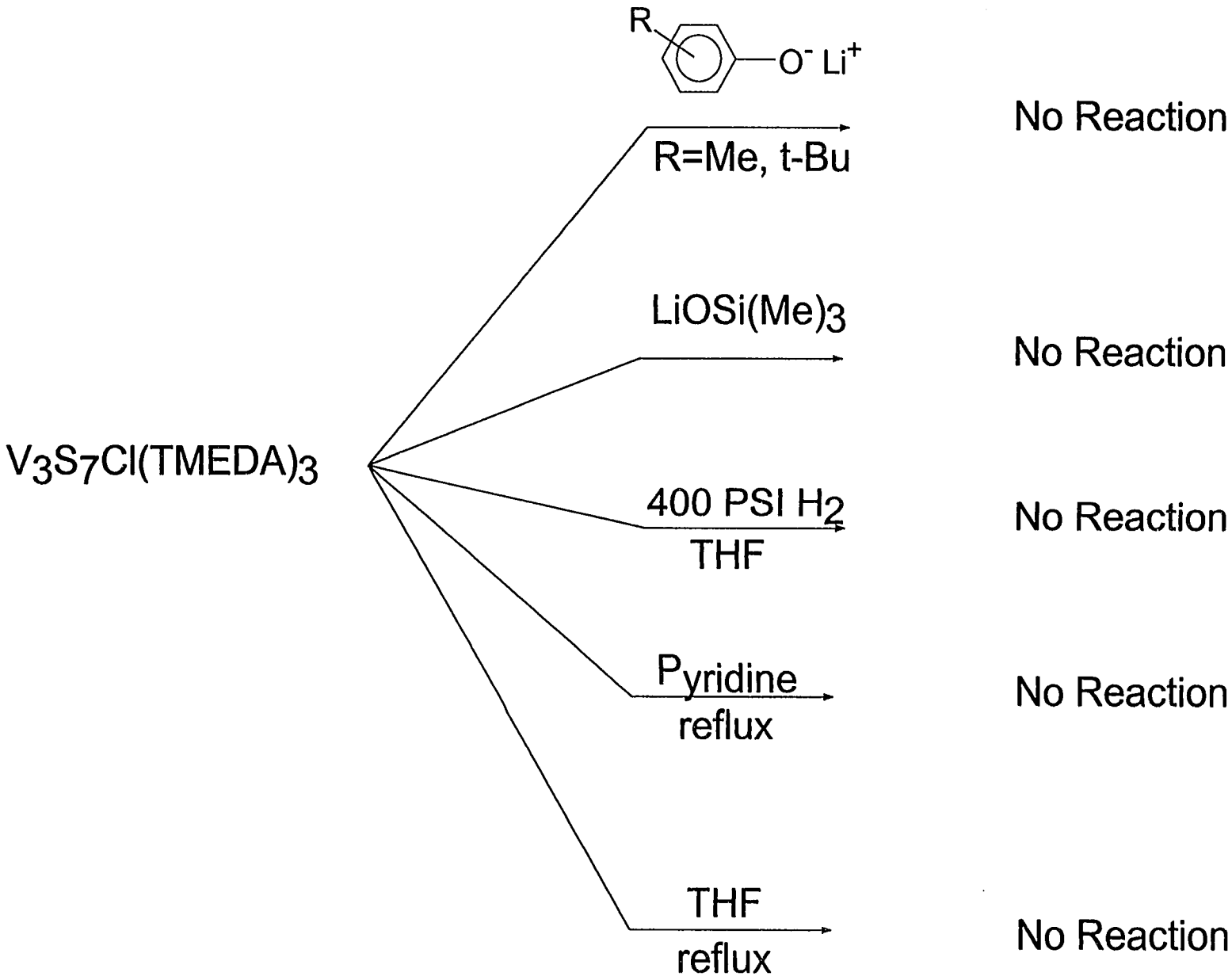
R
O⁻ Li⁺
R=Me, t-Bu
No Reaction
LiOSi(Me)3
No Reaction
V3S7Cl(TMEDA)3
400 PSI H2
THF
No Reaction
Pyridine
reflux
No Reaction
THF
reflux
No Reaction

Figure 16

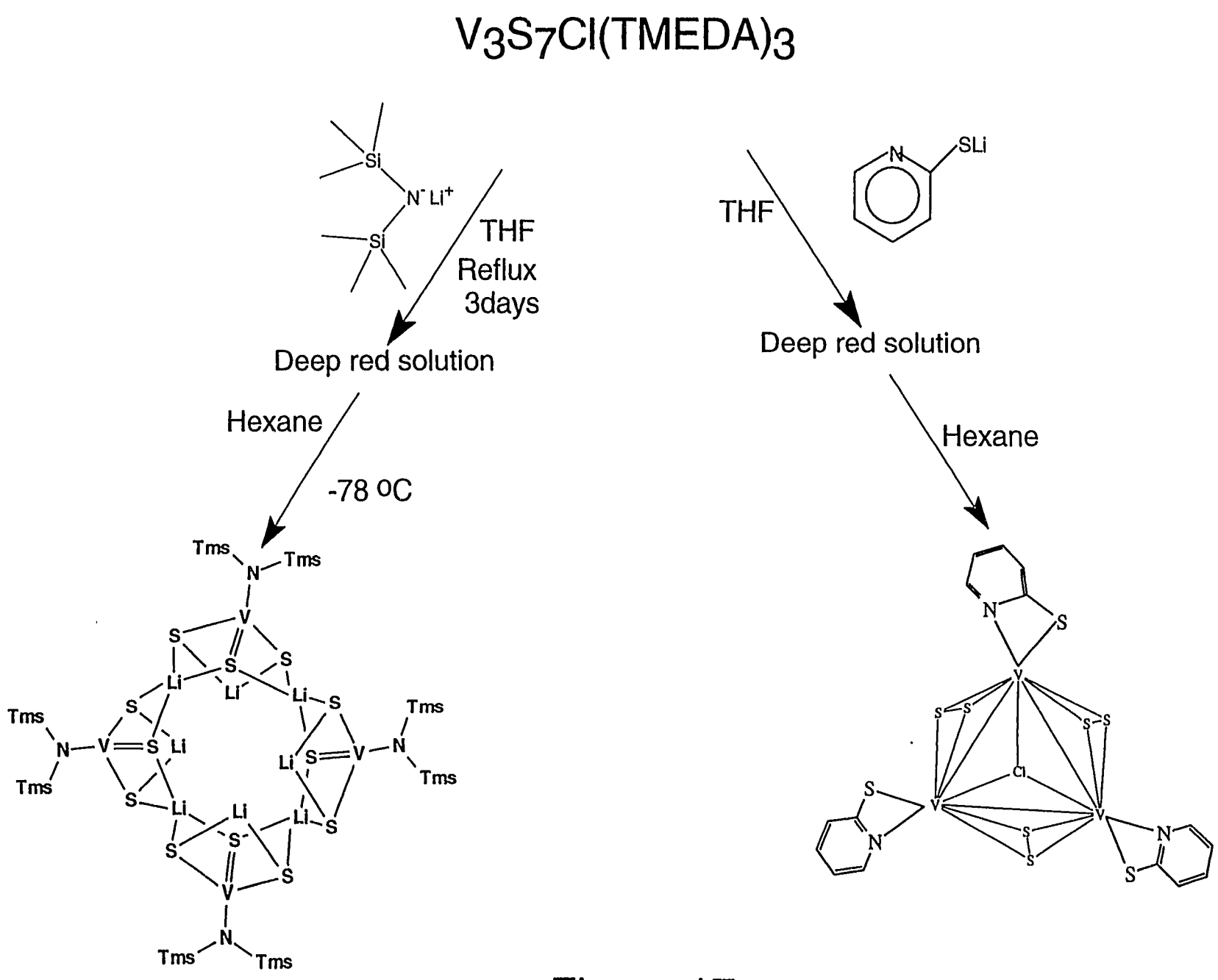
V3S7Cl(TMEDA)3
Si
N- Li+
Si
THF
Reflux
3days
Deep red solution
Hexane
-78 oC
Tms
N
Tms
V
S
Li
Tms
N
Tms
Tms
N
Tms
V
N
SLi
THF
Deep red solution
Hexane
N
S
V
S
S
S
S
Cl
V
V
S
N
S
S
N
S
N

Figure 17

S4=2.381(3) Å, V1-S6=2.380(3) Å, V2-S8=2.369(3) Å, V2-S4=2.375(3) Å, V3-S8=2.366(3) Å, V3-S6=2.371(3) Å, (ave. 2.37 Å)] and one longer [V1-S5=2.453(3) Å, V1-S7=2.459(3) Å, V2-S5=2.440(3) Å, V2-S9=2.454(3) Å, V3-S7=2.450(3) Å, V3-S9=2.466(3) Å, (ave. 2.45 Å)] bound to each vanadium atom. Each vanadium atom is located on the vertices of almost an equilateral triangle [V2-V1-V3=60.92(6)°, V1-V2-V3=59.84(6)°, V1-V3-V2=59.23(5)°, V1-V2=2.710(2) Å, V1-V3=2.727(2) Å, V(2)-V(3)=2.757(2) Å] with average V-V distance and angles of 2.74 Å and 60°. As for the ligand, the rather long V-S distance (ave. 2.5 Å) suggests a single bond. One interesting feature to point out is that the sulfurs S1 and S2 of the ligand are above the plane formed by the three vanadium atoms, while S3 is below it (Figure 17-a). On the basis of these findings it is suggested that the structure of **7c** may be a persulfido trivanadium cluster.

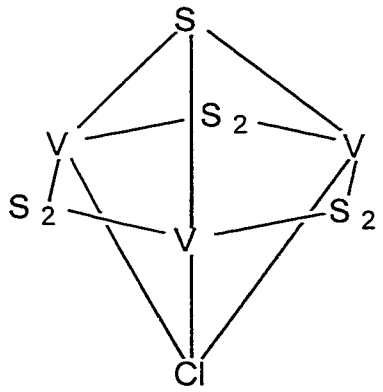

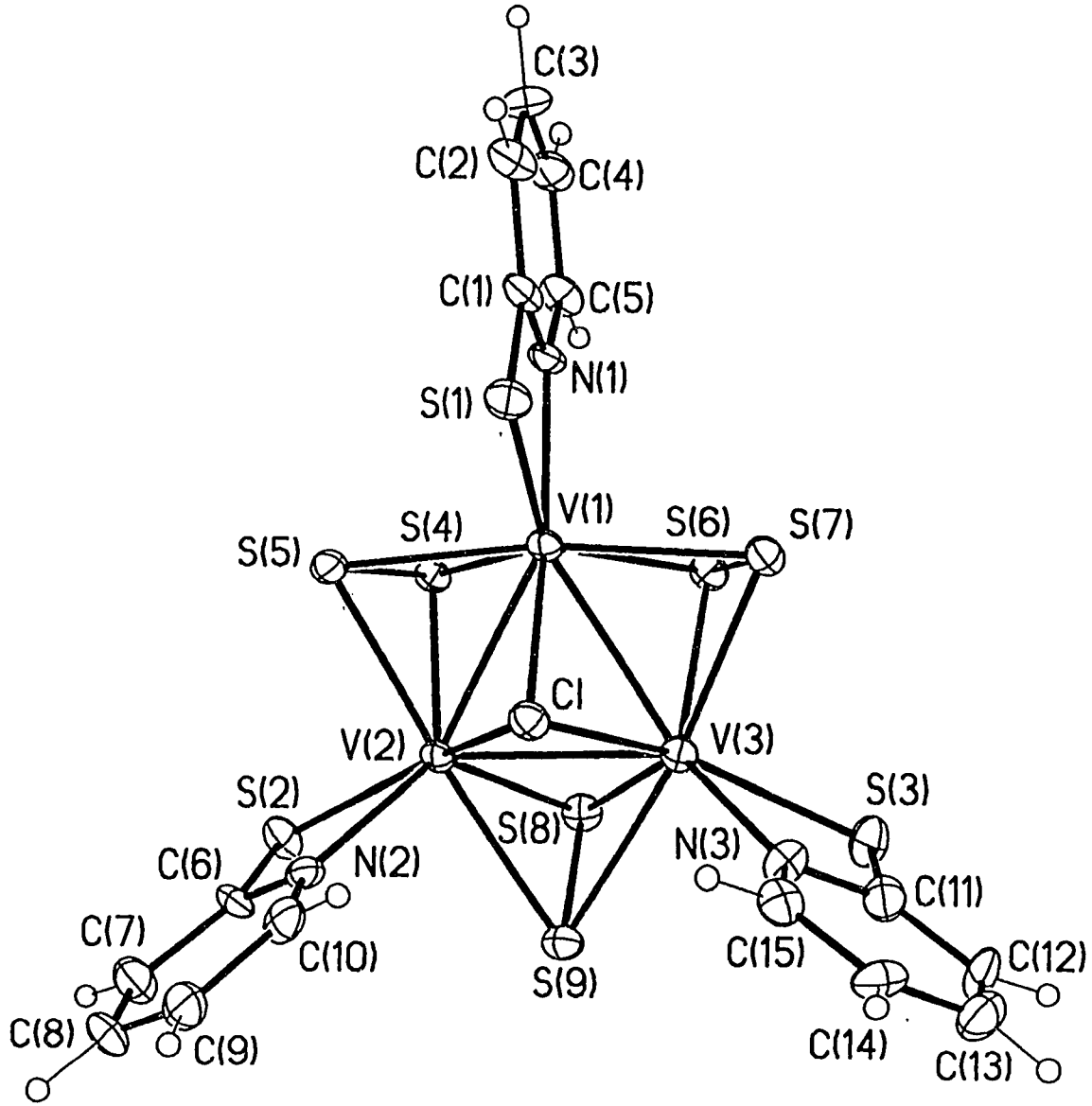

Figure 17-a: ORTEP plot of **9** : V1-S4=2.381(3) Å, V1-S6=2.380(3) Å, V2-S8=2.369(3) Å, V2-S4=2.375(3) Å, V3-S8=2.366(3) Å, V3-S6=2.371(3) Å, (ave. 2.37 Å) , V1-S5=2.453(3) Å, V1-S7=2.459(3) Å, V2-S5=2.440(3) Å, V2-S9=2.454(3) Å, V3-S7=2.450(3) Å, V3-S9=2.466(3) Å, (ave. 2.45 Å) , V2-V1-V3=60.92(6)°, V1-V2-V3=59.84(6)°, V1-V3-V2=59.23(5)°, V1-V2=2.710(2) Å, V1-V3=2.727(2) Å, V(2)-V(3)=2.757(2) Å.

In order to support this idea, we have also reacted complex **7c** with $[(TMS)_2N]Li$. The reaction gave the new diamagnetic complex **7d** in which the metal has an oxidation state of +5. The structure of **7d** was determined by X-ray analysis. The complex is tetrameric, and consists of four $[(TMS)_2N]VS_3Li(THF)_2Li$ units linked together by four Li-S-Li bridges, thus forming an eight member macrocycle (Figure 17b). The geometry around the vanadium atom is slightly distorted tetrahedral [Sl-V-S2=107.54(12)°, S1-V-S3=108.63(11)°, S1-V-N1=110.3(2)°, S2-V-N1=111.0(3)°, S2-V-S3=107.46(11)°], and is defined by one nitrogen atom of one unit [V-N1=1.886(7) Å] and three sulfur atoms [V-S1= 2.139(3) Å, V-S2 = 2.125(3) Å, V-S3 = 2.137(3) Å]. The coordination geometry around the nitrogen is trigonal planar [Si2-N1-Si1=123.2(4)°, Si2-N1-V=117.9(4)°, Si1-N1-V=118.0(4)°] with rather short V-N distances. The VS_3 core could be regarded as occupying the corner of a cube with each of the atoms on one of the vertices. The rather short V-S distances may be indicative of some multiple bond character. Both carbon atoms of THF and TMS showed signs of thermal activity.

Gathering and putting all the evidence in perspective, we notice that the reaction of V(II) with sulfur led to the oxidation of the latter from +2 to +3 oxidation state, thus yielding a sulfur-rich complex possessing the formula $V_3S_7Cl(TMEDA)_3$. The reaction can be summarized by the following equation:

$$8VCl_2(TMEDA)_2 + 7S \xrightarrow{THF} V_3S_7Cl(TMEDA)_3 + 5VCl_3(TMEDA)(THF)$$

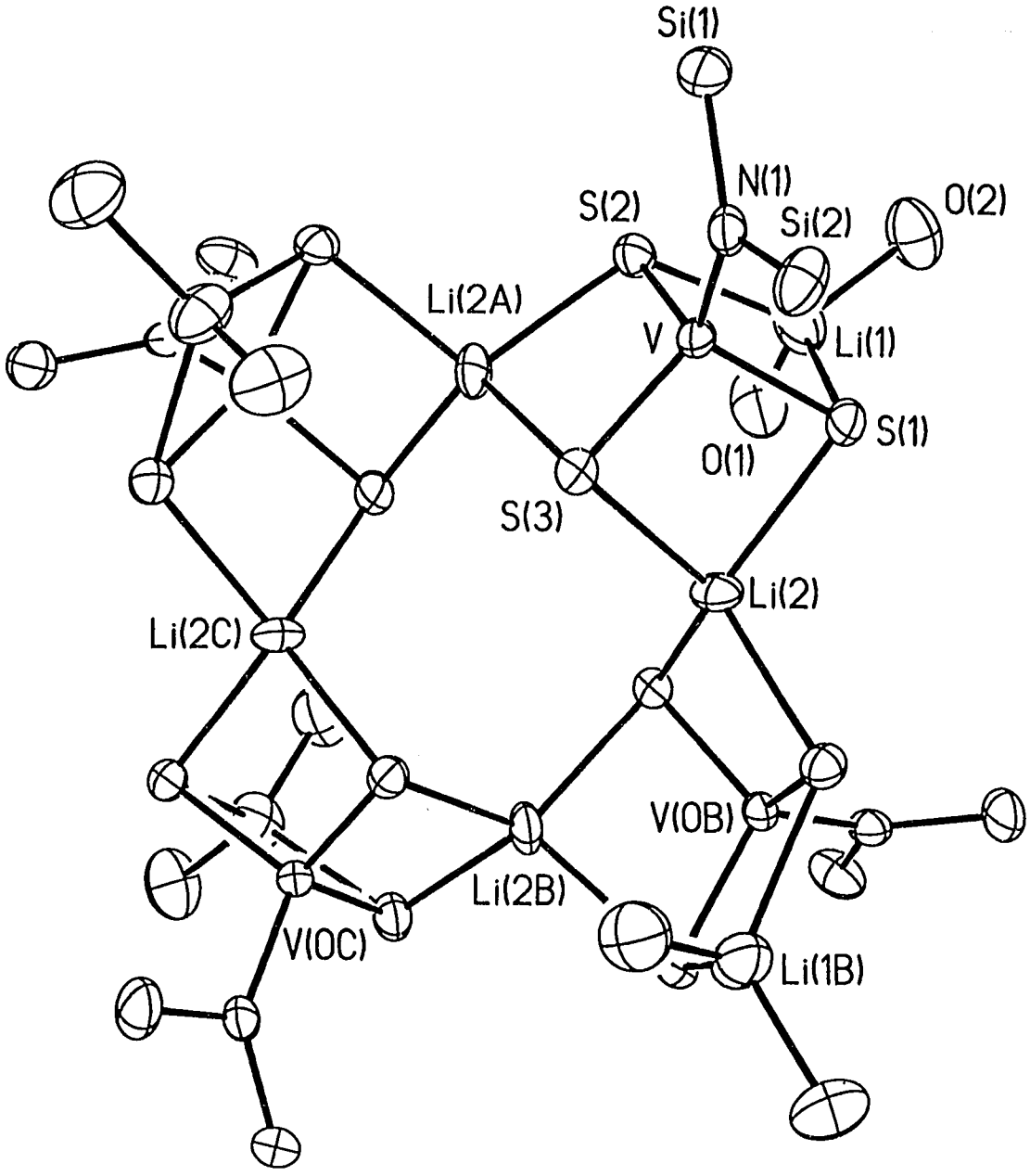

Figure 17-b: ORTEP plot of **7d** : Sl-V-S2=107.54(12)°, S1-V-S3=108.63(11)°, S1-V-N1=110.3(2)°, S2-V-N1=111.0(3)°, S2-V-S3=107.46(11)° , V-N1=1.886(7) Å , V-S1= 2.139(3) Å, V-S2 = 2.125(3) Å, V-S3 = 2.137(3) Å , Si2-N1-Si1=123.2(4)°, Si2-N1-V=117.9(4)°, Si1-N1-V=118.0(4)°.

The 8 electrons necessary for the transformation of 7 S atoms into one sulfide, S^{2-} and three persulfide S_2^{2-} are provided by the one electron oxidation of eight vanadium(III) atom.

Reaction of $V_3S_7Cl(TMEDA)_3$ with $(C_5H_5N)SLi$ led to the replacement of the TMEDA with the ligand and the elimination of one molecule of lithium sulfide via the following reaction:

$$V_3S_7Cl(TMEDA)_3 + 3PyS^-Li^+ \longrightarrow V_3S_6Cl(PyS)_3 + Li_2S + 3TMEDA$$

The transformation of **7c** into complex **9** is not a redox process, since the oxidation state +3 is preserved. The reaction arises from the formal replacement of S^{2-} by two molecules of mercaptopyridinate anions with elimination of LiS_2 and the addition of a third molecule thus forming the final anionic species.

Conversely, reaction of $[(TMS)_2N]Li$ with $V_3S_7Cl(TMEDA)_3$ led to molecular rearrangement in which the original cluster broke in two fragments. The first one is $[(TMS)_2N]VS_3Li(THF)_2Li$ which clustered to form the tetramer and the other one is thought to be $\{[(TMS)_2N]V\}_2(\eta^2:\eta^2:\mu S_2^{2-})_2$ **(7e)**. Unfortunately, attempts to isolate or identify **7c** failed so far.

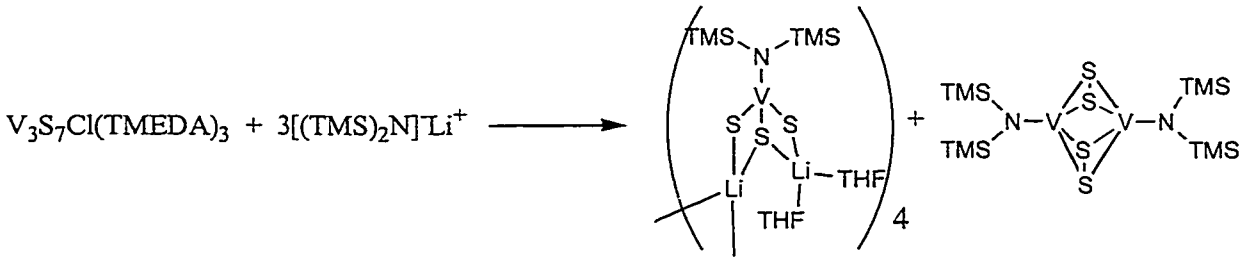

In spite of efforts to control the stoichiometry of this transformation, the reaction led to sulfur rich V-S cluster. In order to prevent formation of persulfido containing structures other sulfur donating agents were taken into consideration.

The reaction of vanadium(III) with one equivalent of hydrogen sulfide led to the formation of a green precipitate and a brown solution. However no effort was made to identify the structure of the green precipitate since XRF analysis showed that the latter was rich in vanadium and chlorine, and depleted in sulfur. Although SH bands were detected in the I.R. spectrum at 2566 (cm^{-1}), 2458 (cm^{-1}), they may also be produced by impurities. Layering the brown mother liquor with hexane led to the formation of a crystalline mass containing two different types of crystals. Due to the poor quality of the crystals, and the numbers of products formed, no other efforts were made in this reaction. As a possible alternative, propylene sulfide was used as sulfur source instead of H_2S since with this type of compound, the sulfur transfer reactivity should be milder and more controllable. However the reaction of $VCl_2(TMEDA)_2$ with one equivalent of $CH_3CH_2CH_2(\mu\text{–}S)$ led to the formation of a purple solution from which brown microcrystalline powder separated. Unfortunately, attempts to obtain suitable crystals for X-ray analysis failed. However XRF and combustion elemental analysis suggest the formula $V_2Cl_4S(TMEDA)_2$. In an attempt to obtain better quality crystals, the product was redissolved in pyridine and the solution was allowed to stand at room temperature. After a few days , a small amount of solid

separated from which a single crystal was analyzed by X-ray diffraction. To our surprise the final structure of the product revealed no sulfur but rather the presence of an oxygen atom possessing a linear geometry bridging two vanadiums (Figure 18). The vanadium-oxygen linear complex is probably generated by an epoxy impurity (CH_2CH_2-μO), which cannot be easily removed. This fact led us to consider alternative sulfurising reagents such as organic persulfides. The reaction of $VCl_2(TMEDA)_2$ with one equivalent of diphenyldisulfide led to a color change of the solution from blue to purple, via transient formation of a green intermediate. After few days, purple crystals of $(TMEDA)_2V_2Cl_2(\mu\text{-}SPh)_2(\mu\text{-}Cl)$ (7b) separated. The structure of **7b** was determined by X-ray analysis. The structure consists of two vanadiums linked together by one bridging chlorine, and two bridging phenylsulfido groups (Figure 19). The coordination geometry around each vanadium is distorted octahedral [N(1)-V(1)-N(2)=79.55(4) °, N(1)-V(1)-Cl(1)=90.74(3) °, N(2)-V(1)-Cl(1)=90.71(3) °, N(1)-V(1)-S(1)=168.96(4) °, N(2)-V(1)-S(1)=91.83(3) °, Cl(1)-V(1)-S(1)=96.29(2) °, N(1)-V(1)-S(1)=88.07(3) °, N(2)-V(1)-S(1)=162.74(4) °, Cl(1)-V(1)-S(1)=101.51(2) °, S(1)-V(1)-S(1)=98.798(14) °, N(1)-V(1)-Cl(2)=96.15(3) °, N(2)-V(1)-Cl(2)=92.60(3) °, Cl(1)-V(1)-Cl(2)=172.80(2) °, S(1)-V(1)-Cl(2)=77.220(11) °, S(1)-V(1)-Cl(2)=76.692(11) °], with rather long vanadium sulfido bonds [V(1)-S(1)#1=2.4344(4) Å, V(1)-S(1)=2.4635(4) Å]. Complex **7b** is a V(II)/V(III) mixed valence species, and therefore its formation requires only one electron

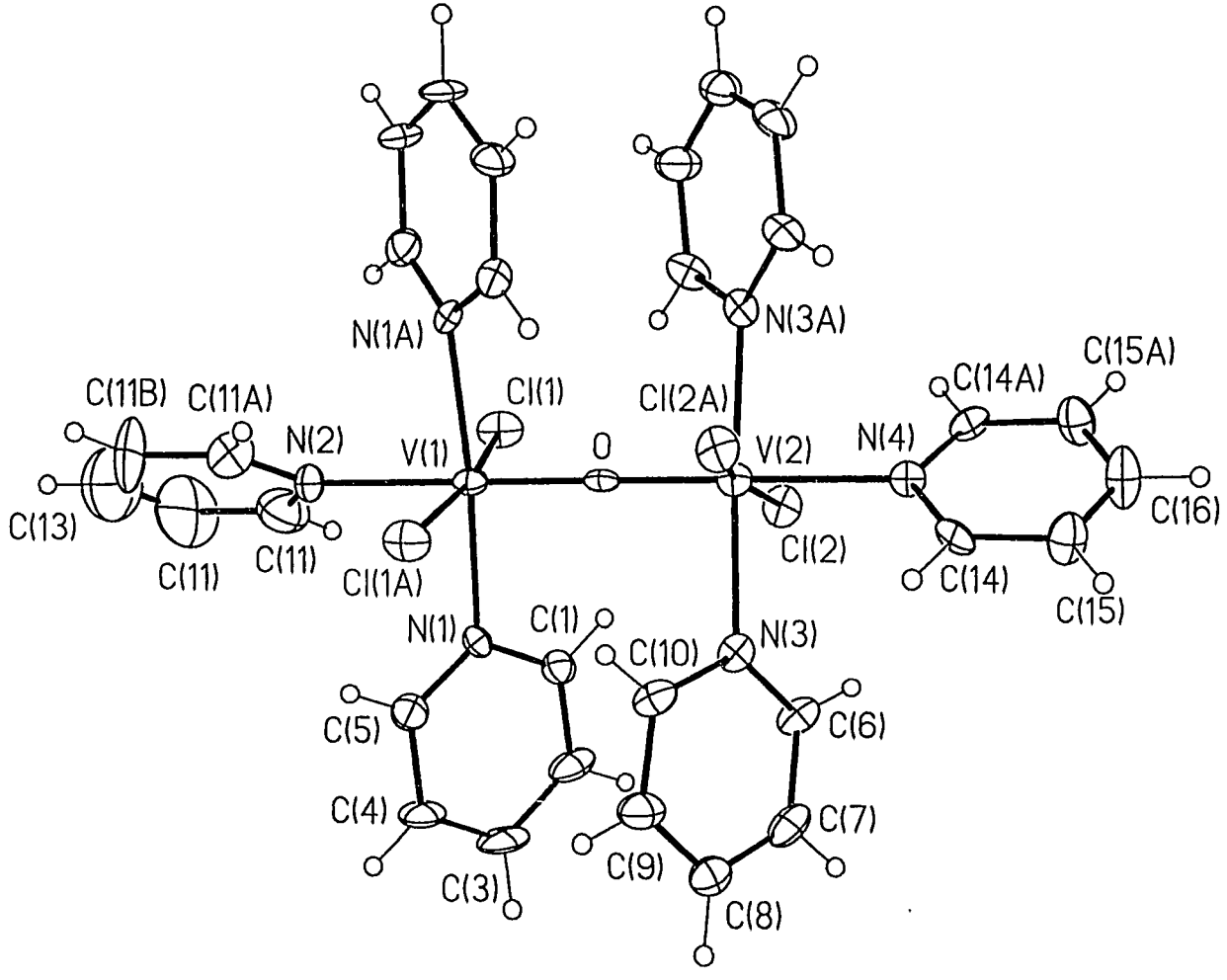
N(1A)
N(3A)
C(15A)
C(14A)
C(11B)
C(11A)
Cl(1)
Cl(2A)
N(2)
V(1)
O
V(2)
N(4)
C(16)
C(13)
C(11)
C(11)
Cl(1A)
Cl(2)
C(14)
C(15)
N(1)
C(1)
C(10)
N(3)
C(5)
C(6)
C(4)
C(7)
C(9)
C(3)
C(8)

Figure 18

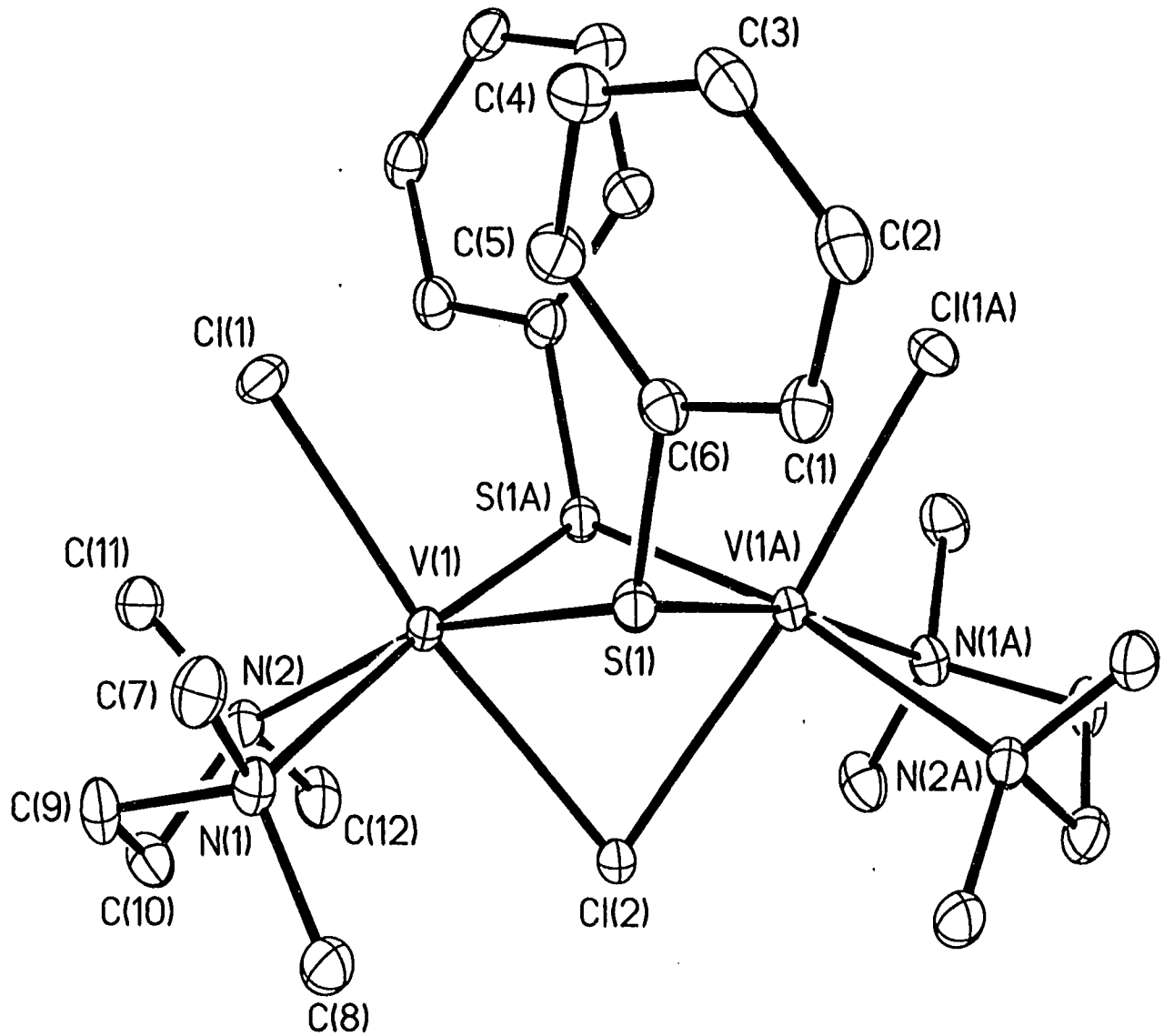

Figure 19: ORTEP plot of **7b:** N(1)-V(1)-N(2)=79.55(4) °, N(1)-V(1)-Cl(1)=90.74(3) °, N(2)-V(1)-Cl(1)=90.71(3) °, N(1)-V(1)-S(1)#1=168.96(4) °, N(2)-V(1)-S(1)#1=91.83(3) °, Cl(1)-V(1)-S(1)#1=96.29(2) °, N(1)-V(1)-S(1)=88.07(3) °, N(2)-V(1)-S(1)=162.74(4) °, Cl(1)-V(1)-S(1)=101.51(2) °, S(1)#1-V(1)-S(1)=98.798(14) °, N(1)-V(1)-Cl(2)=96.15(3) °, N(2)-V(1)-Cl(2)=92.60(3) °, Cl(1)-V(1)-Cl(2)=172.80(2) °, S(1)#1-V(1)-Cl(2)=77.220(11) °, S(1)-V(1)-Cl(2)=76.692(11) °, V(1)-S(1)#1=2.4344(4) Å, V(1)-S(1)=2.4635(4) Å.

being removed from the two metal centers. By contrast, the tranformation of RSSR in two RS^- units is typically a two electron process. However the reaction is accompanied by the formation of $VCl_3(TMEDA)(THF)$ complex. The one electron oxidation of a third vanadium center provides the second electron necessary to the cleavage. We speculate that the reaction may proceed via the intermediate formation of a triangular cluster as described below. The oxidative addition of RSSR to one dinuclear moiety results in the detachment of complex **7b** and the formation of $VCl_3(TMEDA)(THF)$.

$$3V(II) \longrightarrow 2V(III) + V(II) + 2e^-$$

$$RSSR + 2e^- \longrightarrow 2RS^-$$

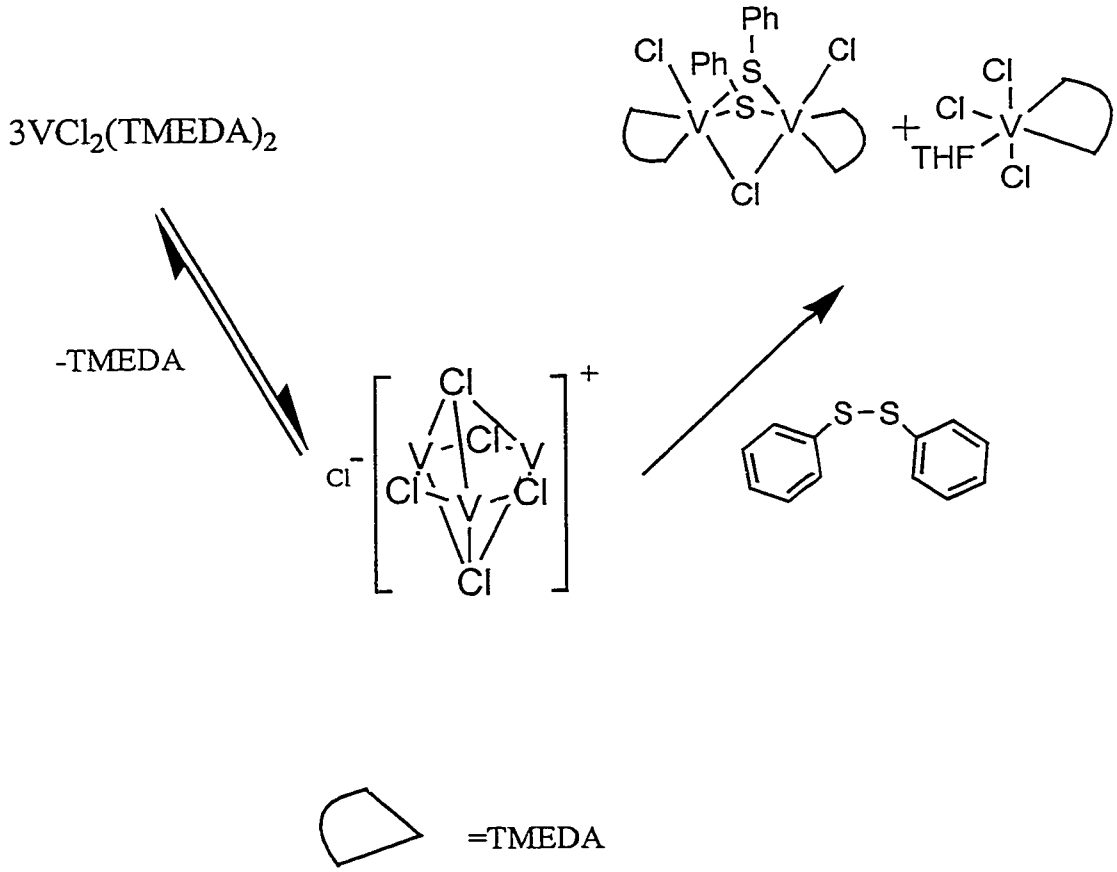

References:

1. J.J.H. Edema, S. Gambarotta, A. Meetsma, *J. Am. Chem. Soc.* **1989**, 111, 6878.

2. (a) J. Chatt, A. J. Pearman, R. L. Richards, *J. Chem. Soc., Dalton Trans.*, **1984**, 469.

   (b) S. Donovan-Mtunzi, R. L. Richards, R. L. Mason, *J. Chem. Soc., Dalton Trans.*, **1984**, 469.

   (c) Y. Mizobe, T. Ishida, Y. Engawa, K. Ochi, T. Tanase, M. Hidai, *J. Coordination Chem.*, **1991**, 23, 57.

   (d) J. Chatt, A. J. Pearman, R. L. Richards, *J. Chem. Soc., Dalton Trans.*, **1977**, 2139.

3. (a) B. R. James, *Adv. Organomet. Chem.*, **1979**, 17, 319.

   (b) R. L. Pruett, *Adv. Organomet. Chem.*, **1979**, 17, 1.

4. R. Ferguson, E. Solari, C. Fluorani, A. Chiesi-Villa, C. Rizzoli, *Angew. Chem., Int. Ed. Eng.*, **1993**, 32, 396.

5. J. K. Buinjik, A. Meetsma, J. H. Teuben, Organometallics, **1993**, 12, 2004.

6. W. A. Nugent, J. M. Mayer, *Metal-Ligand Multiple Bonds,* Wiley, New-York, **1988,** 179

7. (a) M. H. Chisholm, J. C. Huffman, W. G. van der Sluys, *J. Am. Chem. Soc.*, **1987**, 109, 2514.

(b) F. A. Cotton, M. P. Diebold, W. J. Roth, *Inorg. Chem.*, **1985**, 24, 3509.

8. (a) M. J. Scott, W. C. A. Wilisch, W. H Armstrong, *J. Am. Chem. Soc.*, **1990**, 112, 2429.

   (b) C. Floriani, A. Chiesi-Villa, M. Mazzanti, *Angew. Chem., Int. Ed. Eng.*, **1988**, 27, 576.

9. (a) N.G. Connelly, *Comprehensive Organometallic Chemistry;* Wilkinson J. , Pergamon Press, Oxford, **1982**, 3, 656.

   (b) K. Jones, W. Russeler, K. Angermund, C. Kruger, *Angew. Chem. , Int. Ed. Engl.*, **1986**, 25, 927.

   (c) Jensen, J. A.; Girolami, G. S.; *J. Am. Chem. Soc.* **1988**, 110, 4450.

   (d) Halloway, C. E.; Melnik, M.; *J. Organomet. Chem.*, **1986**, 304, 41.

   (e) Smart, J. C.; Pinsky, B. L.; Fredrich, M. F.; Day, V. W.; *J. Am. Chem. Soc.* **1979**, 101, 4371.

   (f) Castellani, M. P.; Geib, S. J.; Rheingold, A. L.; Trogler, W. C.; *Organometallics*, **1987**, 6, 1703.

   (g) Hessen, B.; van Bolhuis, F.; Teuben, J. H.; *J. Am. Chem. Soc.* **1988**, 110, 295.

   (h) Kowalesky, R. M.; Basolo, F.; Trogler, W. C.; Ernst, R. D.; *J. Am. Chem. Soc.* **1986**, 108, 6046.

10. M. F. Lappert, P. P. Power, A.R. Sanger, R. C. Srivastava, *Metal and Metalloid Amides*, Ellis Howood: Chichester, England, **1980**.

11. J. I. Song, S. Gambarotta, *Chem. Eur. J.*, **1994,** 2, 1258.

12. G. W. A. Fowles, C. M. Pleass, *J. Chem. Soc.*, **1957,** 1674.

13. M. G. Fickes, W. M. Davis, C. C. Cummins, *J. Am. Chem. Soc.* **1995**, 117, 6384.

14. C. C. Cummins, R. R. Schrock, W. M. Davis, *Inorg. Chem.* **1994,** 33, 1448.

15. S. Gambarotta, J.J.H. Edema, R. Minhas,. *J. Chem. Soc., Chem. Commun.*, **1993**, 1503.

16. P. Berno, M. Moore, R. Minhas, S. Gambarotta, *Organometallics,* **1996,** 74, 1930.

17. C. E. Laplaza, C. C. Cummings, *Science*, **1995**, 268, 861.

18. J. I. Song, P. Berno, S. Gambarotta, *J. Am. Chem. Soc.*, **1994**, 116, 6927.

19. P. Berno, R. Minhas, S. Hao, S. Gambarotta, *Organometallics* **1994**, 13, 1052.

20. P. Berno, S. Gambarotta, *Organometallics* **1994**, 13, 2569.

21. P. Berno, S. Gambarotta, *Angew. Chem., Int. Ed. Engl,* **1995**, 34, 822.

22. T. B. Rauchfuss, *J. Am. Chem. Soc.*, **1982**, 104, 7313.

23. R. B. King, *Inorg. Syn.*, **1963**, 7, 100.

24. C. T. Prewitt, *Inorg. Chem.*, **1966**, 5, 892.

25. J. Darkwa, *J. Am. Chem. Soc.*, **1988**, 110, 141.

26. Z. Duan, M. Schmidt, V. G. Young, X. Xie, R. E. McCarley, J. G. Verkade, *J. Am. Chem. Soc.* **1996**, 118. 5302 and references cited therein.

27. Bolinger, C. M.; Rauchfuss, T. B.; Rheingold ..A. L. *J. Am. Chem. Soc.* **1983,** 105, 6321.

28. (a) C. M. Bolinger, T. B.Rauchfuss, A. L. Rheingold, *Organometa*llics **1982,** 1, 1551.

(b) T. R. Helbert, L. L. Hutchings, R. Rhodes, E. I. Stiefel *J. Am. Chem. Soc.* **1986,** 108, 6437.

(c) S. C. Sendlinger, I. R. Nicholson, F. B. Lobkovsky, J. C. Huffman, 0. Rehder, G. Chrtistou, *Inorg. Chem.* **1993,** 32, 204.

(d) S. A. Duraj, M. T. Andras, P. A. Kibala, *Inorg. Chem.* **1990,** 29, 1232.

29. L. Scoles, S. Gambarotta, *Inorg. Chim. Acta* **1995,** 235, 375.

CHAPTER III

Introduction

One of the most important concepts in chemistry, and perhaps the greatest one in inorganic chemistry, is the concept of the coordination complex, which was developed by Alfred Werner at the turn of this century. This concept enabled Werner to rationalize an enormous amount of experimental data that could not be otherwise explained in the structural and bonding theory existing at that time.

The basic idea of the coordination theory of Werner is that a metal ion surrounds itself with ligands and that the nature of the ligands, the character of the metal-ligand bonds. and the geometrical arrangement of the ligands around the metal atom determine the physical and chemical properties of the compound. Although this simple theory must be considered as a milestone of the modern coordination chemistry, it should be observed that there is no place in the Wernerian scheme for direct bonding between metal atoms.

Werner recognized the existence of polynuclear complexes and devoted considerable effort towards the elucidation of their properties. However, these species were regarded as a simple combination of two or more mononuclear complexes sharing some ligand atoms. The properties of these complexes were still attributed to the metal-ligand interactions, and direct metal-to-metal (M-M) interactions were never taken into consideration.

The first compounds containing direct metal-metal bonds and the

recognition of the existence of clusters was achieved only about 60 years ago. Although these compounds were known by Werner and his contemporaries, the existence of a direct metal-metal bond was not understood. It was only with the application of X-ray crystallographic techniques during the late 1930s and 1940s that Brosset elucidated the existence of metal-metal bonds (e.g.. in $W_2Cl_9^{-3}$ and MoO_2) and metal atom clusters (of the $Mo_6Cl_8^{+4}$ type).

Today the chemistry of the M-M bond is well established. A metal atom cluster may be defined as a core of two or more metals in which there are substantial and direct bonds between the metal atoms. Thus a cluster complex is more than just an ordinary polynuclear complex. There are, of course, borderline cases, i.e. compounds in which the metal-to-metal distances and other properties are such that one cannot say unequivocally whether M-M bonding is "chemically significant." That does not negate the value of recognizing the existence of an enormous number of true, unambiguous metal atom cluster compounds in which the M-M bonds are as important as any other bonds in determining the chemistry and properties of the substance.

Unlike main group chemistry, where atomic orbitals can interact in a σ or π fashion, with the highest possible bond order of 3, (a combination of one σ bond and two π bonds) when two transition metal atoms interact, the most important interactions are realized via the direct overlap of their outermost *d* orbitals. These d orbitals can combine to form σ , π and δ orbitals as shown in Figure 1. If the z axis is chosen as the internuclear axis, the strongest interaction

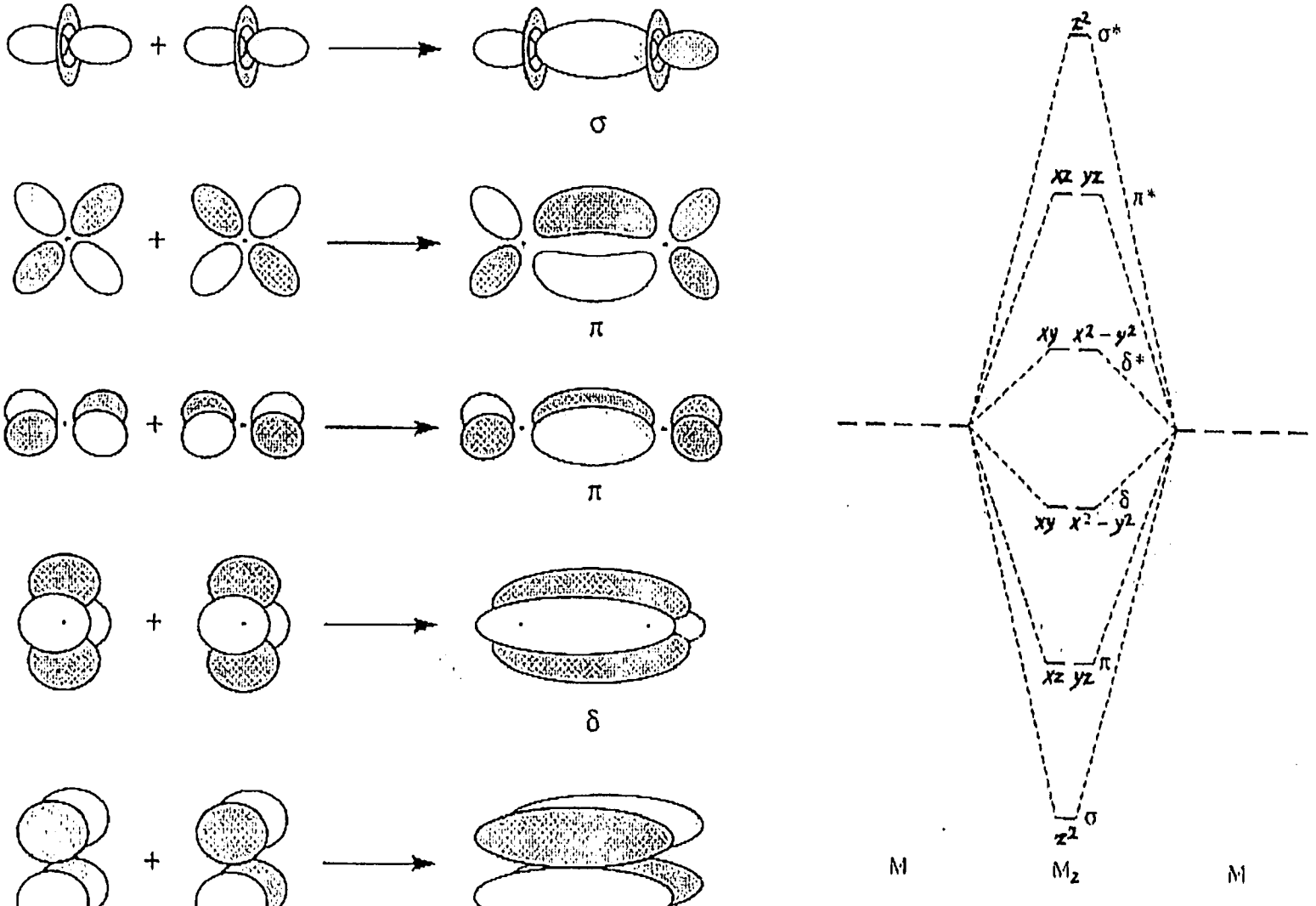

Figure 1

(involving greatest overlap) is the sigma interaction between the *d* orbitals. Next in effectiveness of overlap are the d_{xz} and d_{yz} orbitals, which form π orbital . The last, and weakest, of these interactions are originated by the d_{xy} and $d_{x^2-y^2}$ orbitals; these orbitals interact in four regions forming δ molecular orbitals.

The relative energies of the resulting molecular orbitals are shown in Figure1. In the absence of ligands, an M_2 fragment would have five bonding orbitals resulting from *d-d* interactions, with molecular orbitals increasing in energy in the order σ, π, δ, δ*, π*, σ*.

The unique reactivity of M-M bonds suggests that they may function as an electron reservoir. Several cases of addition of organic functionalities to M-M multiple bonds are established in the literature. Therefore, the unique cuboidal structure of the FeMo cofactor of nitrogenase suggests that M-M interactions may be responsible for the unique ability of this cluster to reduce extremely stable molecules such as N_2.

In order to reduce dinitrogen to NH_3, the vanadium sulfur cubane cluster must be able to provide at least 4 of the 6 electrons necessary for the cleavage. In order to accomplish this, the system must be able to store the electrons without undergoing dramatic changes of geometry. This means that (i) the incoming electron(s) should preferably not populate an MO with an antibonding character and (ii) an intricate "web" of electron density delocalized over the whole structure should be present.

In this chapter our efforts will be focused on clarifying the electronic

aspects of several metal-sulfido clusters. We will also investigate the molecular orbitals (shape, energy distribution, degeneracy) that are responsible for metal-metal bonding and the effect of the ligand on this interaction.

Results and discussion

Extended Hückel calculations were performed on a cubane cluster, with the atomic coordinates of the non-hydrogen atoms obtained from the X-ray crystal structure of CpVS. The Cp ligand was replaced by the hypothetical NH_2 group. The calculation correctly predicted a multiplicity of 3 for the system, due to the near degeneracy of HOMO and HOMO-1 (gap 0.01 eV). The bond order between the vanadium atoms (bo=1/3) is rather low. The HOMO (-10.77 eV) (Figure 2) consists of a delocalized lobe over the faces of the cuboidal structure, thus bridging the sulfur to the vanadium atoms. The next MO of interest are HOMO-1 (-10.78 eV) and HOMO-2 (-10.79 eV) (Figure 3) whose shapes clearly show the possibility that the vanadium atoms electronically communicate with all of their sulfur neighbors. Another MO featuring similar characteristics is HOMO-3 (-11.87 eV) (Figure 4) which shows a large lobe over the three V-S-V centers, thus generating σ type bonds between the two vanadium atoms and the sulfur. The next MOs are HOMO-5 (-12.04 eV), HOMO-6 (-12.11 eV) and HOMO-7 (-12.22 eV) (Figure 5). These orbitals have a strong M-M σ-bond character. However, the direct overlap between the vanadium orbitals seems to be rather weak, while the contribution of the sulfur atomic orbitals is dominant. HOMO-11 (-13.08 eV)

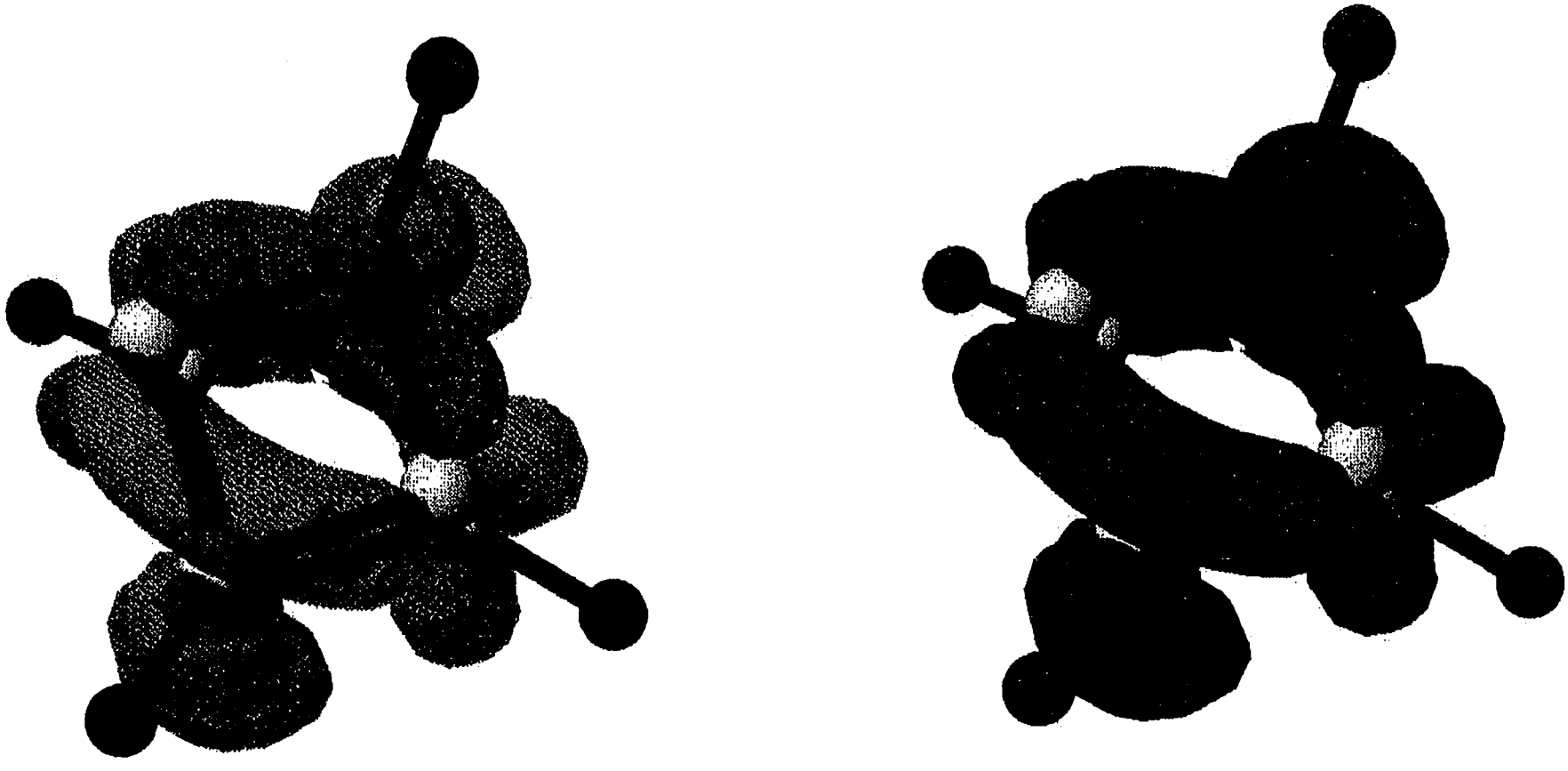

Figure 2

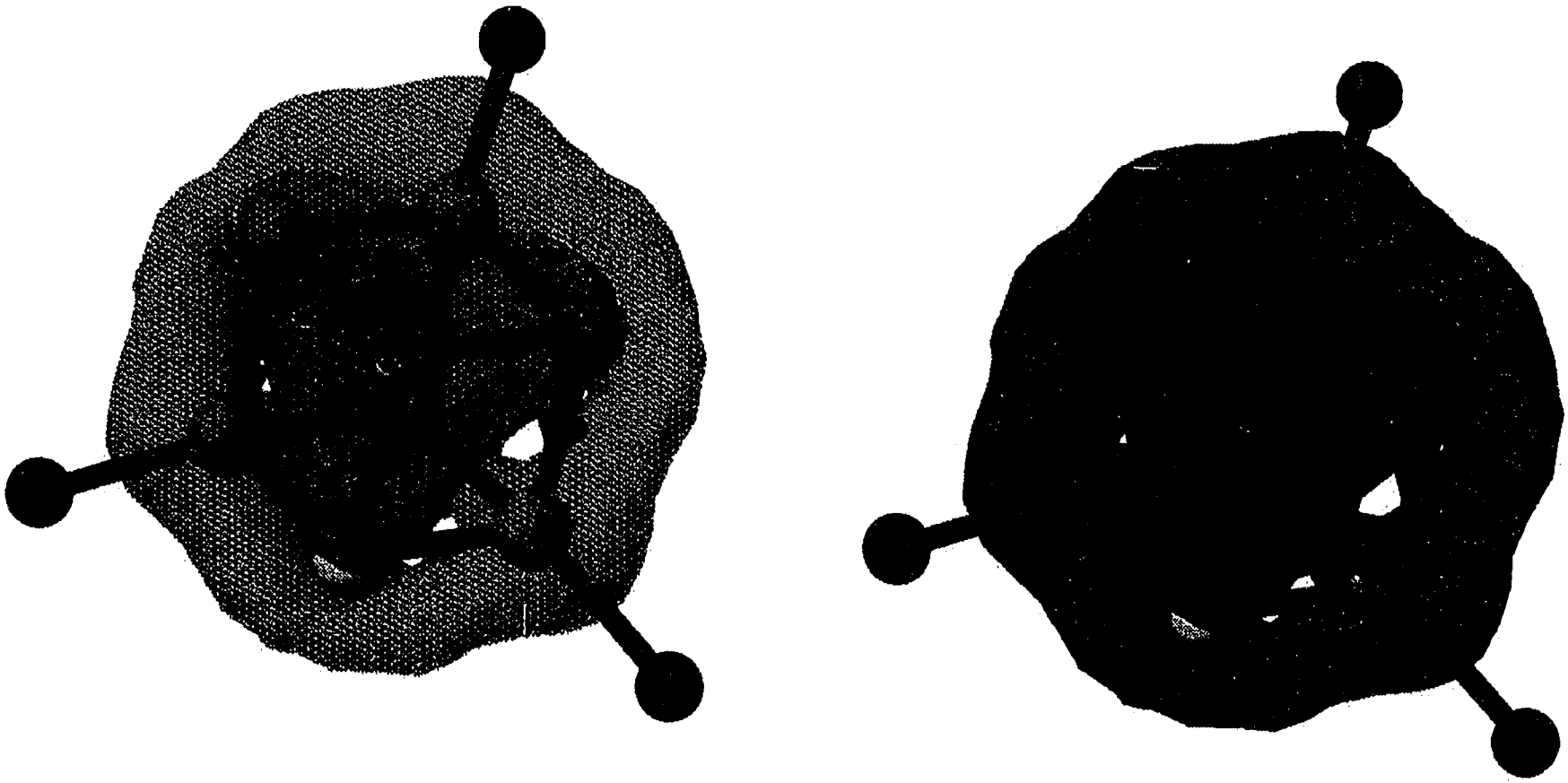

Figure 3

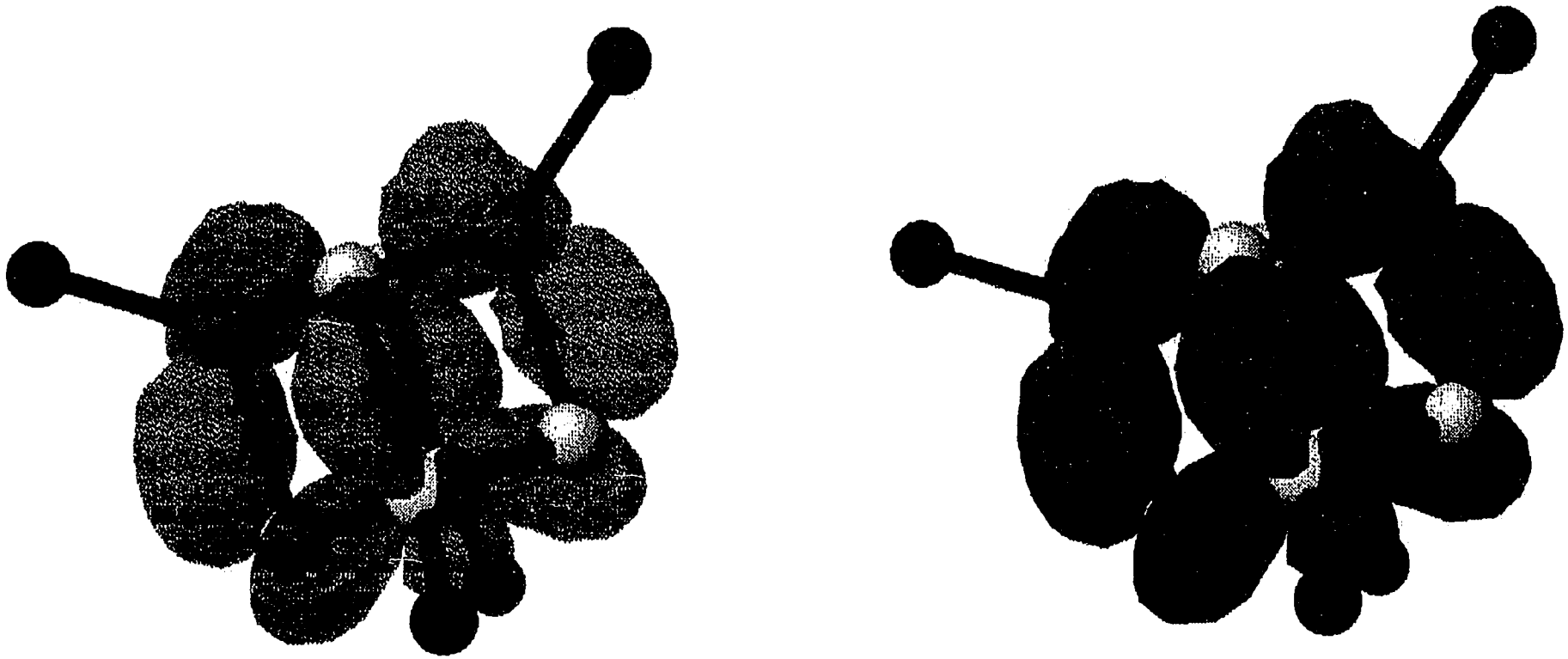

Figure 4

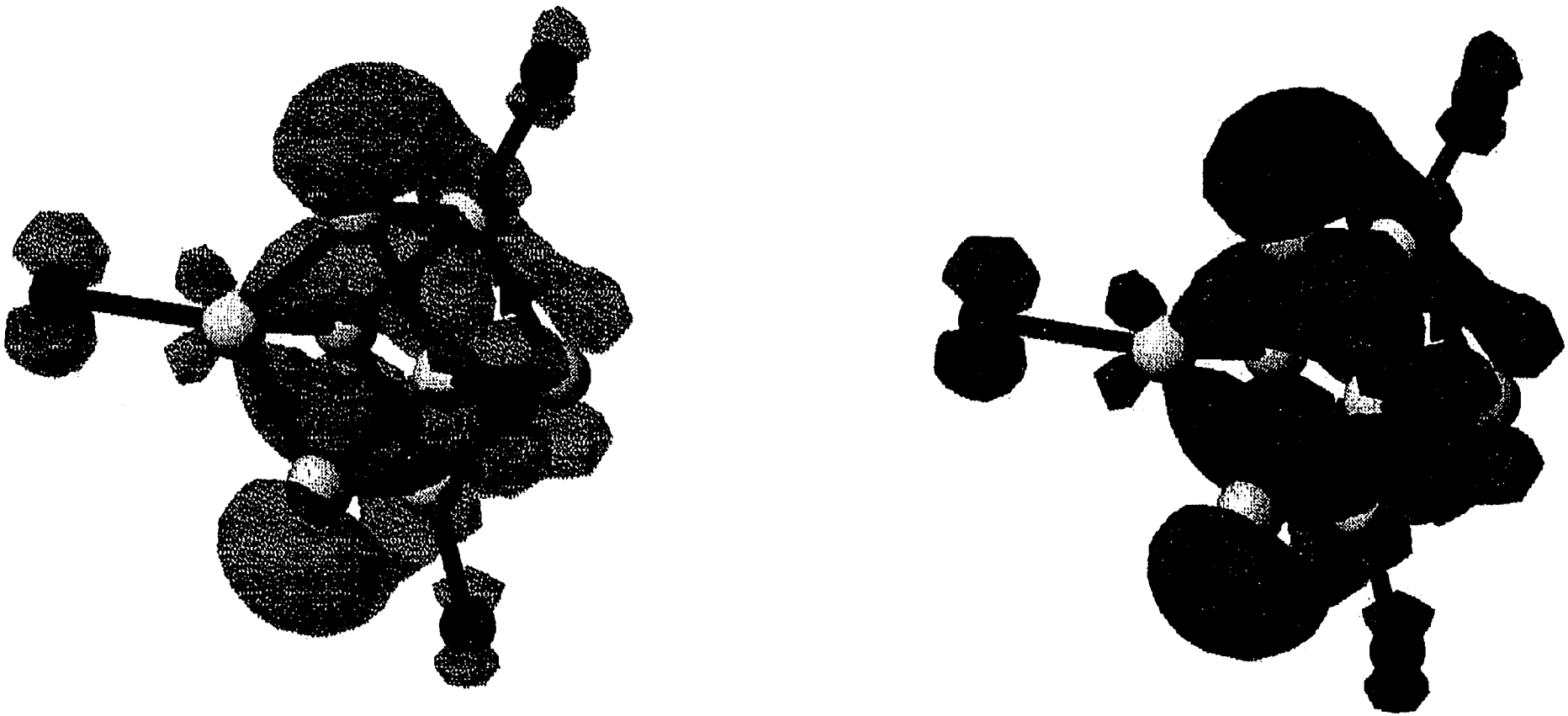

Figure 5

(Figure 6) consists of an electronic density covering four faces of the cuboidal structure. This type of overlap ensures electronic communication between all the sulfur and vanadium atoms. A similar situation is found in HOMO-15 (-13.56eV) (Figure 7), although in this case the overlap of vanadium and sulfur atomic orbitals form a unique centrosymmetric orbital located in the center of the cuboidal frame. The only MO featuring a direct M-M interaction without the participation of sulfur AOs is HOMO-24 (-15.088 eV) (Figure 8). This MO consists mainly of a V-N σ bond with significant electronic density inside the cavity of the cube, allowing electronic communication between all four metal centers.

Although the cubane cluster features remarkable MO shapes, it is difficult to clearly define the AO responsible for their formation due to the high level of hybridization. Therefore, in order to better understand the electronic configuration of the cuboidal structure, simpler systems such as M_2X_2 cores were studied. These systems have the advantage of being less complicated, but are still the building block of the cuboidal structure.

For this reason ab initio and extended Hückel calculations were carried on M_2X_2 cores. Several aspects such as the metal, the bridging ligand and the steric hindrance were changed in order to understand the effect on the MO and the paramagnetism of the system and the conditions that favor metal-metal bonding.

The absence of a straightforward correlation between magnetic behavior and intermetallic separation is striking in the particular case of dinuclear

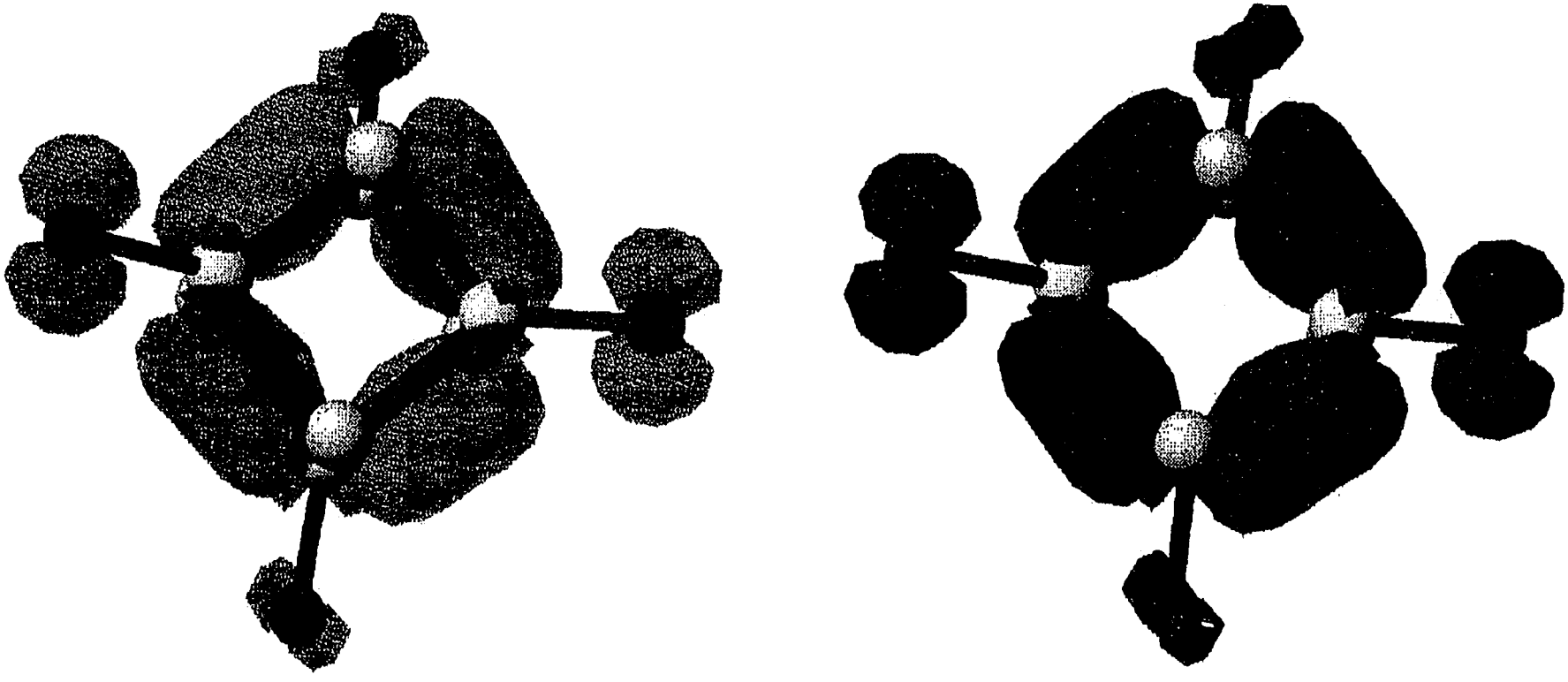

Figure 6

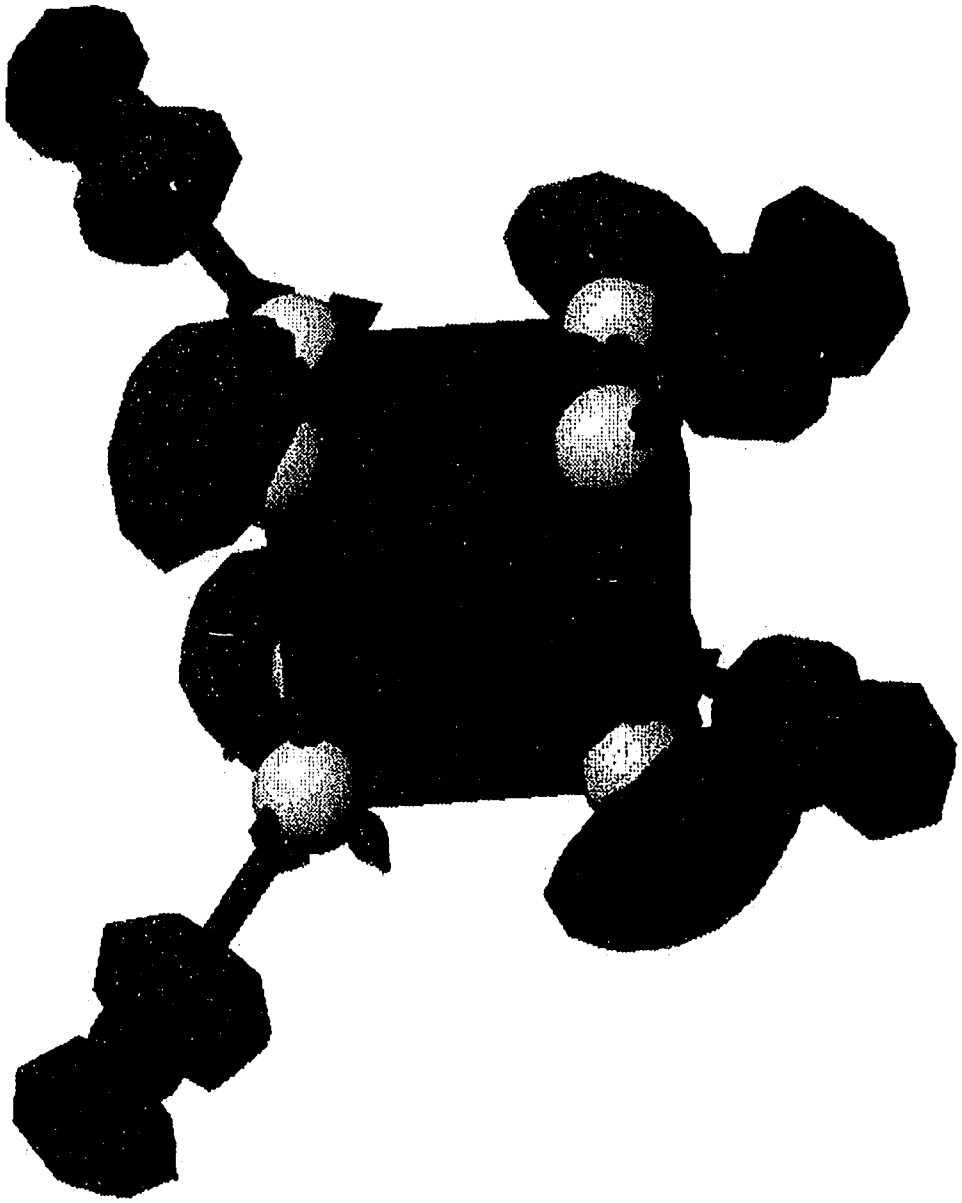

Figure 7

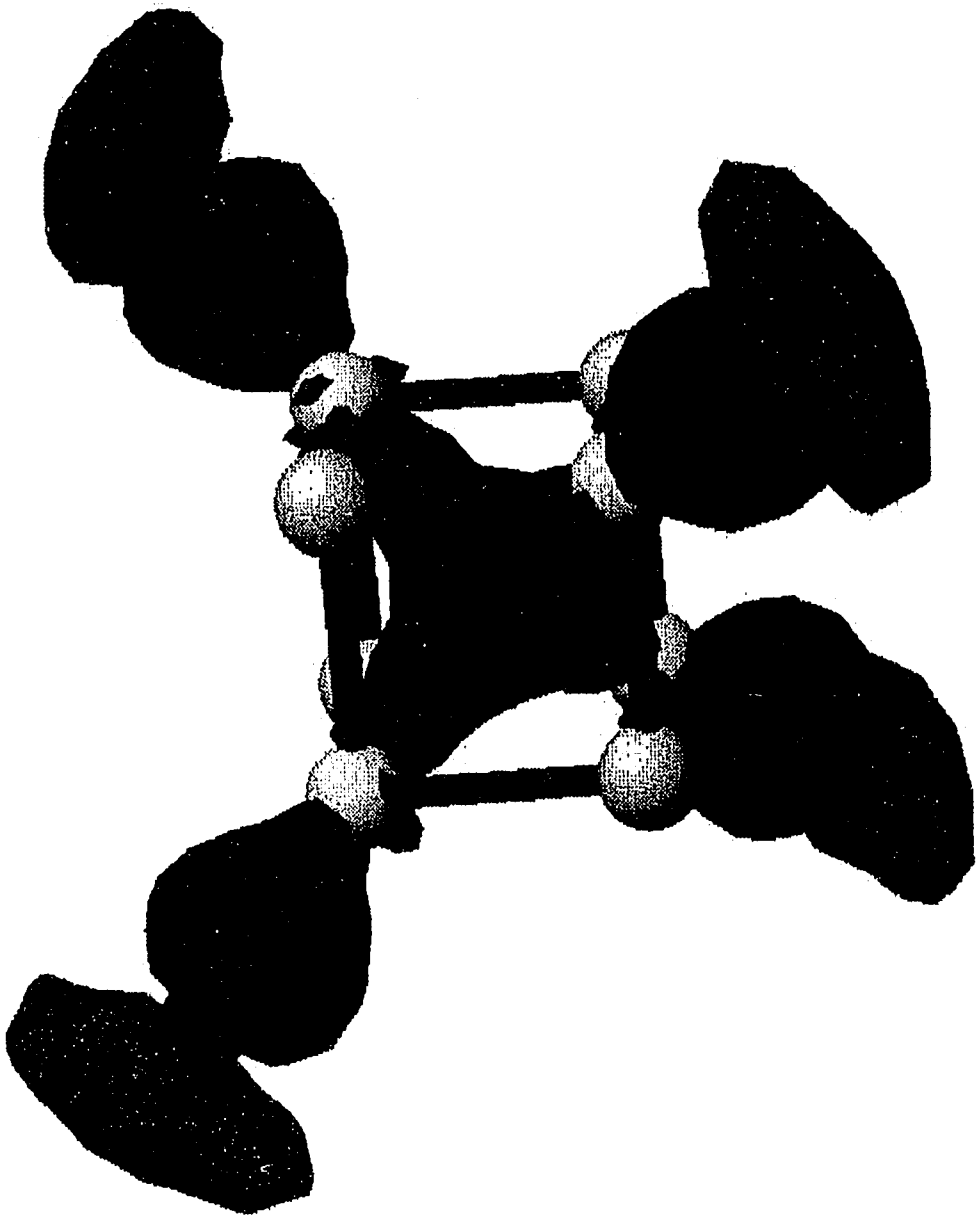

Figure 8

vanadium(IV) complexes. Diamagnetic complexes have been obtained with V-V distances up to 2.97 Å [1], while paramagnetic species have been found with V-V distances as short as 2.514 Å [2]. Even more striking, two divanadium complexes with the same bridging persulfide group have been reported, one being diamagnetic and the other paramagnetic, with long and short intermetallic distances, respectively [2]. An other example of this contradictory behavior is seen in the magnetic behavior of the following two isostructural complexes: $\{[(Me_3Si)_2N]_2V\}_2(\mu\text{-}O)_2$ and $\{[(Me_3Si)_2N]_2V\}_2(\mu\text{-}S)_2$.

Recently, Verkade et al. have described the preparation and characterization of the $\{[(Me_3Si)_2N]_2V\}_2(\mu\text{-}O)_2$ (Figure 9) dimer featuring a V-V distance of 2.612 Å [3].

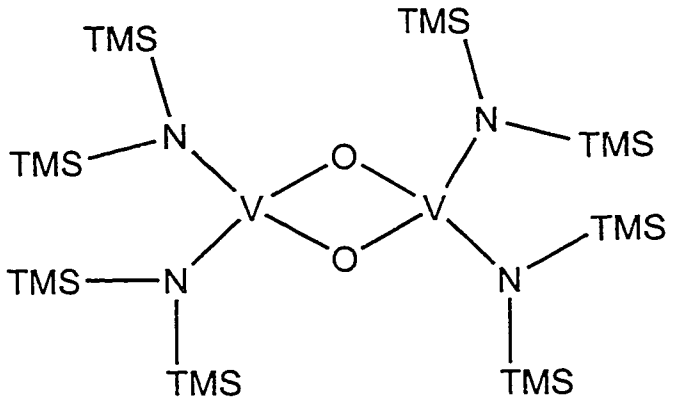

Figure 9

The paramagnetism of this species was nicely explained by eHMO calculations with the presence of a pair of nearly degenerate HOMO's primarily metal centered and with V-V bonding character (σ and π). By using a different synthetic approach, we have now obtained and characterized an essentially

isostructural compound, $\{[(Me_3Si)_2N]_2V\}_2(\mu\text{-}S)_2$, where the bridging oxides were replaced with sulfide (Figure 10).

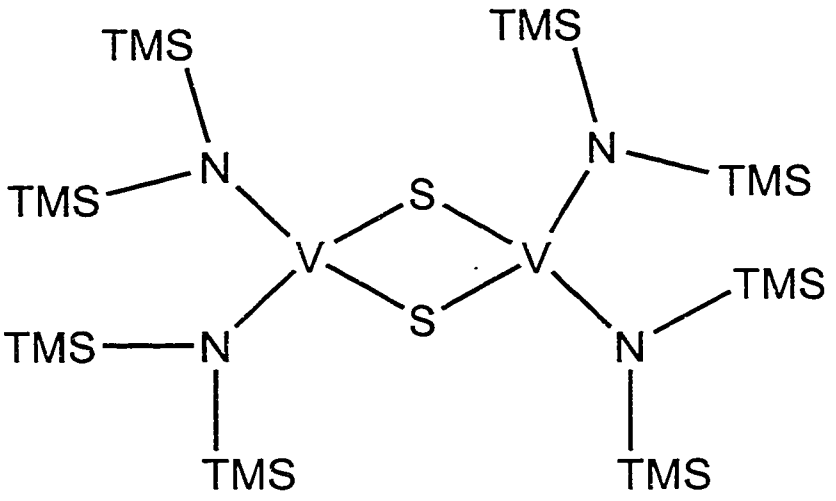

Figure 10

As mentioned in chapter II, this new compound, *in spite of having a longer intermetallic distance, is diamagnetic.* Thus to clarify the nature of the V-V interaction in these two complexes we have carried out *ab initio* HF/STO-3G calculations using $\{[(H_3Si)_2N]_2V\}_2(\mu\text{-}S)_2$ as a model. The intermetallic vector was selected as the z axis, while the x axis was perpendicular to the plane of the V_2X_2 core (X=S, O). The geometrical parameters of the non-hydrogen atoms were those obtained from the X-ray crystal structure. The HOMO-LUMO gap is not particularly large (0.334 eV), but it is still sufficient to account for the diamagnetism (Figure 12). Of the 121 populated bonding MOs only the HOMO (-0.129 eV) showed a significant V-V bond character. This molecular orbital is mainly generated by the overlap of two identical hybrid combinations of d_{x2-y2} and

d_{z2} atomic orbitals (MO factor 0.44 and 0.43. respectively) of each vanadium atom with the p_y orbitals of the bridging sulfur atoms. The shape of this orbital, which lies on the intermetallic vector, is strongly reminiscent of a M-M σ-bond. However, the overlap between the vanadium orbitals seems to be rather weak, and the contribution of the sulfur p_y orbitals to its formation (MO factor = 0.13) is significant. The next two lower MOs are located at -0.224 and -0.231 eV and are mainly sulfur-centered with a minor V-S π character. Two V-S σ-bonds, mainly arising from the overlap of the vanadium d_{yz} orbitals with the p orbitals of the two sulfur atoms, are respectively the HOMO-3 (-0.258 eV) and HOMO-5 (-0.282 eV). A third V-S σ-bond (HOMO-10) was located lower in energy at -0.353 eV. This orbital is constructed with the same combination of vanadium atomic orbitals which form the V-V σ-bond and the p_z orbitals of the bridging sulfur atoms. A V-S π-bond (HOMO-6) was found at -0.305 eV and is formed by the combination of the vanadium d_{xz} orbitals with the p_x orbitals of the two sulfur atoms, forming two largely delocalized lobes on the two sides of the V_2S_2 plane, thus conferring a formal bond order significantly higher than unity to the V-S bond (average V-S bond order = 1.22). This bond can be regarded as possessing weak V-V π-bond character. The p orbitals of the amido nitrogen atoms also significantly contribute to the formation of this largely delocalized molecular orbital.

The results of these calculations clearly indicate that the magnetic coupling between the two metal centers of the sulfido complex is mainly realized via a direct V-V σ-bond. While this is not particularly surprising *per se,* it makes

the paramagnetism of the corresponding oxo analogue even more difficult to understand especially when considering that this species has a considerably shorter V-V distance. In fact one could reasonably expect that if the magnetic coupling in the sulfido complex is realized via direct V-V interaction, the shorter intermetallic distance of the oxo analogue should lead to an even better overlap of the d orbitals. Since this is in contrast to the experimental observations, we have recalculated the oxo derivative by using the same *ab initio* theoretical approach. The energy gap between the LUMO and the singly occupied HOMO (0.347 eV) compares well with that calculated for the sulfido compound (Figure 11 and 12). The HOMO and the SOMO are located respectively at -0.142 and -0.205 eV and are very different in character. Similar to the sulfido complex , the HOMO is mainly a V-V centered molecular orbital and is formed by the same hybrid combination of d_{x2-y2} and d_{z2} (MO factors = 0.42 and 0.43. respectively) atomic orbitals of the vanadium atoms with the p_y orbitals of the two oxygen atoms. The difference with respect to the analogous orbital of the sulfido complex is that the contribution of the p_y orbital of the bridging atoms is now more pronounced (MO factor = 0.21) than in the case of sulfur, probably as a result of the shorter V-V distance. The next singly populated MO orbital (SOMO -0.205 eV) is nonbonding with respect to V-V. A π molecular orbital (HOMO-11 -0.356eV), mainly originating from the overlap of the d_{xz} of the two vanadium atoms and the p_x orbitals of the two oxygens, forms two large lobes delocalized on the two sides of the V_2O_2 plane. Although this orbital has some V-V π-bond character, the

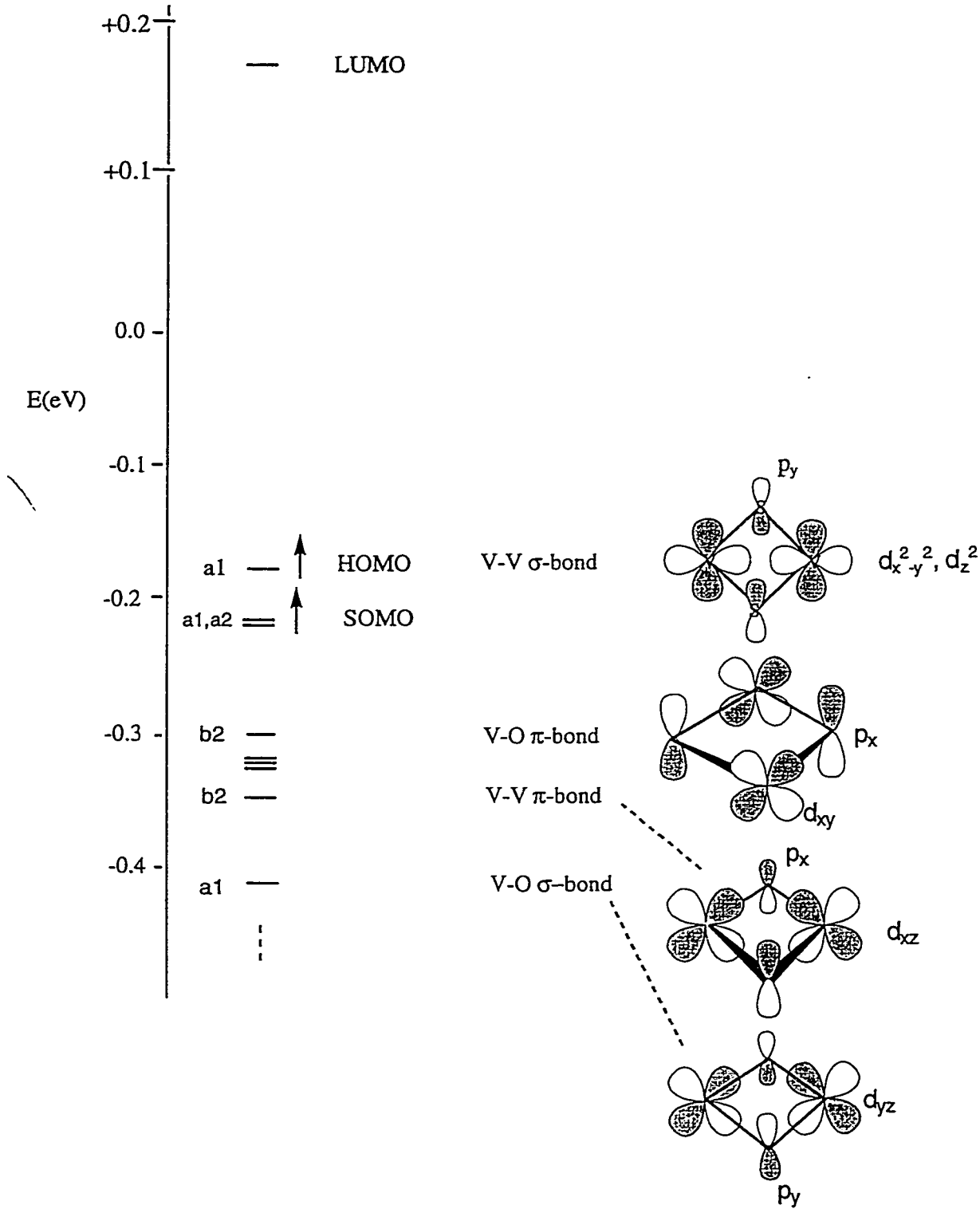
+0.2
LUMO
+0.1
0.0
E(eV)
-0.1
a1
HOMO
-0.2
a1,a2
SOMO
-0.3
b2
b2
-0.4
a1
V-V σ-bond
V-O π-bond
V-V π-bond
V-O σ–bond
py
dx2-y2, dz2
px
dxy
px
dxz
dyz
py

Figure 11

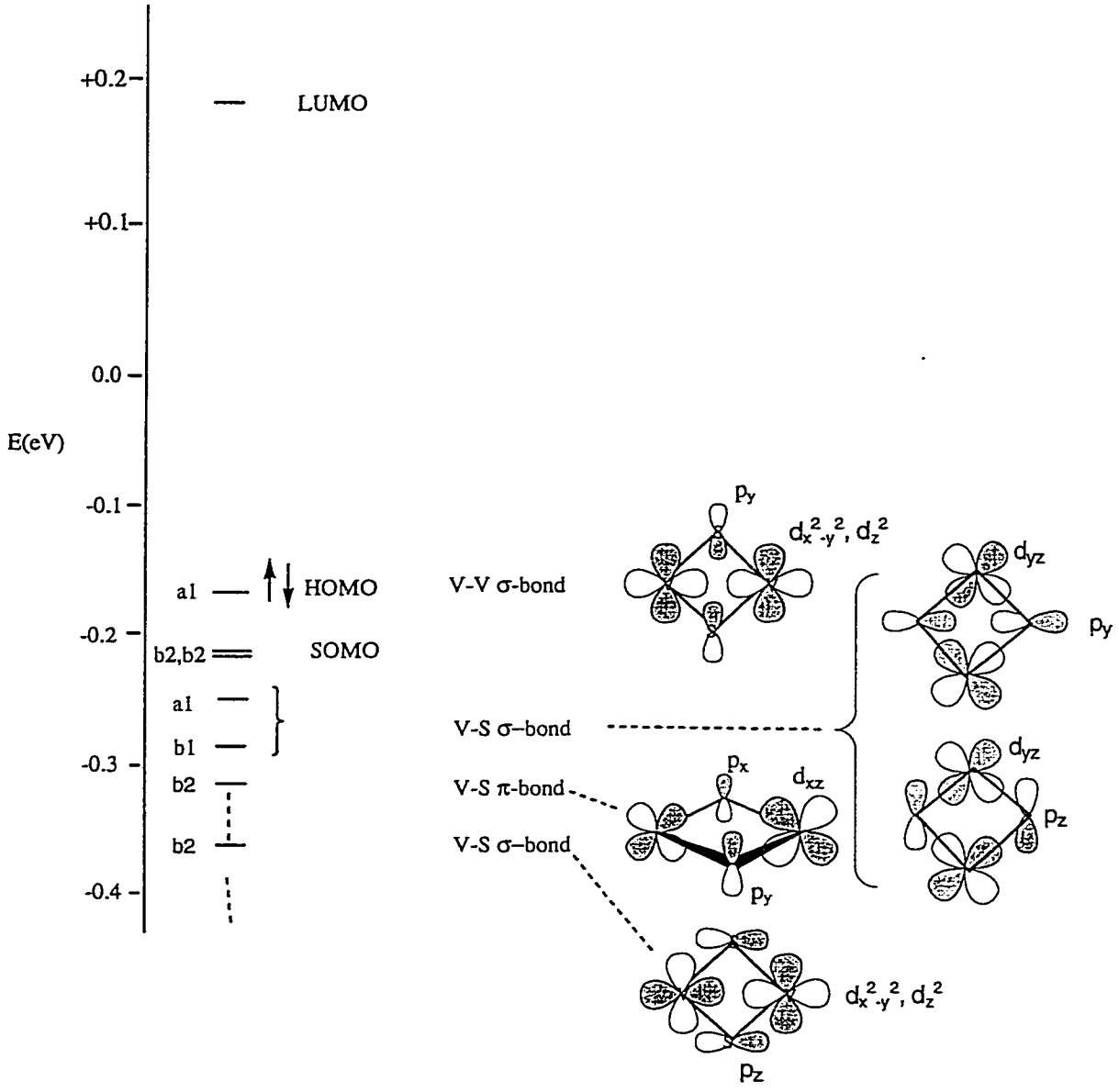
+0.2
LUMO
+0.1
0.0
E(eV)
-0.1
a1
HOMO
-0.2
b2,b2
SOMO
a1
b1
-0.3
b2
b2
-0.4
V-V σ-bond
V-S σ–bond
V-S π-bond
V-S σ–bond
py
dx2-y2, dz2
dyz
py
dyz
px
dxz
pz
py
dx2-y2, dz2
pz

Figure 12

contribution of the oxygen atomic orbitals is comparable (MO coefficient 0.22) to that of the vanadium d orbitals (MO coefficient 0.31). The combination of atomic orbitals which compose this particular MO is the same as that which composes the V-S π-orbitals of the sulfido complex. However, while in the case of the sulfido complex the V-V π-bond character is only minor, it appears to be more significant in the case of the oxide complex. Once again this is probably the result of the shorter intermetallic distance caused by the two bridging oxides. The formation of two different V-V bonds, both σ and π in character, is in good qualitative agreement with the results of the previously reported EHMO calculation. A V-O-V π-bond is found at -0.303 eV (HOMO-6) and is mainly generated by the π-overlap of the d_{xy} of the two vanadium atoms and the p_x orbitals of the two bridging oxides. Curiously such an orbital was not found in the case of the sulfido complex. The V-O-V σ-bond was located at -0.406 eV (HOMO-16) and is formed by the overlap of the vanadium d_{yz} orbitals with the p_y of the oxygens.

On the basis of this theoretical work, we are unable to provide a simple and straightforward explanation of the striking difference between the magnetic properties of the two complexes other than trivial arguments based on the near HOMO-SOMO degeneracy. We observed that, in the case of 1, at least two MOs (HOMO-9 and -16) show a significant S-S σ-bond character. Similar orbitals are not present among the MOs of the oxo-bridged complex. On the other hand, given the long S-S distance (3.3 Å), we are unable to evaluate the significance of these

orbitals and the relative contribution of this additional interaction to the coupling of the d electrons. However, these MOs involve a rather substantial participation of the vanadium orbitals. At this stage it is tempting to speculate that this additional S-S interaction plays an important role in determining the diamagnetism of the sulfido complex.

Even though these complexes possess efficient electronic communication between the metal center and the ligand, they show very little direct metal-metal interaction. This is clearly seen in the V-V bond order which is considerably lower than one. In contrast with vanadium, chromium has more ability to form metal-metal bonds. On the other hand, multiple Cr-Cr bonds are intriguing since they are expected to be very weak. In other words, they may work as electronic reservoir, which may be important for N_2 activation process. However, Cr-Cr bonds were described only for the divalent state and the particular paddle-wheel systems. In an attempt to generalize the behavior of the Cr-Cr interaction we have attempted calculations on the Cr_2X_2 units. Semi-empirical PM3(tm) calculations were selected as a compromise between efficiency and accuracy.

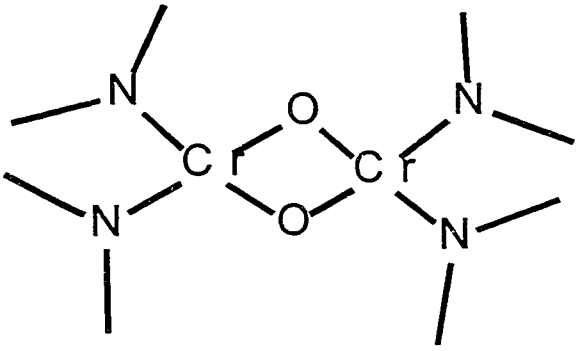

Figure 13

The fractional atomic coordinates of the crystal structures of the Cr_2O_2 core type complex (Figure 13) prepared by K.B.P. Ruppa[4], were converted to the corresponding cartesian coordinates. The adamantyl and the phenyl groups were converted to methyl groups, for simplicity. The output of the calculation on the triplet state showed a small gap between the HOMO (-7.45 eV) and HOMO-1 (-7.66 eV) which nicely accounts for the observed paramagnetism. There are four MOs which account for the direct Cr-Cr interaction (Figure 14). The orbital HOMO-3 (-9.02 eV) is a very weak Cr-Cr σ-bond. The bond is realized via a marginal overlap of the two lobes of d_{z^2},d_{yz} hybrid combinations of each chromium atom lying on the intermetallic vector. The bridging oxygen atoms contribute to some extent to the formation of the MO by using the hybrid combinations p_x/p_y. The other three are located much lower in energy. The first is again a sort of Cr-Cr σ-bond (HOMO-32, -16.84 eV) and is realized with the overlap of the lobes of the $d_{x^2-y^2},d_{yz}$ hybrid combinations placed on the

intermetallic vector, with hybrid p_z,p_y

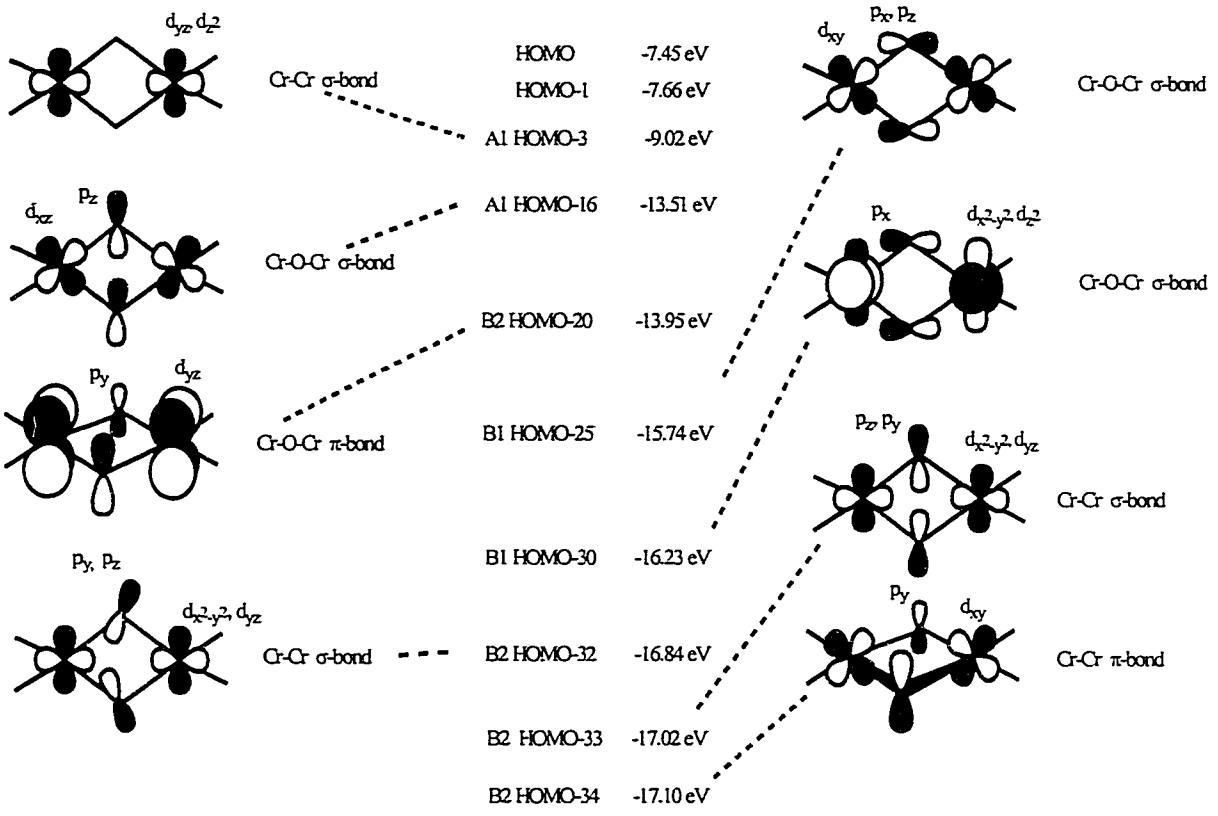

Figure 14

combination of the bridging oxygen atoms. This MO forms a large lobe delocalized in the center of the Cr_2O_2 core. The same hybrid combination with the participation of the p_y orbitals of the bridging oxygen atoms is used for the next MO (HOMO-33, -17.02 eV) to originate a weak Cr-Cr σ-bond. A Cr-Cr π-bond (HOMO-34, -17.10 eV) is originated by the overlap of the d_{xy} orbitals of the two

chromium atoms with a strong participation of the bridging oxygen p_y orbitals. The MO thus consists of two rather symmetric lobes on the two sides of the Cr_2O_2 core. These four MOs bring all together the overall Cr-Cr bond order to 0.4. In order to verify if chromium will present diamagnetic behavior with sulfur, like vanadium, and to clarify the magnetic behavior and the nature of the Cr-Cr interaction, *ab initio UHF/STO-3G* calculations were performed on $[(RR'N)_2Cr]_2(\mu\text{-}S)_2$ [R = R' = Cy ; R = Ad, R' = 3,5-Me_2Ph] [5] using $[(Me_2N)_2Cr(\mu\text{-}S)]_2$ (Figure 15) as a model, with the atomic coordinates of the non-hydrogen atoms obtained from the X-ray crystal structure.

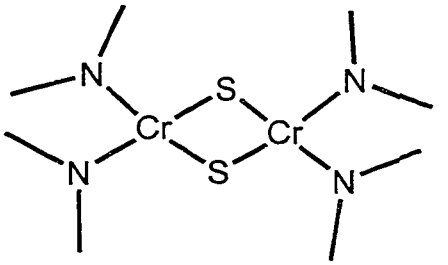

Figure 15

The adamantyl and the phenyl groups were converted to methyl groups during calculation for simplicity's sake. Given the value of the magnetic moment, [μ_{eff} = 2.15 μ_B *per dimeric unit* at room temperature], the triplet state was considered to be the most reasonable basis for the calculations (calculations carried out on the quintet state yielded a significantly higher value of the total energy). The result showed a rather small HOMO-LUMO gap of 0.245eV, which may well account for the low paramagnetism (Figure 15-a). The two unpaired electrons were located in two frontier orbitals, namely the HOMO (-0.216eV) and

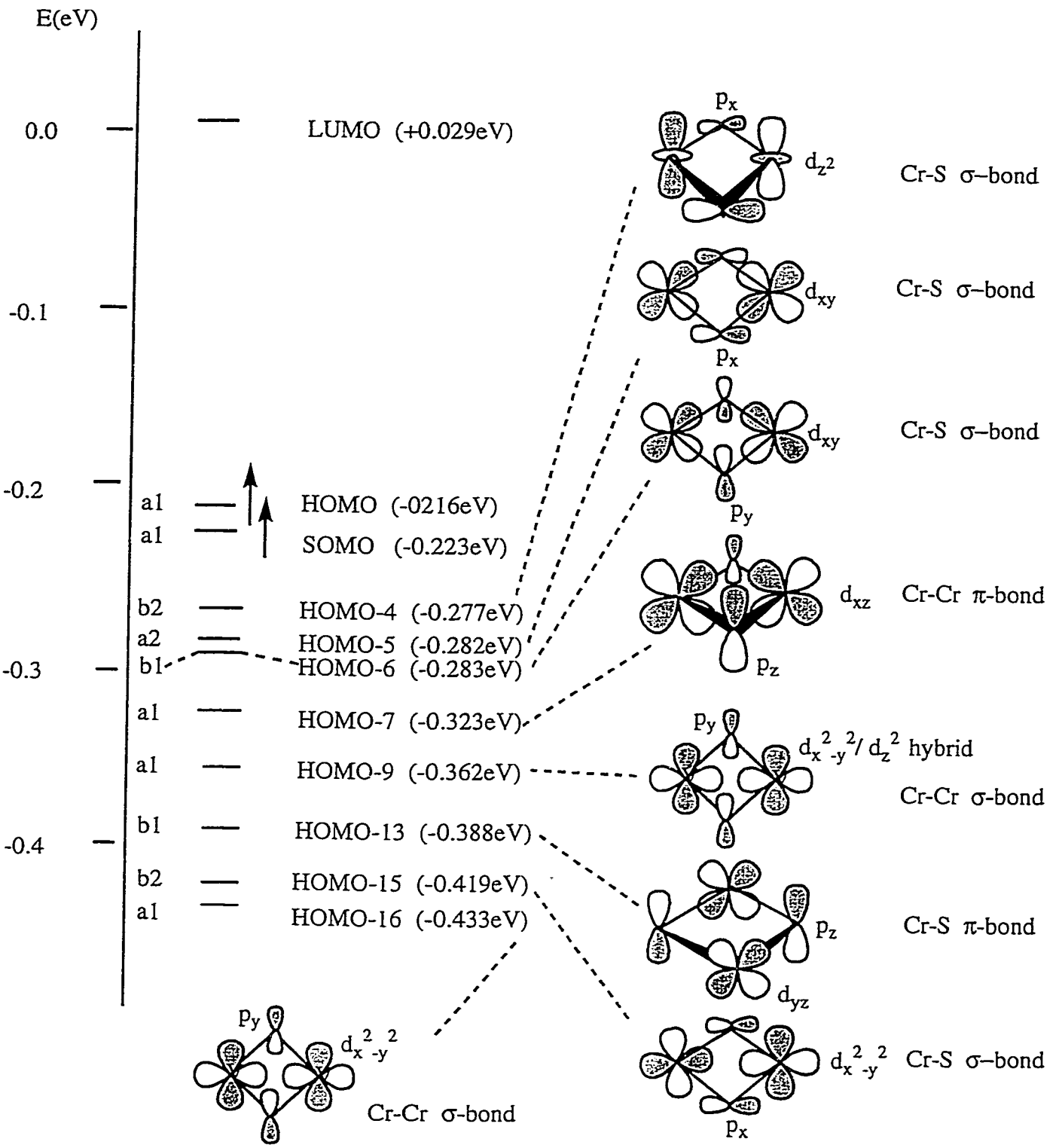
E(eV)
0.0
-0.1
-0.2
-0.3
-0.4
LUMO (+0.029eV)
HOMO (-0216eV)
SOMO (-0.223eV)
HOMO-4 (-0.277eV)
HOMO-5 (-0.282eV)
HOMO-6 (-0.283eV)
HOMO-7 (-0.323eV)
HOMO-9 (-0.362eV)
HOMO-13 (-0.388eV)
HOMO-15 (-0.419eV)
HOMO-16 (-0.433eV)
a1
a1
b2
a2
b1
a1
a1
b1
b2
a1
Cr-S σ–bond
Cr-S σ–bond
Cr-S σ–bond
Cr-Cr π-bond
dx2-y2/ dz2 hybrid
Cr-Cr σ-bond
Cr-S π-bond
Cr-S σ–bond
Cr-Cr σ-bond

Figure 15-a

the next lower MO [HOMO-1 (-0.223eV)]. The near degeneracy of these two orbitals nicely explains the significant decrease of the magnetic moment observed at low temperatures. These two orbitals are Cr-N centered with a weak Cr-S antibonding character. The bonding of the Cr_2S_2 core is mainly realized with five molecular orbitals. Four of them [HOMO-4 (-0.277eV), HOMO-5 (-0.282eV), HOMO-6 (-0.283eV) and HOMO-15 (-0.419eV)] possess a marked σ-character with respect to the Cr-S bond, while the fourth one [HOMO-13 (-0.388eV)] is mainly a Cr-S π-bond. The four Cr-S σ-bonds are originated by the chromium *d* orbitals (or hybrid combinations) with in-plane *p* orbitals of the bridging sulfide. Conversely, the Cr-S π-bond is formed by the two out-of-plane d_{yz} chromium orbitals with p_z of the two bridging sulfur. Three more MO's also are Cr-S bonds but display some significant Cr-Cr bond character. Two of them [HOMO-9 (-0.362eV) and HOMO-16 (-0.433eV)] are reminiscent of Cr-Cr σ-bonds. The two orbitals are similar in shape and are formed by the overlap of the sulfur p_y orbitals with either the d_{x2-y2} or a hybrid combination of d_{z2} with d_{x2-y2} orbitals of the two chromium atoms. Both orbitals are characterized by the presence of a large lobe delocalized between the four core atoms and which may be regarded as Cr-Cr σ-bonds. However, the participation of the bridging atoms atomic orbitals is very substantial. A third orbital (HOMO-7) located at -0.323 eV is formed by the overlap of the sulfur p_z with the two d_{zx} orbitals of the two chromium atoms, thus forming two large lobes on the two sides of the Cr_2S_2 core. This MO may be regarded as a sort of Cr-Cr π-bond which, again, involves the atomic orbitals of

the bridging sulfur atoms in a rather important manner. The overall Cr-Cr bond order is 0.21.

These observations indicate that the electronic coupling between the two d^2 Cr atoms may involve mechanisms other than a direct M-M bond. While the direct Cr-Cr interaction appears to be weak, and certainly unable to hold together the dinuclear frame in the absence of bridging atoms, the Cr-Cr "bonds" made with the determinant participation of the bridging atom orbitals provide a rather efficient coupling between the two metal centers and, ultimately, are probably responsible for the low magnetic moments. The fact that the bond order between the two metallic centers, in the four previous examples, is low does not come as a surprise. This phenomenon is probably due to the fact that for the elements of the fourth period, the most outer *d* orbitals are less diffuse than those of the fifth and sixth period.

Therefore the electronic properties of several complexes containing heavier transition elements such as niobium were investigated in order to understand more about the nature of the interaction between the two metals. In particular, we have decided to focus on Nb, since it belongs to the same group of vanadium.

Several complexes of the group V metals containing single and double metal-metal bonds have been reported over the last few years. Complexes with double M-M bonds (M=Nb,Ta) have been synthesized by reduction of the pentahalides in the presence of ligands such as SMe_2 [6], THT

(THT=tetrahydrothiophene) [7], PMe_3 [8], and PMe_2Ph [9]. The bridging thioester originates face sharing bioctahedral complexes of the type $M_2X_6L_3$ whereas the phosphine ligands give edge sharing bioctahedral spieces of the kind $M_2X_6L_4$. A rich and diverse chemistry has been reported for both types of compound. These species have been used to form other niobium and tantalum complexes containing single and double M-M bonds [10]. Compounds with single bonds have also been obtained upon reduction of the penthalides with one equivalent of a reducing agent or by reacting monomeric $NbCl_4L_2$ (L= THF, CH_3CN) with ligands such as MeOH or PMe_3 [11].

The M-M bond in these species are surprisingly long, and thus to evaluate their properties it is important to prepare a variety of multiply bonded systems with the greatest possible diversity of ligand environments.

The complex $Nb_2Cl_6(TMEDA)_2$ (Figure 16) features an intermetallic distance of 2.764 Å, which corresponds to a M-M single bond distance [12]. In order to elucidate the bonding, an STO-3G *ab initio* calculation was carried out with the coordinates of the non hydrogen atoms obtained from the crystal structure. Given the paramagnetism, a triplet state was considered to be the most reasonable basis for the calculation. The result showed a HOMO SHOMO gap of (0.05 eV) which nicely explains the paramagnetism of the molecule.

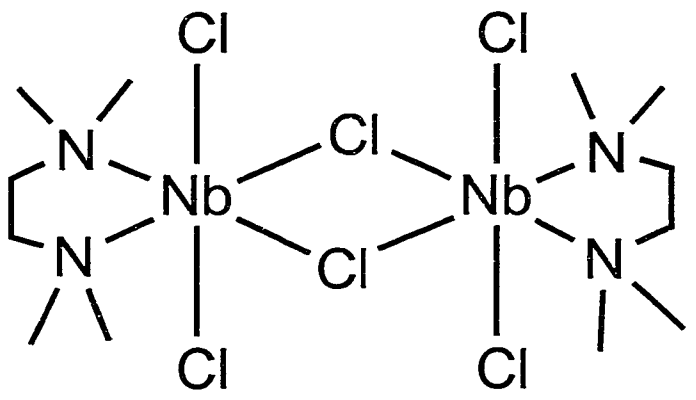

Figure 16

The HOMO located at -0.100eV is mainly centred on the metal atoms. The molecular orbital is formed by the d_{xy} of each niobium atom[Mo factor: d_{xy} (0.66)]. The next occupied orbital (HOMO-1) (Figure 17), is nearly degenerate with the HOMO and shows some π character. This MO is formed by the overlap of the d_{yz} orbitals of each niobium. The last MO relevant to M-M bonding (HOMO-2 -0.19 eV) (Figure 18) is formed by a hybrid combination of atomic orbitals of each niobium atom [MO factors: d_{x2-y2} (0.20), d_{z2} (0.59)]. The overlap of these hybrid orbitals generates a σ bond between the two metallic centres. The calculation also reveals a significant bond order of 1.36 between the two niobium centres which accounts for a σ bond and a partial π bond.

$Nb_2(\mu\text{-}Cl_3)(\mu\text{-}Li)(TMEDA)_3$ (1)(Figure 19) prepared by M. Tayebani [13] reavealed a very short Nb-Nb distance [Nb-Nb 2.4001(5) Å] and a diamagnetic behaviour. In this case the shortness of the intermetallic distance contrasts with those of the few previously reported divalent diniobium or ditantalum THF

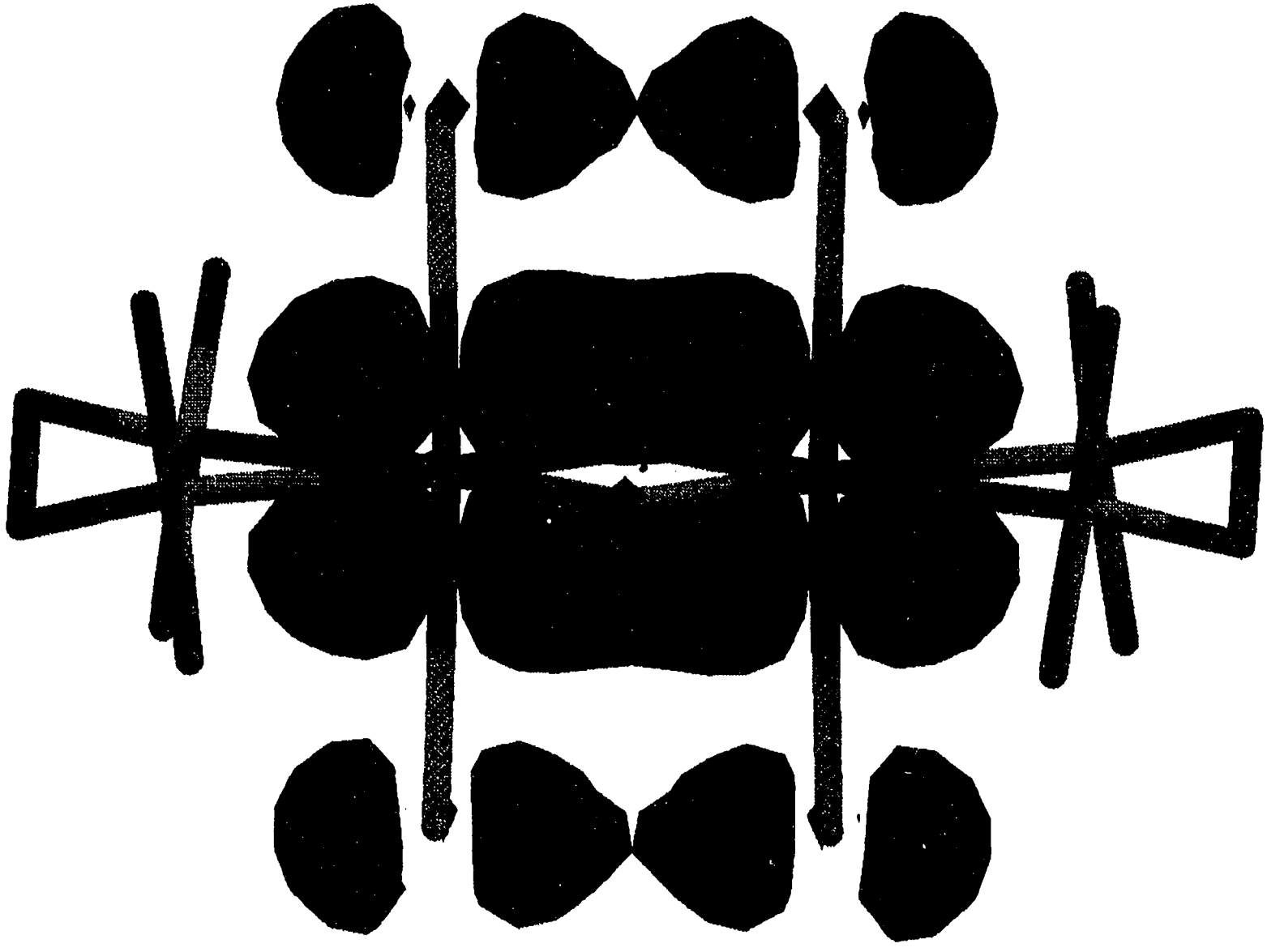

Figure 17

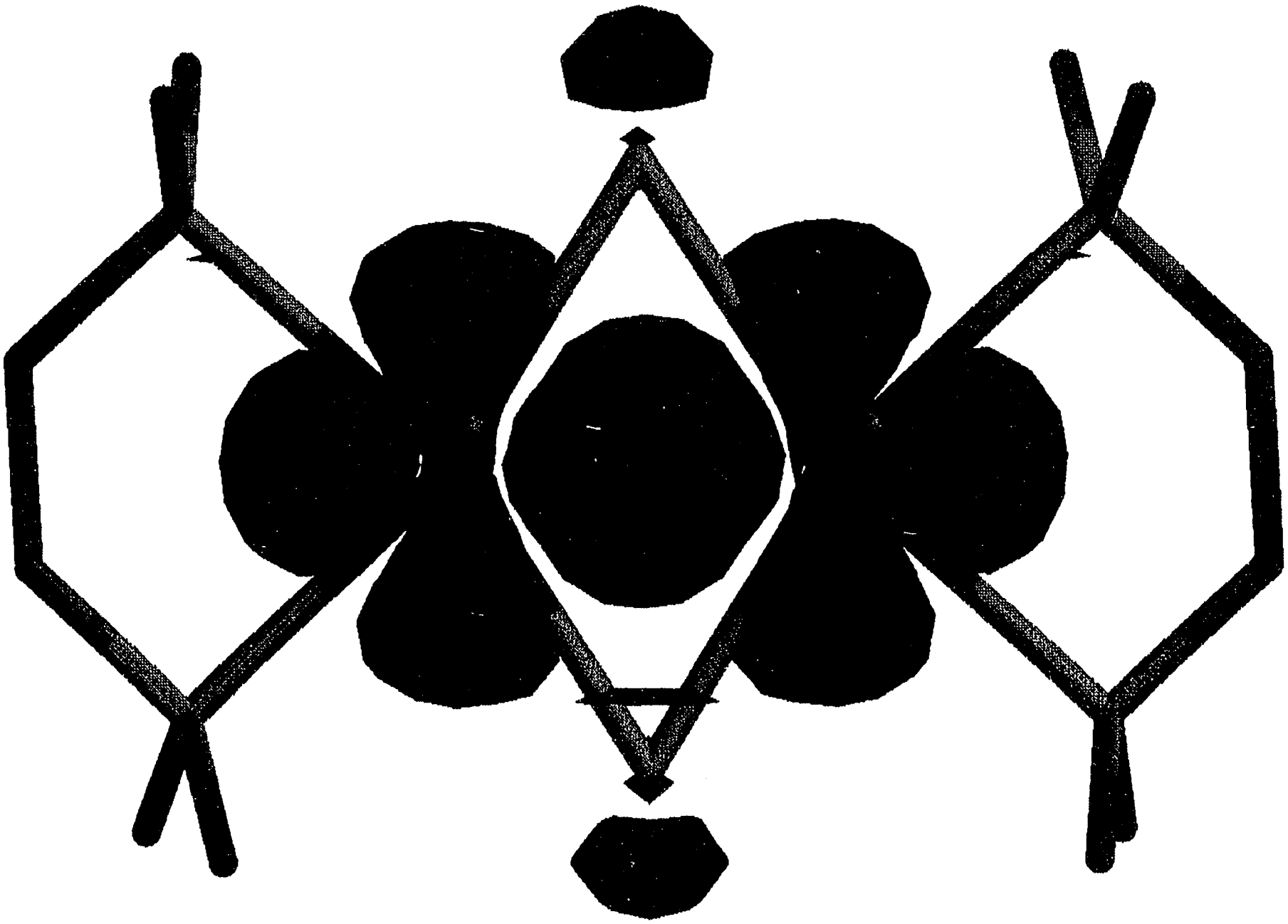

Figure 18

bridged complexes, whose unusually long M-M distances were ascribed to an intrinsic weakness of the metal-metal bonds [14].

Figure 19

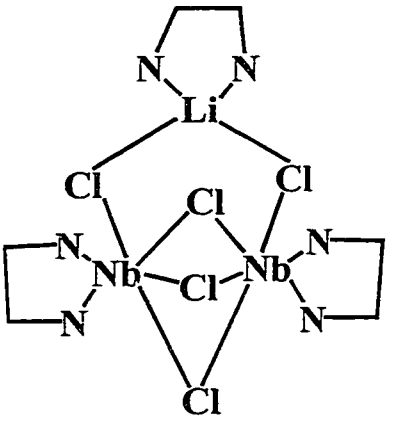

Theoretical calculations carried out on the atomic crystallographic coordinates show that the three highest occupied molecular orbitals are mainly Nb-Nb centred with a metal atom contribution of predominantly d-orbital character and a minor but significant contribution from the p orbitals of the bridging chlorine atoms. The HOMO-LUMO gap is rather small yet sufficient to account for the observed diamagnetism in solution (Figure 24). The three MOs are formed by the overlap of hybrid atomic orbitals of the two niobium atom. The shape of the HOMO (Figure 20) is reminiscent of a M-M δ bond while the LUMO (-10.32eV) is the corresponding out of phase combination. The next occupied molecular orbital (Figure 21), located at -11.24 eV is also M-M centred and has some π bond character, while the third next orbital (Figure22) (-12.17 eV) is a regular σ bond lying symmetrically on the intermetallic vector. At this stage it

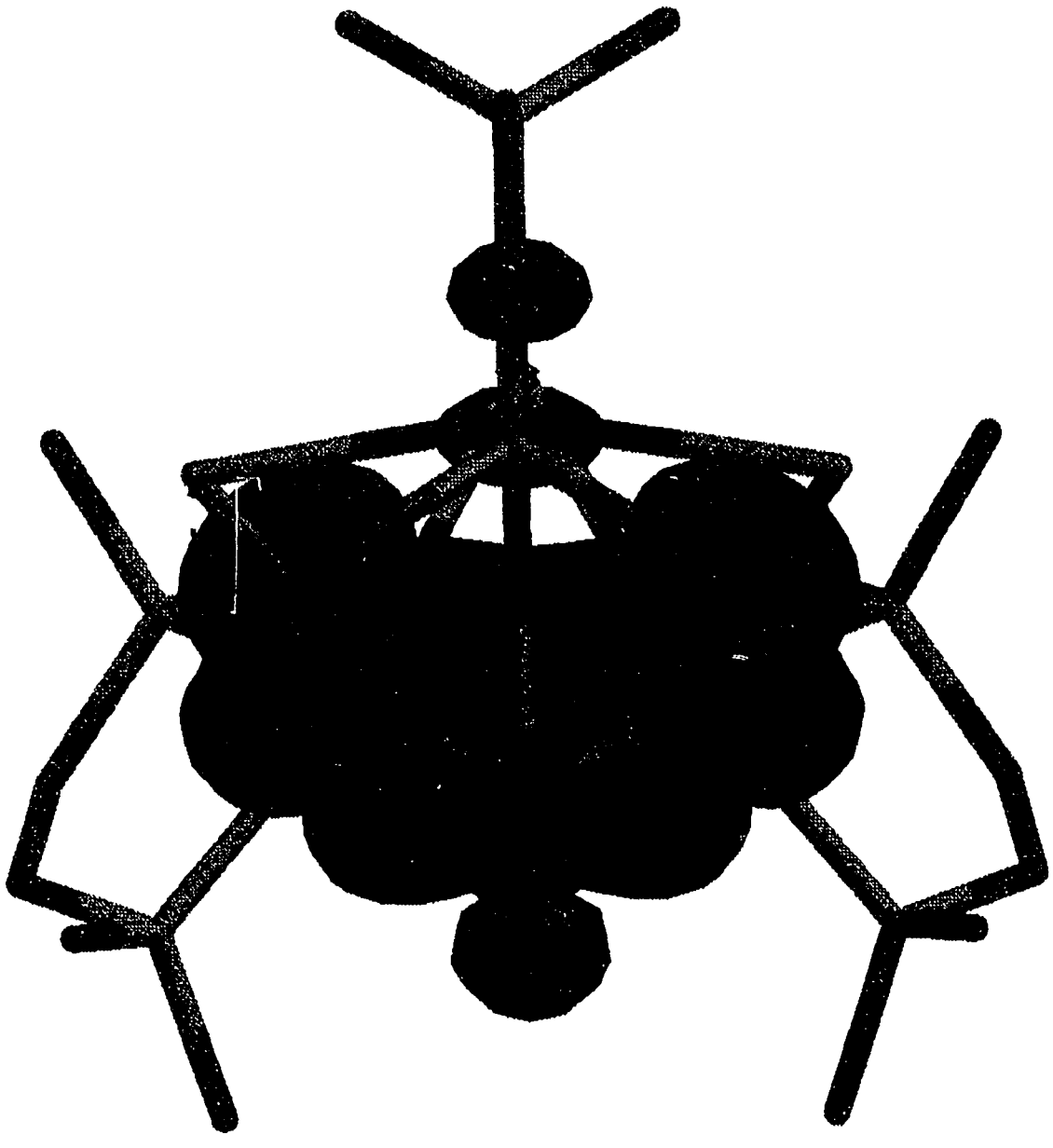

Figure 20

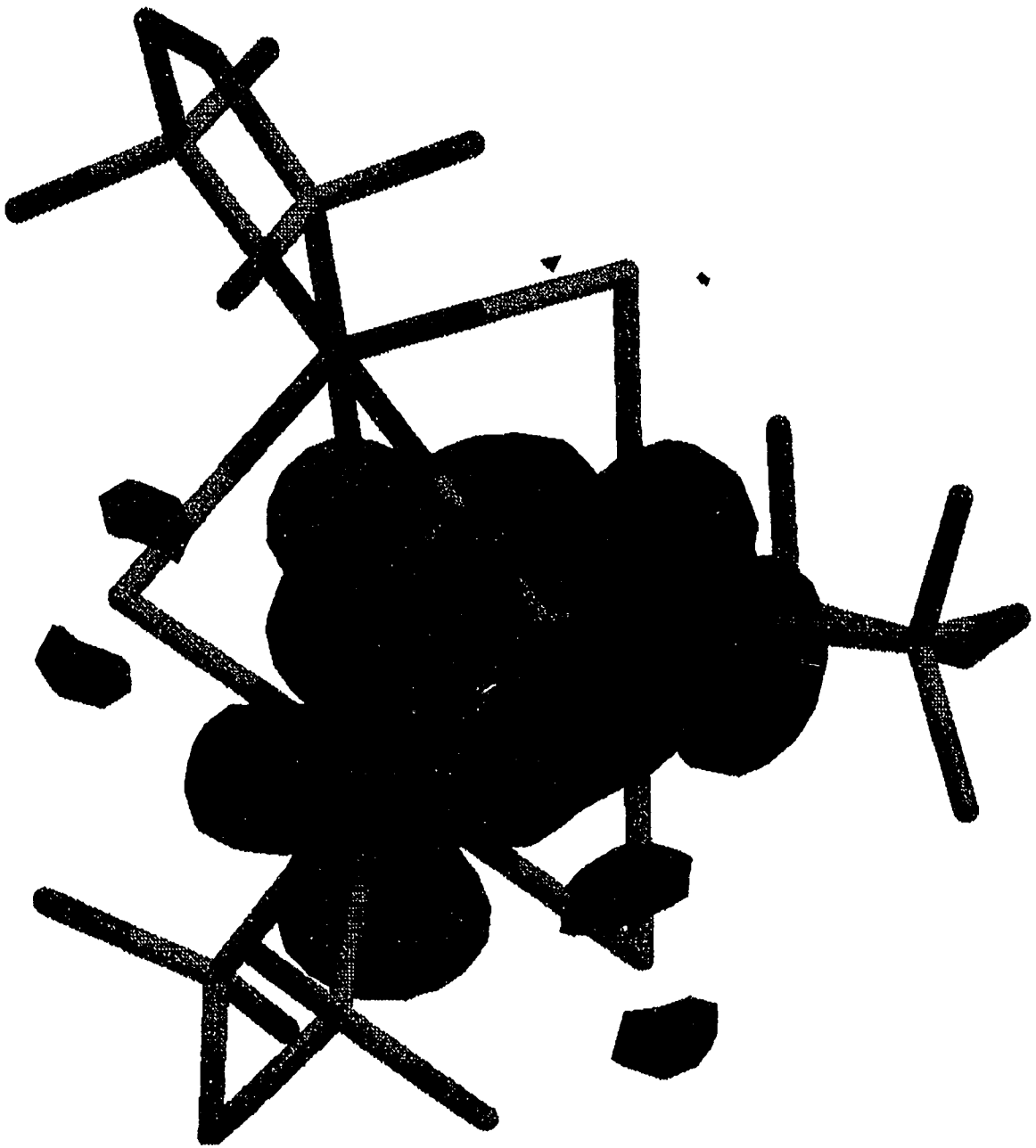

Figure 21

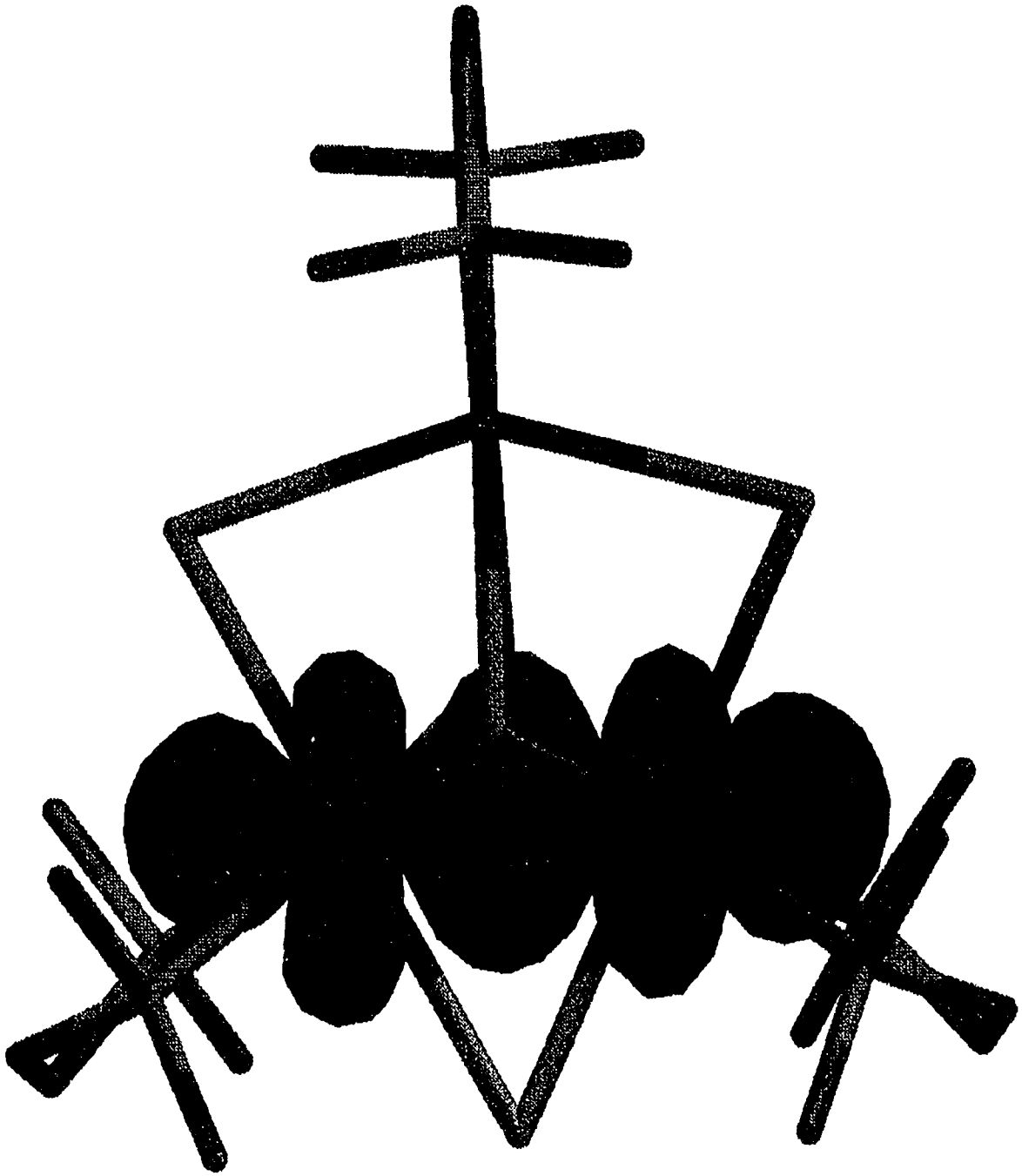

Figure 22

is not clear which factor (electronic or steric) is responsible for the short Nb-Nb distance.

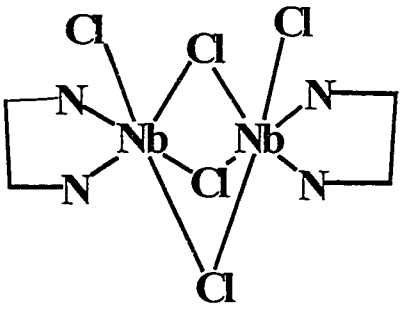

Figure23

The comparison between the geometry of $Cl_2Nb_2(\mu\text{-}Cl)_3(TMEDA)_2$ [13] **(2)** (Figure 23) with that of complex **1** is somewhat interesting. The most visible difference lies in the absence of the lithium cation and the value of the Nb-Nb distances [respectively 2.545(1)Å and 2.4001(5)Å, for **2** and the starting material]. The deviation from the regular octahedral coordination geometry of the metal center is rather similar in the two complexes and only slightly more pronounced in **2** [Cl3-Nb1-Cl4 angle is 174.94(5) against the value of 179.43(3) of $(TMEDA)_2Nb_2Cl_5Li(TMEDA)$ complex], in spite of the absence of coordinated lithium. The absence of the attractive force in **2** applied by the lithium cation between the two vertices of the two octahedra of the starting material, might well be a critical factor in determining the elongation of the intermetallic vector of **2**. However, it is also possible that given that complex **2** is a mixed valence species, the absence of one electron when comparing to the starting Nb(II) complex

depopulates the HOMO (a MO with some Nb-Nb δ-bond character) thus decreasing the formal Nb-Nb bond order, and ultimately lengthening the Nb-Nb distance.

Ab initio STO-3G Hartree-Fock calculations with the doublet state, were carried out on the geometrical parameters of $Cl_2Nb_2(\mu\text{-}Cl)_3(TMEDA)_2$ as determined by the crystal structure. The frontier orbitals (HOMO, HOMO-1 and HOMO-2) are basically the same calculated for complex 1 (Figure 24) with a comparable HOMO-LUMO gap. As for the starting material, these orbitals are mainly Nb-Nb centered MOs with a metal atom contribution mainly of *d*-orbital character and a significant contribution from the bridging chlorine *p* orbitals. For both complexes, the orbitals originate from the same hybrid combinations of *d* orbitals. In the case of 1, the contribution of the bridging halide *p* orbitals to the formation of the M-M bonds is even higher than in the starting material. As a probable result of an increased involvement of the bridging ligand orbitals in complex 1 and of the potential depopulation of the HOMO, the formal bond order dropped from 2.76 to 1.45. The most visible difference between the two systems arises from the fact that the orbital which has the higher δ character in complex 1 is more stable than the "π" orbital and becomes the HOMO. Although these calculations are certainly inadequate to assess the strength of the Nb-Nb bond, nevertheless, they give a reasonable qualitative picture. Certainly we cannot rule out the possibility that the lithium cation may ultimately determine the intermetallic distance by bridging the two octahedra, even though it is tempting at

this stage to conclude that the partial depopulation of the HOMO is the factor that determines the lengthening of the Nb-Nb distance.

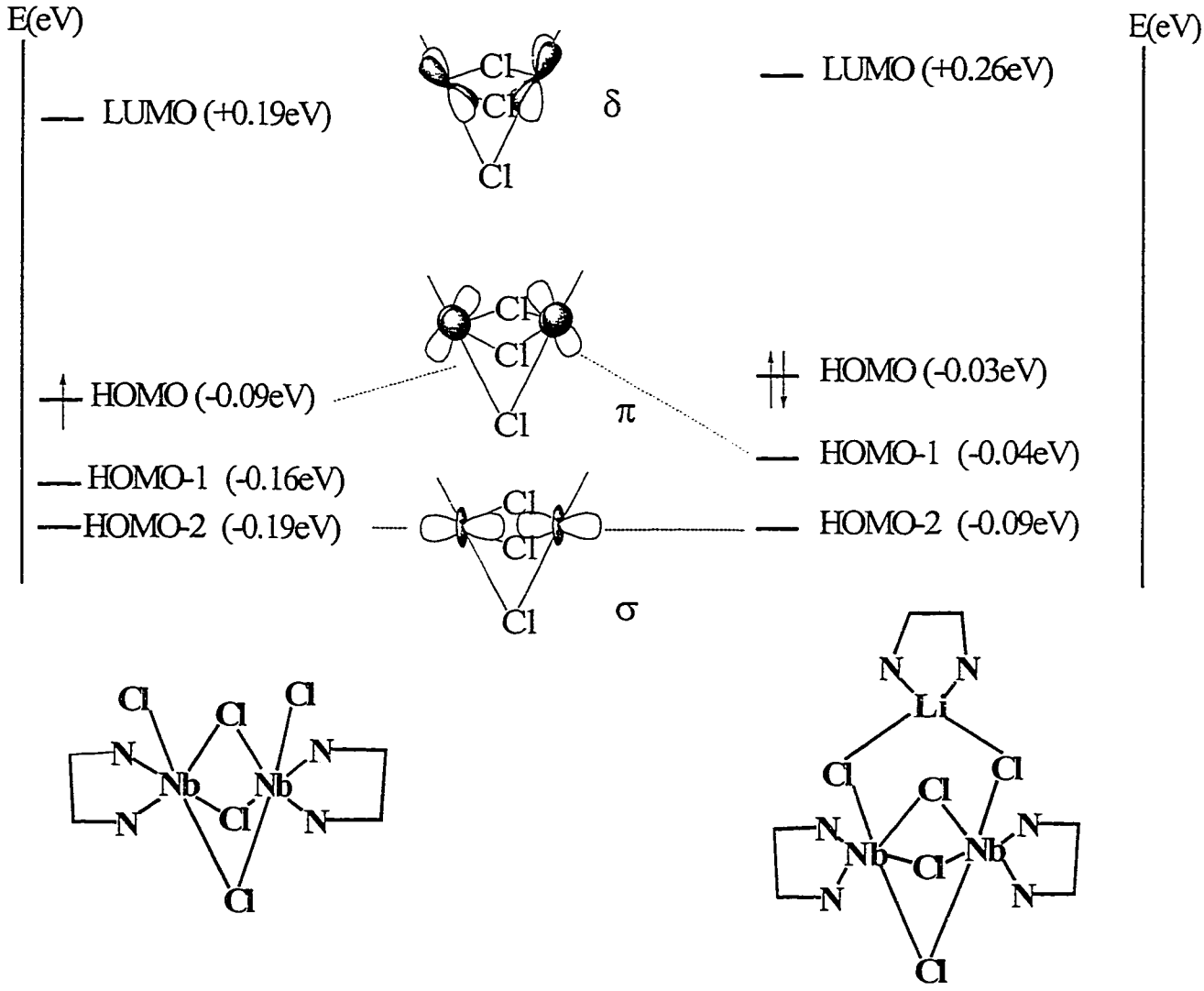
E(eV)
LUMO (+0.19eV)
HOMO (-0.09eV)
HOMO-1 (-0.16eV)
HOMO-2 (-0.19eV)
δ
π
σ
LUMO (+0.26eV)
HOMO (-0.03eV)
HOMO-1 (-0.04eV)
HOMO-2 (-0.09eV)
E(eV)
Cl
Nb
N
Li

Figure 24

References:

1. F. Preuss, G. Overhoff, H. Becker, H.J. Hausler, W. Frank, G. Z. Reiss, *Anorg. Allg.Chem.* **1993,** 619, 1827.
2. C. M. Bolinger, T. B. Rauchfuss, A. L. Rheingold *J. Am. Chem. Soc.* **1983,** 105, 6321.
3. Z. Duan, M. Schmidt, V. G. Young, X. Xie, R. E. McCarley, J. G. Verkade, *J. Am. Chem. Soc.* **1996,** 118. 5302 references cited therein.
4. K. B.P. Ruppa, I. Kovacs, K. Aparna, S. Gambarotta, G. P.A. Yap and C. Bensimon, *article in press.*
5. D. Reardon, I. Kovacs, KBP Ruppa, K. Feghali, S.Gambarotta, J. Petersen *Chem. Eur. J.* **1997,** 9, 1482.
6. A. D.Allen, S. Naito *Can. J. Chem.* **1976,** 54, 2948.
7. E.T. Mass Jr., R.E. McCarley, *Inorg. Chem.* **1973,** 12, 1096.
8. A.P. Sattelberger; R.B. Wilson Jr., J.C. Huffman *J. Am. Chem. Soc.* **1980,** 102, 7111.
9. L. Hubert-Pfalzgraf, J.G. Reiss, *Inorg. Chim. Acta* **1978,** 29, L251.
10. M.E. Clay, T.M.Brown, *Inorg. Chim. Acta* **1983,** 72, 75.
11. L.E. Manzer *Inorg. Chem.* **1977,** 16, 525.
12. M.Canich, F.A. Cotton *Inorg. Chem.* **1987,** 26, 4236.
13. M. Tayebani, A. Kasani, K. Feghali, S. Gambarotta, C. Bensimon *Chem. Comm.* **1997,** 20, 2001.

14. F.A. Cotton, M.P. Diebold, W.J.Roth *J. Am. Chem. Soc.* **1986**, 108, 3538.

CHAPTER IV

Experimental Section

All operations were performed under an inert atmosphere using standard Schlenk techniques. Sulfur and propylensulfide,(Aldrich) were used as received. [$(Me_3Si)_2N$]Li was prepared by reacting the amine with BuLi in hexane and purified by recrystallization in hexane. PySLi was prepared by reacting mercaptopyridine (Aldrich) with one equivalent of methyllithium. Solvents were dried with the appropriate drying agents and distilled prior to use. Infrared spectra were recorded on a Mattson 9000 FTIR instrument from Nujol mulls prepared in a drybox. Samples for magnetic susceptibility measurements were prepared inside a drybox and sealed into calibrated tubes. Magnetic measurements were performed with a Gouy balance (Johnson Matthey) at room temperature. The magnetic moment were calculated by standard methods, and corrections for underlying diamagnetism were applied to the data. NMR spectra were recorded with Varian Gemini 200 MHz spectrometer. Elemental analyses were carried out with a Perkin Elmer 2400 CHN analyzer. Ratios between heavy atoms were determined by X-ray fluorescence by using a Philips 2400 instrument.

X-ray Crystallography

Data were collected with a Siemens CCD instrument at -158°C for air-sensitive crystals mounted with viscous oil on glass fibers using the hemisphere scan method. Cell constants and orientation matrices were obtained from reflections found on 50 initial data frames. Data were corrected for Lorentz, polarization effects and scaled for absorption effects using redundant data. The structures were solved by direct methods in locating all the non-hydrogen atoms, which were refined anisotropically. Hydrogen atom positions were calculated but not refined. Refinement was carried out by using full-matrix least-squares refinement based on $|F|^2$. Atomic scattering factors and anomalous dispersion terms were taken from SHELXTL (5.03) program library.

Molecular Orbital Calculations

Molecular orbital calculations were performed on a Silicon Graphics computer using the software package SPARTAN 4.0 and on a Pentium computer using the CAChe software package (Oxford 1995) for Extended Huckel calculations. Default parameters were used in the calculations on the model compounds. Calculations were also performed by imposing higher symmetries without significantly modifying the final results.

Preparation of $VCl_3(THF)_3$ (1):

A suspension of anhydrous VCl_3 (50 g, 317 mmol) was refluxed in THF (500 mL) under vigorous stirring for 44 hours. The mixture was cooled to room temperature, (red crystals were observed), filtered and extracted with 500 ml of dry THF. When extracts became colorless, the solution was allowed to stand at 4°C overnight, upon which red crystals separated. The crystalline solid was filtered and dried under vacuum (81 g, 214 mmol, 68%). IR (Nujol, KBr, cm^{-1}) ν: 1342 (s), 1295 (m), 1260 (m), 1242 (m), 1176 (m), 1041 (s), 1010 (s), 922 (m), 848 (s), 684 (m).

Preparation of $VCl_2(TMEDA)_2$ (2):

A suspension of $VCl_3(THF)_3$ (44 g, 279 mmol) was stirred and refluxed in the presence of zinc powder (25 g, 385 mmol) in THF (500 mL) for 12 hours. The green crystals formed were filtered dried and redissolved in CH_2Cl_2. The product was then precipitated by addition of hexane. After filtration the product was redissolved in boiling THF and TMEDA was added dropwise until the green product disappeared. The blue solution was then cooled to 4°C overnight then filtered to collect the blue crystals (59 g, 168 mmol, 60%). IR (Nujol, KBr, cm^{-1}) ν: 1354 (m), 1285 (s), 1260 (m), 1239 (m), 1164 (m), 1122 (s), 1071 (s), 1014 (s), 956 (s), 925 (m), 792 (s).

Preparation of $[(TMS)NHCH_2CH_2]_2NTMS$ (3):

A solution of DABCO (diaminebicyclooctane 50 g, 0.45 mol) in ether (700 mL) was treated with chlorotrimethylsilane (62.17 mL, 0.45 mol) at room temperature. Upon mixing the color of the solution changed from colorless to white. After stirring for 60 minutes, diethyltriamine (15.3 mL, 0.15 mol) was added to the mixture and stirring was continued overnight. The solution was then filtered and ether was removed under vacuum to yield a yellow oil. After the removal of the unreacted DABCO by sublimation the amine was distilled yielding a colorless oil (21 g, 65 mmol). IR (KBr, cm^{-1}) ν: 3450 (m), 1330 (s), 850 (s), 660 (s), 592 (s). ^{1}H-NMR($CDCl_3$, 200MHz, 25°C): δ 0.1 (m, 9H, TMS), 2.7(m, 4H, CH_{ethyl}). ^{13}C-NMR($CDCl_3$, 200MHz, 25°C): δ 42 (s, TMS), 52 (s, TMS) 54 (s, CH_{ethyl}).

Preparation of $[(TMS)NLiCH_2CH_2]_2NTMS$ (3a):

The addition of buthyllithium (52 mL, 2.5M) to a solution of **3** in hexane (150 mL) at -80°C afforded a white precipitate. The solution was allowed to warm to room temperature, stirred for 1h, and filtered to collect the lithiated compound **3a** (19.3g, 58 mmol, 89%). IR (Nujol, KBr, cm^{-1}) ν: 1258(m), 1083(m), 944(w), 884(w), 825(m), 729(w). ^{1}H-NMR($CDCl_3$, 200MHz, 25°C): δ 0.15 (s, 9H, TMS), 0.34(s, 18H, TMS), 2.9 (m, 4H, CH_{ethyl}).

Preparation of $\{[(TMS)NCH_2CH_2]_2N(TMS)\}_2V_2(\mu\text{-}Cl)_2$ (4):

A solution of $VCl_3(THF)_3$ (5.8 g, 15.5 mmol) in THF (100 mL) was treated with one equivalent of **3a** (5.2 g, 15.5 mmol) at room temperature. The color of the solution immediately darkened upon mixing and stirring was continued for 30 minutes. THF was removed in vacuo and the resulting red powder was redissolved in hexane (150mL). The solution was then filtered to eliminate LiCl and allowed to stand at 0°C, for 24 hrs, upon which dark red crystals of **4** separated. (5.1 g, 6.2 mmol, 80%). IR (Nujol, KBr, cm^{-1}) ν: 1377 (m), 1250 (s), 1074 (s), 937 (s), 911 (s), 825 (s). μ_{eff}: 2.93 μ_B. Anal. Calcd.(found): C, 38.64 (38.53) ; H,8.73 (8.61); N 10.40 (10.34).

Preparation of $\{[(TMS)NCH_2CH_2]_2N(TMS)\}VCH_3Py$ (5):

A solution of **4** (1.1 g, 1.4 mmol) in ether (100 mL) was treated with one equivalent of mehyllithium (2 mL, 1.4M) at room temperature. After mixing the color of the solution changed to pink red and stirring was continued for 30 minutes. The solvant was removed *in vacuo*, the solid residue was redissolved in hexane (50 mL) and the solution was then filtered to eliminate LiCl. The addition of dry pyridine (5 mL), turned the color of the solution to purple. The mixture was allowed to stand at -80°C, for 36 hrs, upon which dark purple crystals of **5** separated (0.98 g, 2.1 mmol, 75%). μ_{eff}: 2.90 μ_B.

The extreme air-sensitivity prevented IR analysis as well as combustion analysis determinations.

Reaction of (4) with S_8 (6):

A solution of **4** (1.0 g, 1.2 mmol) in THF (100 mL) was treated with S_8 (0.08 g, 0.3 mmol) at room temperature. Upon mixing the color of the solution changed to brown. After stirring for 10 minutes, the solvant was removed *in vacuo* and the resulting powder was redissolved in ether (100 mL). The solution was then filtered and allowed to stand at -30°C, for 24h, upon which a dark brown solid separated (0.4 g, 0.5 mmol, 43%). IR (Nujol, KBr, cm^{-1}) ν: 1255 (s), 1215 (w), 1056 (m), 932 (w), 842 (s), 799 (s), 756 (m). ^{1}H-NMR (C_6D_6, 200MHz, 25°C): δ 0.15 (s, 6H, TMS), 0.51 (s 3H TMS).Anal. Calcd.(found): C, 38.97 (38.12) ; H, 8.80 (8.75); N 10.49 (10.11).

Preparation of $\{[(Me_3Si_2N]_2V\}_2(\mu\text{-}S)_2$ (7).

A suspension of $[(Me_3Si)_2N]_2VCl(THF)$ (1.38 g 2.9 mmol) in toluene (60 mL) was treated at room temperature with S_8 (0.1 g. 0.39 mmol). The color of the mixture changed rapidly from the original blue green to dark red-brown . After the solution was stirred for about 30 min at room temperature, the solvent was evaporated *in vacuo* to give a red-brown powder. The solid was resuspended in ether (20 mL). The mixture was filtered to eliminate a small amount of insoluble solid. The resulting deep-red solution was allowed to stand at -30°C overnight and

at -78°C for a few days, whereupon crystals of 7 separated (0.25 g. 0.3 mmol. 21%). Anal. Calcd (found) for $C_{24}H_{72}Si_8N_4S_2V_2$: C, 35.70 (35.43); H, 8.99(8.38); N, 6.94 (6.53); S, 7.94 (7.32). IR (Nujol mull. NaCl. cm $^{-1}$): ν 1385 (w), 1070(w), 853 (vs, br), 786(s), 706 (s), 7()4 (s), 670 (s), 617 (w). ^{1}H-NMR (500MHz. 25°C): δ 0.51 (Me_3Si), ^{13}C-NMR (125.7 MHz. 25 0C): δ 8.90. ^{51}V-NMR (131.4 MHz. 25°C): δ 2531.

Reaction of $VCl_2(TMEDA)_2$ with H_2S.

A suspension of $VCl_2(TMEDA)_2$ (2.0 g, 5.6 mmol) in THF (100 mL) was treated at room temperature with H_2S (125 mL, 5.6 mmol). The color of the mixture changed slowly from the original blue color to light green. The solution was stirred for about 30 min at room temperature, and then was allowed to stand for few minutes upon which a green powder deposited at the bottom and the color of the solution turned to brown. The residual solid was filtered and dried *in vacuo* (1.3 g). IR (Nujol mull. NaCl, cm^{-1}): ν 2566 (m), 2458 (m), 1288 (w) 1024 (w), 1007 (m) 985 (w), 954 (w), 798 (m). XRF: V, 37.3; Cl 46.2; S 2.23. The mother liquor was layered with hexane and was allowed to stand for few days, whereupon a crystalline mass containing two different types of crystals separated.

Reaction of $VCl_2(TMEDA)_2$ with propylenesulfide (7a):

A solution of $VCl_2(TMEDA)_2$ (2.0 g, 5.6 mmol) in THF (100 mL) was treated with propylenesulfide (4.14 g, 5.6 mmol) at 50°C (without stirring). Upon mixing

the color of the solution slowly changed from blue to dark purple. The solution was then allowed to stand for 24h, upon which dark brown microcrystals separated (0.7 g). IR (Nujol, KBr, cm^{-1}) ν: 1280 (w), 1238 (w), 1117 (w), 1065 (m), 1014 (s), 952 (s), 801 (s), 770 (m), 722 (w). XRF: V, 33.1; Cl, 33.5; S, 9.57.

Preparation of $(TMEDA)_2V_2Cl_2(\mu\text{-}SPh)_2(\mu\text{-}Cl)$ (7b):

A solution of $VCl_2(TMEDA)_2$ (2.0 g, 5.6 mmol) in THF (100 mL) was treated with $(Ph)_2(\mu\text{-}S_2)$ (1.0 g, 5.6 mmol) at 50°C . Upon mixing the color of the solution slowly changed from blue to green and finally to purple. The solution was then filtered and allowed to stand, for 24hrs at room temperature, upon which dark purple crystals separated(0.92 g, 1.68 mmol, 90%). IR (Nujol, KBr, cm^{-1}) ν: 1577(w), 1261(w), 1117(w), 1081(m), 1014(s), 952(s), 927(m), 800(s), 750(s), 698(m).

Preparation of $V_3S_7Cl(TMEDA)_3$ (7c):

Method A. A solution of $VCl_2(TMEDA)_2$ (2.0g, 5.6 mmol) in THF (100mL) was treated with elemental sulfur (0.18g, 0.7mmol) at room temperature. Upon mixing, the color of the solution changed from blue to black. After stirring for 30 minutes the solution was filtered to eliminate a black insoluble powder and a dark red extremely air sensitive solution (traces of moisture change the color to intense purple). The solution was then concentrated *in vacuo* to small volume, and allowed to stand at –30 °C, for 2 days, upon which dark colored crystals of

$VCl_3(THF)(TMEDA)$ separated. IR(Nujol, KBr, cm^{-1}) ν: 1277 (s), 1018 (w), 950 (s), 866 (s), 800 (s). The black residue was then extracted with boiling THF for 24h in a Soxhlet apparatus to eliminate any $VCl_3(THF)(TMEDA)$ contaminant, then dried in vacuum (0.42 g, 0.56 mmol, 80%). IR (Nujol, KBr, cm^{-1}) ν: 1261 (s), 1062 (m), 951 (s), 800 (s). Anal. found: C, 15.78; H, 3.58; N 5.38; Cl, 3.25; S, 26.93; V, 19.4. XRF: V, 32.2; Cl, 7.39; S, 35.0.

Method B. Separate solutions of $VCl_2(TMEDA)_2$ and S_8 were stirred overnight in THF, filtered then cannulated into a layering tube. The reaction mixture was allowed to stand for a week at room temperature (in a vibration free environment) upon which black needle shaped crystals separated.

Preparation of $\{[(TMS)_2N]VS_3Li(THF)_2Li\}_4$ (7d):

A suspension of **7c** (4.3g 5.6mmol) in THF (150mL) was treated with $LiN(TMS)_2$ (3.0 g, 18 mmol) . Upon mixing, the color of the solution changed from black to red. After refluxing for 3 days, THF was then removed in vacuo, and the red solid was dissolved in hexane (150 mL). The solution was filtered to eliminate LiCl and then allowed to stand at 4°C, for 3 days, upon which red crystals of **7d** separated (0.5 g, 0.3 mmol 4.8%). IR (Nujol, KBr, cm^{-1}) ν: 1259(br), 1018(m), 817(br), 669(s). ^{1}H-NMR (C_6D_6, 200MHz, 25°C): δ 0.8 (s, TMS), 1.45 (s, 2H THF), 3.9 (s, 2H THF). ^{13}C-NMR (C_6D_6, 200MHz, 25°C): δ 7.0 (s, TMS), 22 (s, THF), 70 (s, THF).

Preparation of (TMS)PhNLi.(Et_2O) (8):

Freshly distilled aniline (25 mL, 0.27 mol) was dissolved in ether (100 mL) and then cooled to -78°C. A solution of MeLi in ether (196 mL, 1.4 M, 0.27 mol) was added dropwise. The reaction mixture was stirred, allowed to warm to room temperature, then cooled again to -78°C. The addition of $(CH_3)_3SiCl$ (35 mL, 0.27 mol) formed a precipitate of LiCl which, after warming up to room temperature, was removed by filtration. The resulting clear solution was cooled to -78°C and treated with an hexane solution of n-BuLi (110 mL, 2.5 M, 0.27 mol). After further filtration, the clear solution was concentrated and cooled to -30°C overnight. Extremely air-sensitive crystals of $Me_3Si(Ph)NLi(Et_2O)$ separated. (33g, 0.13 mol, 48%). I.R. (Nujol, cm^{-1}) ν: 1582(s), 1271(sh), 1269(vs), 1180(m), 1153(m), 1075(m), 1027(m), 991(s), 917(vs), 830(vs), 762(s), 695(s), 669(m), 623(m). ^{1}H-NMR (C_6D_6, 25°C, 200MHz) δ: 7.19(dd, 2H, Ph), 6.82(dd, 2H, Ph), 6.78(t, 1H, Ph), 3.06(q, 4H, ether), 0.76(t, 6H, ether), 0.32(s, 9H, silyl). ^{13}C-NMR (C_6D_6, 25°C, 75MHz) δ: 159.3, 129.8, 123.0, 115.3(Ph), 64.8(ether), 14.3(ether), 2.8 (silyl). The extreme air-sensitivity prevented combustion analysis.

Reaction of the 7c with (8):

A suspension of **7c** (2.3g, 3mmol) in THF (150mL) was treated with (TMS)PhNLi.(Et_2O) (3.1g, 12 mmol). Upon mixing, the color of the solution changed from black to orange-red. The solution was refluxed for 24 h, after which THF was removed under vacuum, and the red solid was dissolved in hexanes (10 mL). The solution was filtered and was allowed to stand at -30°C, for 2 days, and at -80°C for 4 days upon which orange-red powder separated. IR (Nujol, KBr, cm^{-1}) ν: 1251 (s), 1065(s), 937(m), 910(m), 823(br), 669(s). ^{1}H-NMR (C_6D_6, 200MHz, 25°C): δ 0.35 (s, 9H, TMS) 6.9(m, 5H, Ph).

The small quantity of powder isolated and the extreme air-sensitivity prevented ^{13}C NMR and combustion.

Reaction of the 7c with [CyN-C(H)-NCy]Li

A suspension of **7c** (1.2g 1.6mmol) in THF (150mL) was treated with [CyN-C(H)-NCy]Li (2.2g, 10 mmol) . Upon mixing the color of the solution changed from black to orange-red. After refluxing for 24 hrs. THF was then removed under vacuum, and the red solid was dissolved in hexanes (20 mL). The solution was filtered and was allowed to stand at -80°C, for several days upon which orange-red powder separated. IR (Nujol, KBr, cm^{-1}) ν: 1559 (s), 1288(m), 1260(m), 1151(m), 1117(s), 1051(m), 888(w), 796(w), 727(s) 694(m).

The extreme air-sensitivity prevented combustion analysis determinations.

Preparation of $[V_3(\mu_3\text{-}Cl)\text{-}(\mu\text{-}S_2)_3](PyS)_3Li(THF)_4$ (9)

A suspension of the black powder **7c** (2.0 g, 2.6mmol) in THF (150mL) was treated with PySLi (1.2g, 9 mmol) . Upon mixing the color of the solution changed from black to red. After refluxing for 24 h. THF was then removed *in vacuo* and the red solid was dissolved in hexane (75 mL). The solution was filtered and allowed to stand at room temperature for several days upon which red crystals separated (0.37 g, 0.39 mmol, 15%). IR (Nujol, KBr, cm^{-1}) ν: 1576 (s), 1544(m), 1414(s), 1259(m), 1136(s), 1087(w), 1039(s), 888(w), 303(w), 752(m) 734(m).

IMAGE EVALUATION TEST TARGET (QA-3)

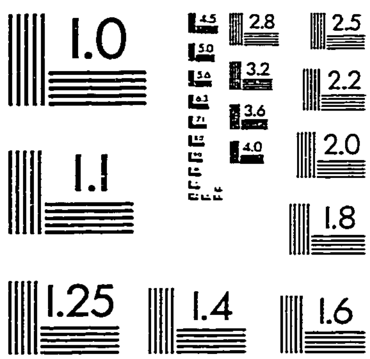

150mm

6"

APPLIED IMAGE . Inc
1653 East Main Street
Rochester, NY 14609 USA
Phone: 716/482-0300
Fax: 716/288-5989